AVC-VTN-17G09

Improvement of GT Classification of Soviet PNEs

Final Report
Contract No. SAQMMA14M1834
Report Period: September 24, 2014 – March 31, 2016
Date Report Submitted: February 28, 2017

Submitted by

Kevin Mackey[1], Kazuya Fujita[1] and Eric Bergman[2]

[1]Dept. of Earth & Environmental Sciences
Michigan State University
288 Farm Lane #207
East Lansing, MI 48824-1115

[2]Global Seismological Services
1900 19th St.
Golden, CO 80501

Sponsored by
U.S. Department of State
Bureau of Arms Control, Verification, and Compliance
2201 C Street NW, Washington DC 20520

Unclassified; Distribution Unlimited

REPORT DOCUMENTATION PAGE			*Form Approved OMB No. 0704-0188*
1. REPORT DATE 2/28/2017	**2. REPORT TYPE** Final Technical Report		**3. DATES COVERED** 9/24/2014-3/31/2016
4. TITLE AND SUBTITLE **Improvement of GT Classification of Soviet PNEs**			**5a. CONTRACT NUMBER** SAQMMA14M1834 **5b. GRANT NUMBER** **5c. PROGRAM ELEMENT NUMBER**
6. AUTHOR(S) Kevin Mackey, Kazuya Fujita and Eric Bergman			**5d. PROJECT NUMBER** **5e. TASK NUMBER** **5f. WORK UNIT NUMBER**
7. PERFORMING ORGANIZATION NAME(S) AND ADDRESS(ES) Department of Earth and Environmental Sciences Michigan State University, 288 Farm Lane #207, East Lansing, MI 48824			**8. PERFORMING ORGANIZATION REPORT NUMBER**
9. SPONSORING / MONITORING AGENCY NAME(S) AND ADDRESS(ES) U.S. Department of State Bureau of Arms Control, Verification, and Compliance Washington, DC 20520			**10. SPONSOR/MONITOR'S ACRONYM(S)** DoS/AVC **11. SPONSOR/MONITOR'S REPORT NUMBER** AVC-VTN-17G09
12. DISTRIBUTION / AVAILABILITY STATEMENT: Unclassified//Distribution Unlimited			
13. SUPPLEMENTARY NOTES			

14. ABSTRACT

From the 1960's through the late 1980's, the Soviet Union conducted 122 Peaceful Nuclear Explosions (PNEs; Figure 1) across its territory. These PNEs are now very important to the seismological community as so-called Ground Truth (GT) events. The PNE locations are widely distributed, thus GT0-1 locations are very useful as calibration events for the development of seismic velocity models, model validation, seismic discrimination, etc. The monitoring/verification community generally utilizes PNE locations from Sultanov et al. (1999) as known or verified GT events. In reality, 43 of the 122 locations were determined seismically and are erroneous by up to 40 km.

We have determined GT0-1 values for 26 of the seismically located events, and to validate or correct the locations of 59 PNEs thought to be GT0-1. Some PNEs currently classified as GT1 or better also have larger errors of up to 16 km. Locations were determined using an integrated approach encompassing published open literature, analysis of satellite imagery and regional seismic data. In addition, ten PNE sites in were visited allowing GPS coordinates to be obtained in the field.

15. SUBJECT TERMS Lop Nor, Kazakhstan, Nuclear Explosions, Seismograms, Phases, Yield, Locations

16. SECURITY CLASSIFICATION OF: Unclassified			**17. LIMITATION OF ABSTRACT**	**18. NUMBER OF PAGES**	**19a. NAME OF RESPONSIBLE PERSON** Rongsong Jih (COR)
a. REPORT U	**b. ABSTRACT** U	**c. THIS PAGE** SAR	SAR	xiv + 145	**19b. TELEPHONE NUMBER** 202-647-8126

Standard Form 298 (Rev. 8-98)
Prescribed by ANSI Std.

TABLE OF CONTENTS

LIST OF FIGURES

LIST OF TABLES

ERRATA

In the main location table of Mackey and Fujita (2014), a previous version of this report, the longitude coordinates for Lira 1-1 and Lira 1-2 are transposed. They are corrected in this version.

FINAL REPORT - IMPROVEMENT OF GT CLASSIFICATION OF SOVIET PNEs

Kevin Mackey[1], Kazuya Fujita[1] and Eric Bergman[2]

[1]Michigan State University
[2]Global Seismological Services

Sponsored by the U.S. Department of State

Order No. SAQMMA14M1834

1. INTRODUCTION

From the 1960's through the late 1980's, the Soviet Union conducted 122 Peaceful Nuclear Explosions (PNEs; Figure 1) across its territory. These PNEs are now very important to the seismological community as so-called Ground Truth (GT) events. The PNE locations are widely distributed, thus GT0-1 locations are very useful as calibration events for the development of seismic velocity models, model validation, seismic discrimination, etc. The monitoring/verification community generally utilizes PNE locations from Sultanov et al. (1999) as known or verified GT events. In reality, 43 of the 122 locations were determined seismically and are erroneous by up to 40 km.

We have been able to determine GT0-1 values for 26 of the seismically located events, and to validate or correct the locations of 59 PNEs thought to be GT0-1. Some PNEs currently classified as GT1 or better also have larger errors of up to 16 km. Locations were determined using an integrated approach encompassing published open literature, analysis of satellite imagery and regional seismic data. In addition, five PNE sites in Kazakhstan were visited in 2015 allowing GPS coordinates to be obtained in the field. A sixth PNE site, that for Batholith 2, could not be found. This report also includes GPS coordinates for 5 additional PNEs visited by the author and reported in Mackey and Fujita (2014) and Mackey and Bergman (2014).

This project is an extension of previous work supported by the US DoS (Mackey and Fujita, 2014; Mackey and Bergman, 2014) and the US DoE (Fujita et al., 2013). We include all material from Mackey and Fujita (2014) for continuity and completeness. Many new events are included in this report and new details, photos, and information are added for some previously verified events. Information in his report should supersede earlier reports and publications. Note however, that we do not repeat all information for Yakutia PNEs contained in Fujita et al. (2013) or for the Mangyshlak PNE sequence contained in Mackey and Bergman (2014).

Figure 1 displays all 122 PNE sites, and plots the revised and confirmed locations in green and red. Table 1 is a comprehensive list of PNEs following the Sultanov et al. (1999) parameters along with our revised coordinates and differences. Green indicates that our verified or revised location confirms the GT quality published by Sultanov et al. (1999). Red indicates that our verified or revised location shows that the location error of the Sultanov et al. (1999) published location exceeds their stated GT quality. For several PNEs, shown in yellow, we expended considerable effort but have been unable to conclusively determine or verify the location. For example, we field checked the published coordinates of Batholith-2 (Figure 1), the location of which is indicated as GT-10, but were unable to locate the borehole in two days of field searching. Although we know that the borehole is not at the published coordinates, the

location may still meet the GT-10 criteria. Additional information must be obtained or a more intensive field effort must be undertaken to verify the location for Batholith-2.

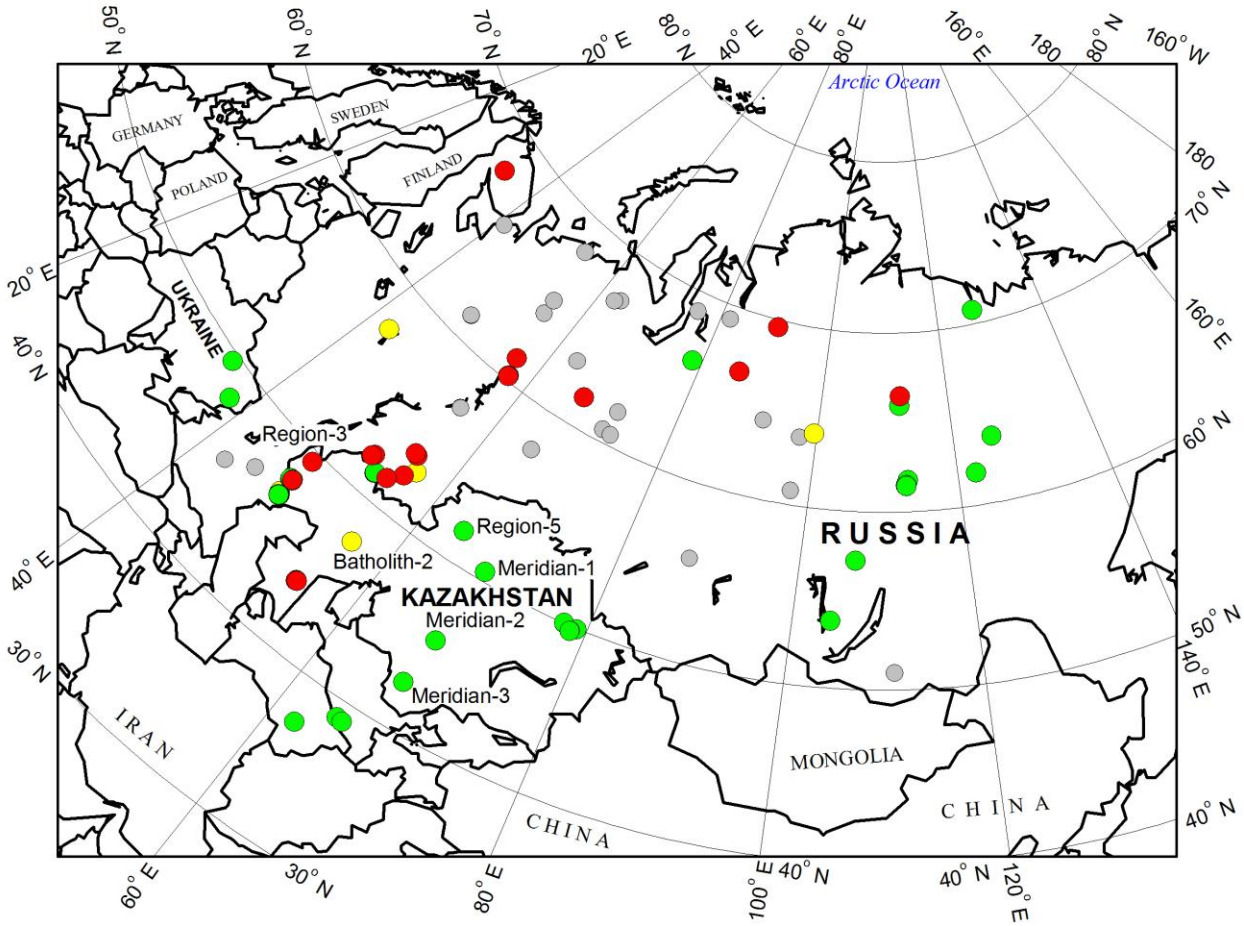

Figure 1. PNEs of the Soviet Union. Green events represent GT0-1 locations determined or verified. Red events indicate GT0-1 locations determined where the new coordinates exceed the location errors published by Sultanov et al. (1999). Yellow events were studied but the locations could not be determined or verified, or evidence exists that the true location error is greater than that published by Sultanov et al. (1999). Grey events have not yet been investigated in depth.

Table 1. All PNEs conducted within the territory of the Former Soviet Union. Green backgrounds are revised or verified GT-0 or GT-1 locations that fall within the GT confidence reported by Sultanov el al. (1999). Red backgrounds are revised GT-0 or GT-1 quality locations that fall outside the GT confidence reported by Sultanov et al. (1999). Yellow backgrounds are events that we researched but were not able to verify or revise the Sultanov et al. (1999) location. In some cases, there is evidence that the Sultanov et al. (1999) location may exceed the stated error. White background events were not extensively researched.

Date	PNE Name	Yield (kt)	Depth (m)	Sul. Lat.	Sul. Lon.	Sul. GT	Lat.	Lon.	GT	Diff. (km)	Notes	Section
65.01.15	Chagan	140	178	49.935ºN	79.009ºE	0.2-1	49.935ºN	79.009ºE	0	0	Hole 1004	2.1
65.03.30	Butane 1-1	2.3X2	1375, 1341	52.9ºN	56.5ºE	-					Hole 617, 618	2.2
65.06.10	Butane 1-2	7.6	1350	52.9ºN	56.5ºE	-					Hole 622	2.2
65.10.14	Sary-Uzen	1.1	48	49.991ºN	77.636ºE	0.2-1	49.9911ºN	77.6351ºE	0	0.07		2.3
66.04.22	Azgir A-1	1.1	161	47.829ºN	47.935ºE	0.2-1	47.8288ºN	47.9336ºE	0		GPS - IGR	2.4
66.09.30	Urtabulak	30	1532	38.968ºN	64.517ºE	0.2-1	38.9671ºN	64.5195ºE	0	0.23		2.5
67.10.06	Tawda	0.3	172	57.70ºN	65.20ºE	5-10						
68.05.21	Pamuk	47	2440	38.918ºN	65.032ºE	0.2-1	38.918ºN	65.032ºE	1	0	Same as Sul.	2.6
68.07.01	Azgir A-2-1	27	597	47.909ºN	47.912ºE	0.2-1	47.9071ºN	47.9105ºE	0	0.23	GPS - IGR	2.4
68.10.21	Telkem1	0.24	31.4	49.728ºN	78.486ºE	0.2-1	49.728ºN	78.486ºE	0	0		2.7
68.11.12	Telkem2	0.24X3	31.4	49.712ºN	78.461ºE	0.2-1	49.712ºN	78.461ºE	0	0	3 explosions	2.7
69.09.02	Grifon-1	7.6	1212	57.220ºN	55.393ºE	0.2-1					Hole 1001	
69.09.08	Grifon-2	7.6	1208	57.220ºN	55.417ºE	0.2-1					Hole 1002	
69.09.26	Stavropol	10	712	45.848ºN	42.600ºE	0.2-1					Takhta-Kugultinskoe	
69.12.06	Mangyshlak-1	30	407	43.867ºN	54.800ºE	0.2-1	43.8625ºN	54.7727ºE	0	2.3	Hole 2-T	2.8
70.06.25	Magistral	2.3	702	52.20	55.70	10	52.3265ºN	55.7238ºE	0	14.2		2.9
70.12.12	Mangyshlak-2	80	497	43.85ºN	54.80ºE	10	43.9096ºN	54.7937ºE	0	6.7	Hole 1-T	2.8
70.12.23	Mangyshlak-3	75	740	44.025ºN	54.933ºE	0.2-1	43.8858ºN	54.8973ºE	0	15.7	Hole 6-T	2.8
71.03.23	Taiga	15X3	127	61.40ºN	56.20ºE	10	61.306ºN	56.599ºE	0	23.7		2.10
71.07.02	Globe-4	2.3	542	67.283ºN	63.467ºE	0.2-1						

Table 1. Continued

71.07.10	Globe-3	2.3	465	64.167ºN	55.267ºE	0.2-1						
71.09.19	Globe-1	2.3	610	57.508ºN	42.643ºE	0.2-1						2.11
71.10.04	Globe-2	2.3	595	61.358ºN	48.092ºE	0.2-1	61.3593	48.0931				2.12
71.10.22	Sapphire-1	15	1140	51.60ºN	54.45ºE	10	51.5862°N	54.6150°E	0	11.5	Hole E-2	2.13
71.12.22	Azgir A-3-1	64	986	47.897ºN	48.133ºE	0.2-1	47.8980ºN	48.1298ºE	0	0.16		2.4
72.04.11	Crater	15	1720	37.35ºN	62.05ºE	10	37.4158ºN	62.0508ºE	0	7.31		2.14
72.07.09	Fakel	3.8	2483	49.80ºN	35.40ºE	10	49.552ºN	35.471ºE	0	28		2.15
72.08.20	Region-3	6.6	489	49.400ºN	48.142ºE	0.2-1	49.4169ºN	48.16155ºE	0	2.35	GPS	2.16
72.09.04	Dnepr-1	2.1	131	67.75ºN	33.10ºE	10	67.782ºN	33.618ºE	1	22		2.17
72.09.21	Region-1	2.3	485	52.118ºN	52.068ºE	0.2-1	52.1404ºN	52.0929ºE	0	3.0		2.18
72.10.03	Region-4	6.6	485	46.853ºN	44.938ºE	0.2-1						
72.11.24	Region-2	2.3	675	51.990ºN	51.867ºE	0.2-1	51.9933ºN	51.8826ºE	0	1.13		2.19
72.11.24	Region-5	6.6	423	51.842ºN	64.21ºE	0.2-1	51.8415ºN	64.21248ºE	0	0.18	GPS	2.20
73.08.15	Meridian-3	6.3	600	42.775ºN	67.408ºE	0.2-1	42.7740ºN	67.40695ºE	0	0.14	GPS	2.21
73.08.28	Meridian-1	6.3	395	50.527ºN	68.323ºE	0.2-1	50.5279ºN	68.32127ºE	0	0.16	GPS	2.22
73.09.19	Meridian-2	6.3	615	45.758ºN	67.825ºE	0.2-1	45.7588ºN	67.82289ºE	0	0.19	GPS	2.23
73.09.30	Sapphire-2	10	1145	51.65ºN	54.55ºE	10	51.6052°N	54.5991°E	0	6.0	Hole E-3	2.13
73.10.26	Kama-2	10	2026	53.65ºN	55.4ºE	10	53.5615ºN	55.51436ºE	0	12.4		2.24
74.07.08	Kama-1	10	2123	53.70ºN	55.10ºE	10	53.4097ºN	55.6387ºE	0	48.1		2.25
74.08.14	Horizon-2	7.6	534	68.903ºN	75.823ºE	0.2-1						
74.08.29	Horizon-1	7.6	583	67.085ºN	62.625ºE	0.2-1						
74.10.02	Crystal	1.7	98	66.10ºN	112.65ºE	10	66.4573ºN	112.3989ºE	0	41.4		2.26
74.12.07	Lazulite	1.7	75	49.90ºN	77.65ºE	10						
75.04.25	Azgir A-2-2	0.35	600	47.909ºN	47.912ºE	0.2-1	47.9071ºN	47.9105ºE	0	0.23	GPS - IGR	2.4
75.08.12	Horizon-4	7.6	496	70.763ºN	126.953ºE	0.2-1	70.7636ºN	126.9518ºE	0	0.1		2.27
75.09.29	Horizon-3	7.6	834	69.578ºN	90.337ºE	0.2-1	69.5831ºN	90.3179ºE	0			2.28
76.03.29	Azgir A-3-2	10	986	47.897ºN	48.133ºE	0.2-1	47.8980ºN	48.1298ºE	0	0.16		2.4

Table 1. Continued

76.07.29	Azgir A-4	58	1000	47.870ºN	48.150ºE	0.2-1	47.871ºN	48.138ºE	0	0.93		2.4
76.11.05	Oka	15	1522	61.458ºN	112.860ºE	0.2-1	61.4608ºN	112.8592ºE	1	0.30	Hole 42	
77.07.26	Meteorite-2	15	850	69.575ºN	90.375ºE	0.2-1	69.5867ºN	90.3420ºE	0			2.29
77.08.10	Meteorite-5	8.5	494	50.955ºN	110.983ºE	0.2-1						
77.08.20	Meteorite-3	8.5	600	64.108ºN	99.558ºE	0.2-1						
77.09.10	Meteorite-4	7.6	550	57.251ºN	106.551ºE	0.2-1	57.2583ºN	106.5565ºE	0	0.88		
77.09.30	Azgir, A-5	10	1500	47.897ºN	48.161ºE	0.2-1	47.888ºN	48.153ºE	0	1.12		2.4
77.10.14	Azgir A-2-3	0.1	600	47.909ºN	47.912ºE	0.2-1	47.9071ºN	47.9105ºE	0	0.23	GPS - IGR	2.4
77.10.30	Azgir A-2-4	0.01	600	47.909ºN	47.912ºE	0.2-1	47.9071ºN	47.9105ºE	0	0.23	GPS - IGR	2.4
78.08.09	Kraton-4	22	567	63.678ºN	125.522ºE	0.2-1	63.6773ºN	125.5266ºE	0	0.24		2.30
78.08.24	Kraton-3	22	577	65.925ºN	112.338ºE	0.2-1	65.9254ºN	112.3330ºE	0	0.2		2.31
78.09.12	Azgir A-2-5	0.08	600	47.909ºN	47.912ºN	0.2-1	47.9071ºN	47.9105ºE	0	0.23	GPS - IGR	2.4
78.09.21	Kraton-2	15	886	66.598ºN	86.210ºE	0.2-1	66.5887ºN	86.1828ºE	0	1.59		
78.10.08	Vyatka	15	1545	61.55ºN	112.85ºE	10	61.5565ºN	112.9922ºE	1	7.6	Hole 43	
78.10.17	Azgir A-7	18+56	1040, 970	47.850ºN	48.120ºE	0.2-1	47.8467ºN	48.1204ºE	0	0.24	GPS - IGR	2.4
78.10.17	Kraton-1	22	593	63.185ºN	63.432ºE	0.2-1						
78.11.30	Azgir A-2-6	0.06	600	47.909ºN	47.912ºE	0.2-1	47.9071ºN	47.9105ºE	0	0.23	GPS - IGR	2.4
78.12.18	Azgir A-9	103	630	47.860ºN	48.160ºE	0.2-1	47.857ºN	48.161ºE	0	0.35		2.4
79.01.10	Azgir A-2-7	0.5	600	47.909ºN	47.912ºE	0.2-1	47.9071ºN	47.9105ºE	0	0.23	GPS - IGR	2.4
79.01.17	Azgir A-8	12.5+56	995, 934	47.920ºN	48.120ºE	0.2-1	47.9187ºN	48.1238ºE	0	0.32	GPS-IGR	2.4
79.07.14	Azgir A-11	21	849, 916, 982	47.880ºN	48.120ºE	0.2-1	47.8819ºN	48.1201ºE	0	0.22	GPS - IGR	2.4
79.08.12	Kimberlite-4	8.5	982	61.803ºN	122.430ºE	0.2-1	61.7997ºN	122.4161ºE	0	0.8		2.32
79.09.06	Kimberlite-3	8.5	599	64.110ºN	99.562ºE	0.2-1						
79.09.16	Cleavage	0.3	903	48.2ºN	38.3ºE	-	48.214oN	38.284oE	0	2		2.33
79.10.04	Kimberlite-1	22	837	60.675ºN	71.455ºE	0.2-1						
79.10.07	Sheksna	15	1545	61.85ºN	113.1ºE	10	61.7679ºN	113.1554ºE	0	9.6	Hole 47	
79.10.24	Azgir A-10	33	915, 980	47.850ºN	48.140ºE	0.2-1	47.852ºN	48.143ºE	0	0.36		2.4

Table 1. Continued

80.06.16	Butane-2-1	3.2	1400	52.9ºN	56.5ºE	-					Hole 1	2.32
80.06.25	Butane-2-2	3.2	1390	52.9ºN	56.5ºE	-					Hole 2	2.32
80.10.08	Vega	8.5	1050	46.757ºN	48.275ºE	0.2-1	46.7565ºN	48.2738ºE	0	0.11	Hole 1T	2.35
80.11.01	Batholith-1	8	720	60.80ºN	97.55ºE	10						
80.12.10	Angara	15	2485	61.75ºN	66.75ºE	10	61.7088ºN	67.0710ºE	0	18		2.36
81.05.25	Pyrite	37.6	1511	68.20ºN	53.50ºE	10						
81.09.02	Helium-1	3.2	2088	60.60ºN	55.70ºE	10	60.2751ºN	57.2991ºE	0	95	Hole 401	2.37
81.09.26	Vega 2-1	8.5	1050	46.790ºN	48.313ºE	0.2-1	46.7936ºN	48.3088ºE	0	0.52	Hole 2T	2.35
81.09.26	Vega 2-2	8.5	1050	46.771ºN	48.304ºE	0.2-1	46.7760ºN	48.3012ºE	0	0.59	Hole 4T	2.35
81.10.22	Shpat-2	8.5	581	63.80ºN	97.55ºE	10						Appendix B
82.07.30	Rift-3	8.5	554	53.80ºN	104.15ºE	10	53.7696ºN	104.1048ºE	0	4.52		2.38
82.09.04	Rift-1	16	960	69.20ºN	81.65ºE	10						
82.09.25	Rift-4	8.5	554	64.35ºN	91.80ºE	10						Appendix B
82.10.10	Neva-1	15	1502	61.55ºN	112.85ºE	10	61.5006ºN	112.9110ºE	1	6.4	Hole 66	
82.10.16	Vega 3-1	8.5	947	46.759ºN	48.247ºE	0.2-1	46.7582ºN	48.2447ºE	0	0.20	Hole 3T	2.35
82.10.16	Vega 3-2	8.5	991	46.752ºN	48.258ºE	0.2-1	46.7494ºN	48.2569ºE	0	0.30	Hole 5T	2.35
82.10.16	Vega 3-3	8.5	1100	46.766ºN	48.288ºE	0.2-1	46.7688ºN	48.2858ºE	0	0.36	Hole 6T	2.35
82.10.16	Vega 3-4	13.5	1057	46.760ºN	48.300ºE	0.2-1	46.7597ºN	48.2987ºE	0	0.10	Hole 7T	2.35
83.07.10	Lira 1-1	15	907	51.363ºN	53.306ºE	0.2-1	51.3627ºN	53.3055ºE	1	0.04	Hole 1	2.39
83.07.10	Lira 1-2	15	917	51.367ºN	53.327ºE	0.2-1	51.3660ºN	53.3258ºE	1	0.14	Hole 2	2.39
83.07.10	Lira 1-3	15	841	51.380ºN	53.340ºE	0.2-1	51.3802ºN	53.3386ºE	2	0.09	Hole 3	2.39
83.09.24	Vega 4-1	8.5	1050	46.783ºN	48.315ºE	0.2-1	46.7812ºN	48.3197ºE	0	0.41	Hole 8T	2.35
83.09.24	Vega 4-2	8.5	1050	46.788ºN	48.297ºE	0.2-1	46.7872ºN	48.2966ºE	0	0.09	Hole 9T	2.35
83.09.24	Vega 4-3	8.5	920	46.767ºN	48.310ºE	0.2-1	46.7671ºN	48.3079ºE	0	0.16	Hole 10T	2.35
83.09.24	Vega 4-4	8.5	1100	46.749ºN	48.303ºE	0.2-1	46.7500ºN	48.3006ºE	0	0.21	Hole 11T	2.35
83.09.24	Vega 4-5	8.5	950	46.754ºN	48.289ºE	0.2-1	46.7538ºN	48.2877ºE	0	0.16	Hole 12T	2.35
83.09.24	Vega 4-6	8.5	1100	46.766ºN	48.274ºE	0.2-1	46.7657ºN	48.2740ºE	0	0.03	Hole 13T	2.35
84.07.21	Lira 2-1	15	846	51.358ºN	53.319ºE	0.2-1	51.3584ºN	53.3196ºE	1	0.07	Hole 4	2.39

Table 1. Continued

84.07.21	Lira 2-2	15	955	51.371ºN	53.337ºE	0.2-1	51.3717ºN	53.3355ºE	3	0.12	Hole 5	2.39
84.07.21	Lira 2-3	15	844	51.391ºN	53.351ºE	0.2-1	51.3917ºN	53.3495ºE	2	0.12	Hole 6	2.39
84.08.11	Quartz-2	8.5	759	65.05ºN	55.10ºE	10						
84.08.25	Quartz-3	8.5	726	61.90ºN	72.10ºE	10						Appendix B
84.08.27	Dnepr-2	1.7X2	175	67.75ºN	33.00ºE	10	67.782ºN	33.618ºE	1	26		2.17
84.08.28	Helium 2-1	3.2	2065	60.30ºN	57.10ºE	10	60.2695ºN	57.2838ºE	0	11	Hole 402	2.37
84.08.28	Helium 2-2	3.2	2075	60.70ºN	57.50ºE	10	60.2840ºN	57.2840ºN	0	48	Hole 403	2.37
84.09.17	Quartz-4	10	557	55.834ºN	87.526ºE	0.2-1	55.8208	87.5058	0	1.9		2.40
84.10.27	Vega 5-1	3.2	1000	46.90ºN	48.15ºE	10					Hole 14T	2.35
84.10.27	Vega 5-2	3.2	1000	46.95ºN	48.10ºE	10					Hole 15T	2.35
85.06.18	Benzene	2.5	2860	60.6ºN	72.7ºE	-					In oil field	
85.07.18	Agate	8.5	772	65.994ºN	41.038ºE	0.2-1						
87.04.19	Helium 3-1	3.2	2015	60.60ºN	57.20ºE	10	60.260ºN	57.263ºE	0	39	Hole 404	2.37
87.04.19	Helium 3-2	3.2	2055	60.80ºN	57.50ºE	10	60.2609ºN	57.2981ºE	0	61	Hole 405	2.37
87.07.07	Neva 2-1	15	1502	61.50ºN	112.85ºE	10	61.4317ºN	112.8860ºE	1	7.8	Hole 68	
87.07.24	Neva 2-2	15	1515	61.45ºN	112.80ºE	10	61.4172ºN	112.8927ºE	1	6.1	Hole 61	
87.08.12	Neva 2-3	3.2	815	61.45ºN	112.80ºE	10	61.4266ºN	112.8879ºE	1	5.4	Hole 101	
87.10.03	Batholith-2	8.5	1002	47.60ºN	56.20ºE	10					Site Visit	2.41
88.08.22	Ruby-2	15	829	66.280ºN	78.491ºE	0.2-1	66.2809	78.4897	0	0.12		2.42
88.09.06	Ruby-1	8.5	820	61.361ºN	48.092ºE	0.2-1						

2. RESULTS

2.1. CHAGAN – 15 January 1965

Chagan was the first official PNE to occur in the Soviet Union, took place at the test site in Kazakhstan, and was intended to produce a crater. The crater was subsequently flooded and is now called Atomic Lake. The crater is clearly visible on Google Earth imagery and is essentially at the coordinates published in Sultanov et al. (1999; Figure 2). The Chagan PNE is also the subject of a short Soviet documentary film that is available at http://www.youtube.com/watch?v=ZAoSUIASET0 in Russian.

Figure 2. Google Earth image of the crater formed from the Chagan PNE. The blue point represents the coordinates as published in Sultanov et al. (1999).

2.2. BUTANE 1-1 and 1-2 – 30 March 1965 (Butane 1-1), 10 June 1965 (Butane 1-2)

The Butane 1-1 and 1-2 PNEs were conducted for oil stimulation in the Grachevka oil reservoir, 150 km N Orenburg, Bashkiria. Butane 1-1 was composed of two simultaneous 2.3 kt explosions 200 m apart at depths of 1375 and 1341 m (Nordyke, 2000). Yablokov (2003) and Mikhailov (1994) give the location as 40 km east of Meleuz (wells 617, 618, 622), but no coordinates.

Butane 1-2 was detonated at 1350 m depth, 350 m west of Butane 1-1. Grachevka 2, hole 622 (Nordyke, 2000; Mikhailov, 1999). Nordyke (2000) gives the same coordinates as for Butane 1-1.

A series of Russian reports place the explosions in the region of New Kazanovka (Popular Mechanics, Grek, 2006), near Meleuz (Figure 3). Several villages were evactuated (Kolpakov and Momot, 2008). Bulatov (1996) cites the detonations as being near Lipovka (settlement located at 53.0616^{o}N x 55.8162^{o}E), which is east of New Kazankovka (located at 53.069^{o}N x 55.6785^{o}N).

Nordyke (2000) provides relative locations as 15 km NW of Meleuz, Bashkiria, and coordinates of 53.10^{o}N x 55.87^{o}E ("based on description of site"). Sultanov et al. (1999) cite 52.9^{o}N x 56.5^{o}E, which is east of Meleuz and nowhere near the described villages.

Lipovka, as well as the village of Staryi Kazankova are 15 km from Meleuz; the Nordyke (2000) coordinates are 17.5 from Meleuz.

Based on the descriptions, this PNEs are clearly located somewhere in the general area of Figures 3 and 4. Three possible areas are denoted on Figure 4: 1) a small area of disturbed ground mid-way between Lipovka and Novy Kazankova (Butane-1A, 53.059^{o}N, 55.751^{o}E) about 17 km from Meleuz, 2) a petroleum facility north of Lipovka with a prominent circular area, which could also be a pad for a gas flare tower, (Butane-1B, 53.078^{o}N x 55.830^{o}E) 16 km from Meleuz, and 3) a gas field (Figure 5) north of Lipovka (around 53.11N x 55.85E), about 20 km from Meleuz. Without further information, this event cannot be located with any better precision, but options 2 and 3 look promising, but with an error of 5-6 km. There are additional oil fields in the area.

No instrumental data are reported in the ISC Bulletin. The coordinates used by Sultanov et al. for both Butane 1 and 2 are 38.5 km east of Meleuz and fit the description given in Yablokov (2003) and Mikhailov (1994). The area appears to be barren of any oil drilling activity, although there is clearly industrial activity around Yumaguzino 7.5 km to the west (Figures 6 and 7).

Instrumental data, and the Sultanov et al. (1999) coordinates, are from the GS RAS (2001), and is limited, especially for Butane-1 events. The only relatively "close" station for Butane 1-1 and 1-2 is Ekaterinburg (SVE), approximately 500 km away. The second closest station is MHV located near Moscow about 1200 km away. Ekaterinburg is essentially equidistant from both the Sultanov et al. (1999) coordinates and the sites northwest of Meleuz and cannot be used as a discriminant. For Butane 1-1 and 1-2, the average travel time to SVE is 1 min 12.75 sec for Pn or 4.62° (514 km). The Sultanov et al. (1999) coordinates are 511 km and the Butane 1B and 1C locations of Figure 2 cited above are 514-518 km from SVE. This means a difference of about 0.4 sec or probably within reading error of the time. All distances calculated using J-B tables.

The only other station with P arrivals for Butane-1 events is MHV (Mikhenovo Observatory) near Moscow. The average P time for MHV for Butane 1-1 and 1-2 is 2 min 35.65 sec or 10.56° (1175 km). The Sultanov et al. (1999) location is 1247 km from MHV and the locations cited above are 1198-1199 km. The residual for the latter locations is about 2.9 sec while the Sultanov et al. (1999) have a residual of 8.9 sec., thus for both cases, the locations northwest of Meleuz fit the seismic data equally or better.

We attempted to constrain the locations of the Butane-1 and Butane-2 PNEs using calibrated relocation analysis using a regional cluster of PNEs that included the Butane sequence (Appendix A). Unfortunately, the attempt was not successful for the Butane sequence, likely due to insufficient arrival times.

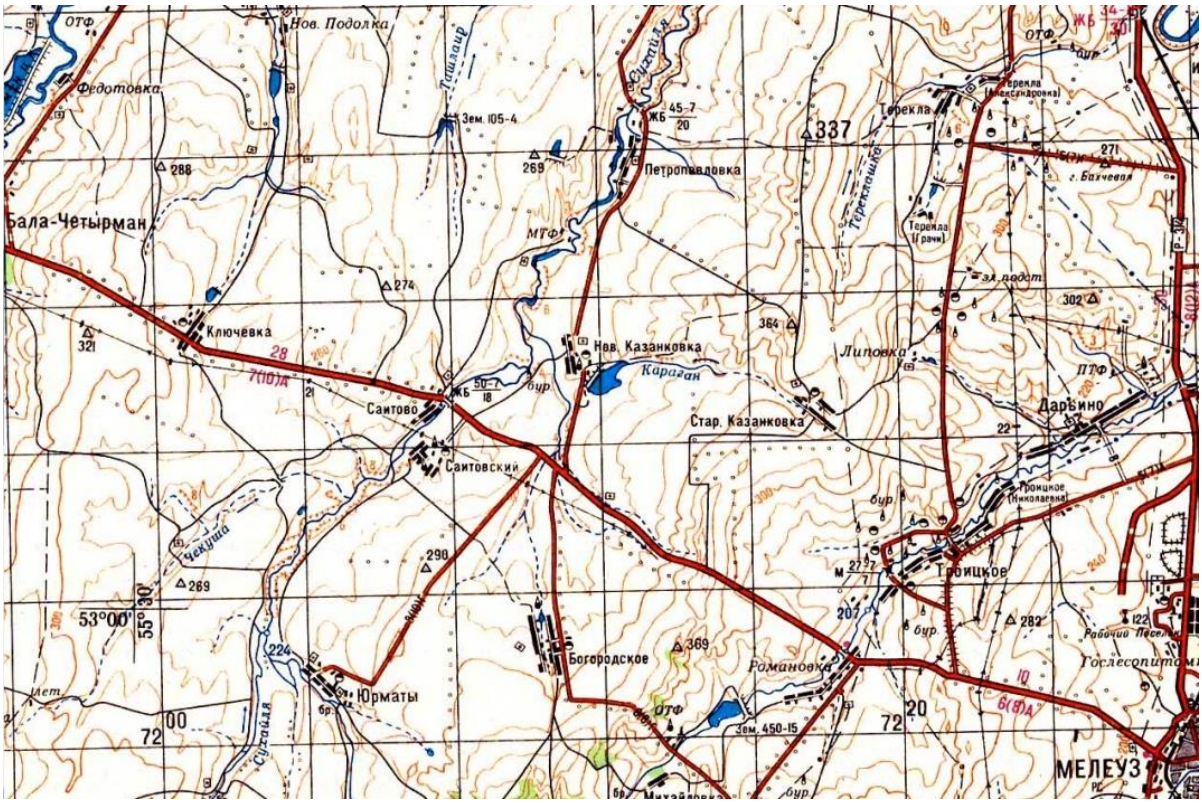

Figure 3. Soviet 1:200,000 base topographic map of the area around Novo Kazanovka and Lipovka, northwest of Meleuz.

Figure 4. Area around Lipovka where Butane 1-1 and Butane 1-2 probably occurred with three possible sited (1A, 1B, and 1C) and the Nordyke (2000) location (Nor But-1). Google Earth Image © 2013 Digital Globe, Landsat.

Figure 5. Oil Field (Grachevka?) near Nordyke (2000) coordinates. Site 3 in text and Butane-1C in Figure 4. Google Earth Image © 2013 Digital Globe.

Figure 6. Yumaguzino and vicinity showing Sultanov et al. (1999) coordinates for Butane 1 (all events) and 2 (both events). Google Earth Image © 2013 Digital Globe, Landsat.

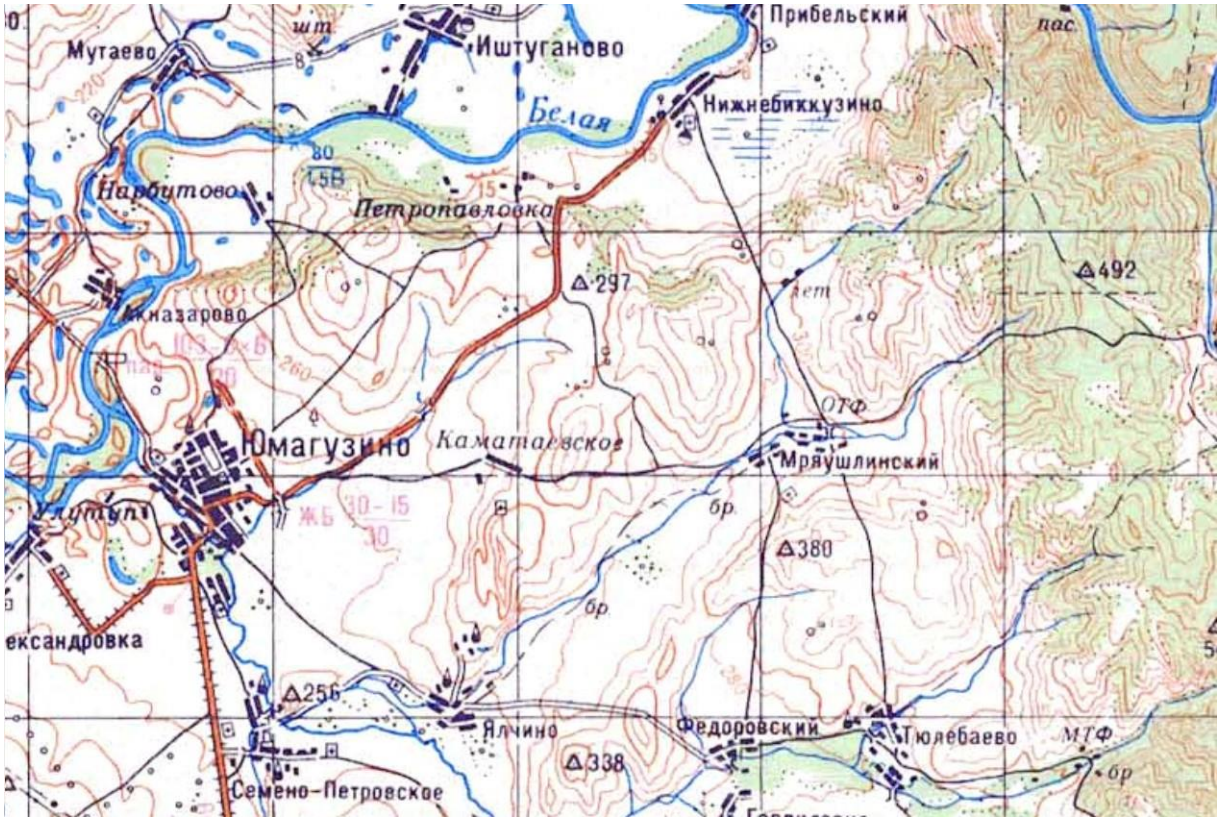

Figure 7. Fragment of 1:200,000 base map of Yumaguzino and vicinity.

2.3. SARY-UZEN – 14 October 1965

Sary-Uzen was the 4th PNE to have been detonated in the Soviet Union and like Chagan, was an excavation explosion. The Sultanov et al. (1999) coordinates for this PNE are good, and fall just inside the rim of the crater, thus our revision to 49.9911°N x 77.6351°E is minor, shifting the location about 70 m. A good high resolution satellite image of the crater is available at www.maps.ovi.com and is shown below in Figure 8.

Figure 8. High resolution satellite image of the Sary-Uzen PNE excavation crater from www.maps.ovi.com. The Sultanov et al. (1999) coordinates fall on the right edge of the crater, which has a diameter of about 150 m.

2.4. AZGIR SEQUENCE – 22 April 1966 – 14 July 1979

The Azgir sequence consisted of 17 PNEs in western Kazakhstan between 1966 and 1979 (Figure 9; Table 1). Some of the PNEs consisted of 2 or 3 devices in the same hole detonated simultaneously. All Azgir PNEs are listed as GT0-1 by Sultanov et al. (1999). Careful examination of Google Earth and Bing Maps satellite imagery revealed that in close proximity to each of the Azgir A-2 through A-11 explosions is an area of disturbed ground with a circular fenced area between about 40 to 80 m in diameter (Figure 10), which we interpret to be the borehole locations. Azgir A-9 is an exception in that a circular lake is present. We also note that relocating these PNEs to the circular structures, the distribution of events becomes constrained to a systematic grid pattern of detonation locations, with many events lining up with each other. From this, we are confident that we can consider Azgir A-2 through A-11 to be GT-0 locations. This also verifies the GT0-1 location quality of Sultanov et al. (1999) for these events. Only Azgir A-5 was moved slightly more at 1.12 km. A fairly detailed map of the Azgir test site is available at http://wikimapia.org/6013134/Nuclear-test-site-Azgir that constrains the specific areas of disturbance and PNE location to within tens of meters, and is consistent with our results for Azgir A-2 through A-11. However, we note that the original source of the information on the wikimapia.org site is unknown. The Institute of Geophysical Research of Kazakhstan (IRG) provided an additional set of coordinates using GPS measurements for Azgir A-1, A-2, A-7, A-8 and A-11.

The Azgir A-1 event is more problematic as a similar ring structure is not visible, though the Sultanov et al. (1999) location is in near proximity to areas of disturbed ground. However, the GPS coordinates provided by the IGR fall within a weakly visible square fenced area on Bing Maps imagery. The IGR also provided a photo of the Azgir A-1 location (Figure 11).

The Azgir A-3-X sequence is relocated to a small area of disturbed ground about 250 m west of the Sultanov et al. (1999) location that places it exactly on a linear trend that connects the Azgir A-4, A-8, and A-10 explosions. At this location, there appears to be two small dome structures that we speculate may be associated with the two PNEs conducted at the Azgir A-3 site. However, we note that the Azgir test site map identifies two regions for Azgir A-3-X, with the second being about 500 m southeast of the first that we identified above. As the Azgir test site map seems to outline the entire area of infrastructure of each test location, we interpret this second area to be part of the Azgir A-3 site, but not necessarily the location of boreholes. There is no evidence of a fence at this location. The Sultanov et al. (1999) location is approximately midway between the two.

An area of disturbance that appears similar in character to the PNE detonation sites is also visible at coordinates 47.8643^{o}N x 48.1141^{o}E. This location falls on the geographical grid of detonation locations. The GPS location table of Azgir experimental boreholes provided by the Institute of Geophysical Research in Kazakhstan identifies this site as Azgir-12. We hypothesize that Azgir A-12 represents the site of a planned, but not conducted, explosion. As apparent on Figure 10, a rectangular structure is clear at the center of the Azgir-11 ring, and visible to a lesser extent in the Azgir-10 ring. A similar structure is also present on the ground at 47.853^{o}N x 48.135^{o}E. It is not clear to us what this site represents, but we can speculate that it also may have been the site of a planned experiment.

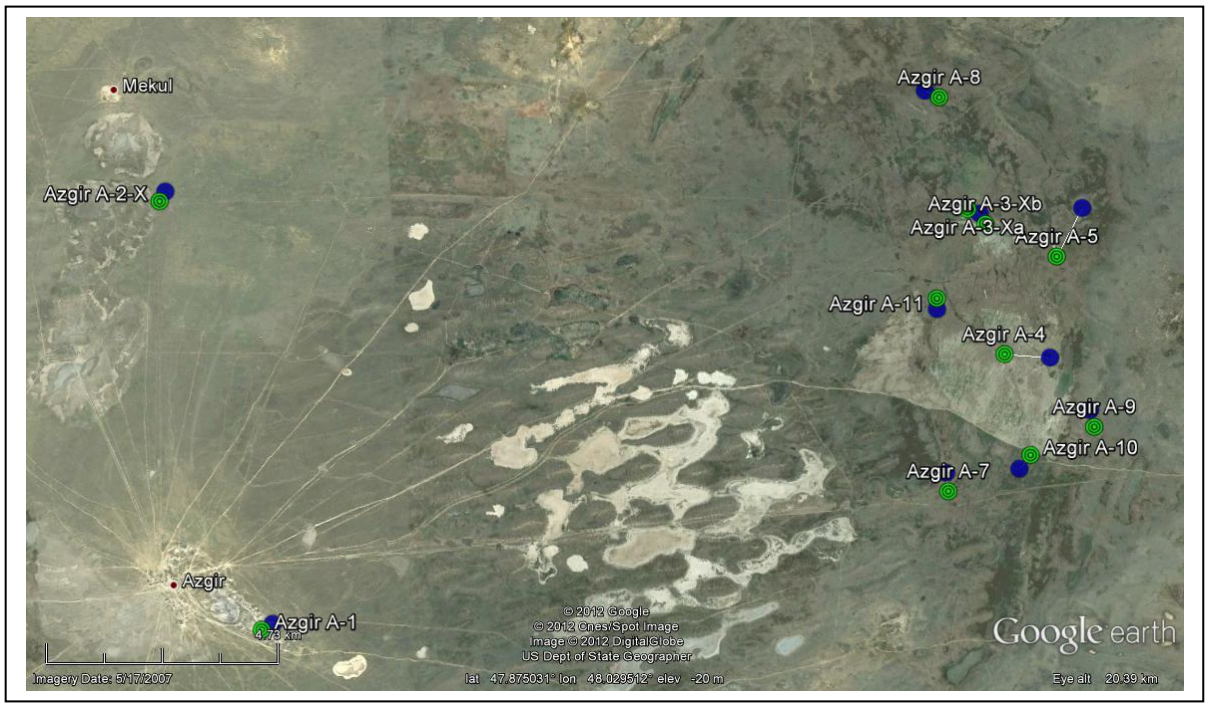

Figure 9. The Azgir test site. Blue points represent locations from Sultanov et al. (1999) and green this report. See Table 1 for coordinates. Image from Google Earth.

Figure 10. Google Earth images of the Azgir A-10 and A-11 sites showing the typical ring or presumed fence that we interpret as enclosing the borehole locations for the Azgir tests.

Figure 11. Borehole photo of Azgir A-1. Photo complements of the Institute of Geophysical Research, Kazakhstan.

2.5. URTABULAK – 30 September 1966

The Urtabulak PNE took place on 30 September, 1966, in Uzbekistan for the purpose of extinguishing a gas well fire. Two short Soviet era documentary films of the PNE available on Youtube at http://www.youtube.com/watch?v=ord-AyaFLaA in Russian and https://www.youtube.com/watch?v=4iB9QYaSVEo&feature=youtu.be in English. Both films show a variety of scenes of work to extinguish the gas well fire as well as preparation, detonation of the PNE, and aftereffects. The English language film includes some scenes with a site overview that allow comparison to satellite imagery to verify the location.

From the videos, we were able to identify and correlate three reference points and two other boreholes with satellite imagery (Figures 12 and 13). We believe that the three reference points are sites of mud and gas blowouts drilled to redirect subsurface pressure. They are visible in the above videos.

Additional film of the Urtabulak PNE detonation and location in found in the video at https://www.youtube.com/watch?v=XUaSGpHNqlk.

The Urtubulak PNE location was used as a calibration location to help constrain the locations of the Pamuk and Crater PNEs (Appendix B).

Figure 12. Composite image from video screenshots shows a site overview of the Urtabulak well fire. Note that the location is inside a large circular berm. Labeled reference points and boreholes are correlate with Figure 13.

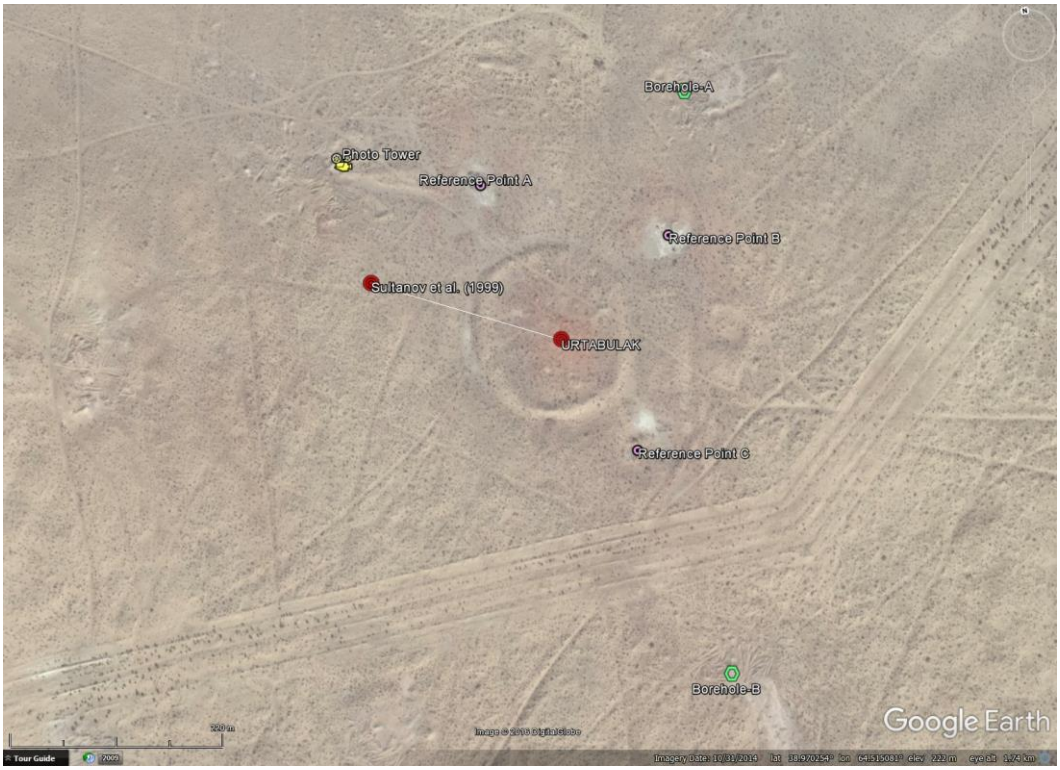

Figure 13. Satellite image showing the circular berm at the Urtabulak PNE site. Labeled reference points and boreholes are correlate with Figure 12. Google Earth Image © 2016 Digital Globe.

2.6. PAMUK – 21 May 1968

Pamuk was a larger PNE at 47 kt that was detonated in southern Uzbekistan about 10 km south of the village of Pamuk. The PNE was detonated in hole 2-R of the Pamuk gas field and successfully extinguished a gas well fire (Nordyke, 2000). Details of the experiment and drilling are summarized by Nordyke (2000).

The Sultanov et al. (1999) location for Pamuk corresponds to a geographic area of disturbance that is associated with an oil field. Our initial verification of this location was to conduct a relative location analysis of Pamuk clustered with the known location of Urtabulak. From this analysis, detailed in Appendix B, we conclude that the Sultanov et al. (1999) location is essentially accurate to the extent that the borehole is within the area of disturbance at the site. However, we can not identify the specific borehole location, thus we assign Pamuk a GT-1 accuracy. An overview of the Pamuk PNE site is shown in Figure 14.

Figure 14. Satellite image showing the site of the Pamuk PNE. Our analysis is consistent with the PNE location as being within the regions of disturbance. As we are unable to identify the specific borehole, we accept the Sultanov et al. (1999) coordinates and assign GT-1 accuracy. Google Earth Image © 2016 Digital Globe.

2.7. TELKEM-1 and TELKEM-2 – 21 October 1968 and 12 November 1968

Telkem-1 and Telkem-2 were both excavation explosions occurring at the test site in Kazakhstan. Telkem-2 was three simultaneous detonations spaced 40 m apart. The Sultanov et al. (1999) coordinates for both Telkem-1 and Telkem-2 fall within the lakes in the craters. Good satellite images are available from www.yandex.ru and are shown below in Figures 15 and 16.

Figure 15. Satellite image from www.yandex.ru for the Telkem-1 PNE excavation crater.

Figure 16. Satellite image from www.yandex.ru for the Telkem-2 PNE excavation crater.

2.8. MANGYSHLAK-1, -2, and -3 - 6 December 1969, and 12 and 23 December 1970

The Mangyshlak Peaceful Nuclear Explosion (PNE) sequence consisted of three detonations in western Kazakhstan in 1969 and 1970. The locations and site verifications described here fully described in Mackey and Bergman (2014). An examination on Google Earth of the locations reported by Sultanov et al. (1999) for the Mangyshlak sites does not reveal the presence of collapse craters or other clear evidence of PNE detonations. The Mangyshlak-1 (Man-1) and Mangyshlak-2 (Man-2) are in non-descript locations in the desert, while Mangyshlak-3 (Man-3) appears to coincide with an animal watering hole at the center of many radial paths that is similar to other features common in the area.

A closer examination of the surrounding land surface reveals two collapse crater structures, one 2.3 km west of the Sultanov et al. (1999) location for Man-1, and one 6.7 km north of the Sultanov et al. (1999) location for Man-2 (Figure 17). The collapse structures were identified by topography and general appearance of the structure on the satellite imagery. Both collapse structures are several meters deep, show what appear to be localized radial cracks, as well as weakly visible collapse structures around the edges of the depression. There is no similar collapse structure in the vicinity of the Sultanov et al. (1999) location for Man-3.

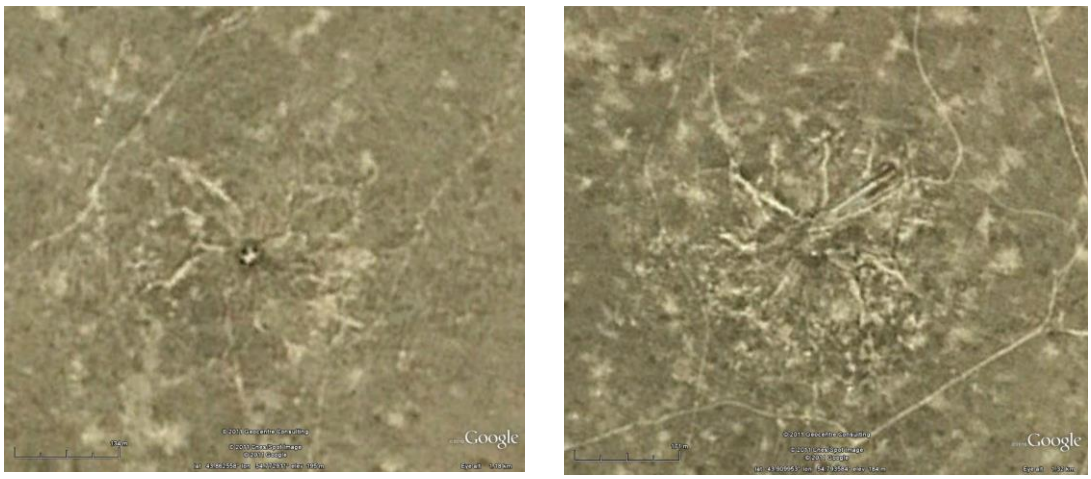

Figure 17. Google Earth images of collapse craters associated with Man-1 (left) and Man-2 (right).

The fact that neither collapse structure is within 1 kilometer of any previously indicated location leads to two conclusions. First, the presumed GT-1 or better accuracy of Sultanov et al. (1999) for the Man-1 location is in error. Secondly, it is not clear which collapse structure corresponds to which PNE. The correct association of the craters becomes more confusing when considering published comments on which Mangyshak PNEs generated collapse craters. Podvig (2001) states that no collapse crater was created by Man-2, thus if this information is correct, the southern collapse crater, based on distance alone, would associate with Man-1 and the northern with Man-3. Nordyke (2000) indicates that it was Man-3 that did not generate a collapse crater, which further confuses the association of events to craters. Nevertheless, the northern collapse structure is approximately 400 m in diameter, and the southern 200 m in diameter. Presumably, the smaller southern crater would be associated with the smaller PNE, which is Man-1 at 30 kt, and the larger crater with either Man-2 or Man-3 at 80 and 75 kt respectively. Nordyke (2000) lists the depth of Man-3 as 740 m, with a greater scaling depth relative to yield than Man-1 or Man-2, and this may be justification for assuming that there was no collapse crater from Man-3.

To better associate the Mangyshlak PNEs with the correct collapse craters, we conducted a multiple event relocation analysis with the three explosions to determine their relative locations. The relocation was done with a version of the Hypocentroidal Decomposition method (Jordan and Sverdrup, 1981) that has been highly developed for application in calibrated location studies (e.g., Walker et al., 2011). This analysis was done using a merged dataset of phases and picks from the local and regional Soviet networks as well as those available from the ISC. For the relocations, the parameters from Sultanov et al. (1999) were used as a starting point (stars in Figure 18). The two x's near Man-1 and Man-2 are the locations of two collapse craters. The solid vector shows how the relative locations of the events changed during the first part of the relocation, in which all available readings were used to estimate improved relative locations but only teleseismic P arrivals (using the ak135 velocity model) to establish the absolute location. In order to match the relative locations of Man-1 and Man-2 to the collapse crater locations, the cluster is shifted about 8 km ENE, which is the dashed vector for each event. The confidence ellipses for the new relative locations are all less than one kilometer.

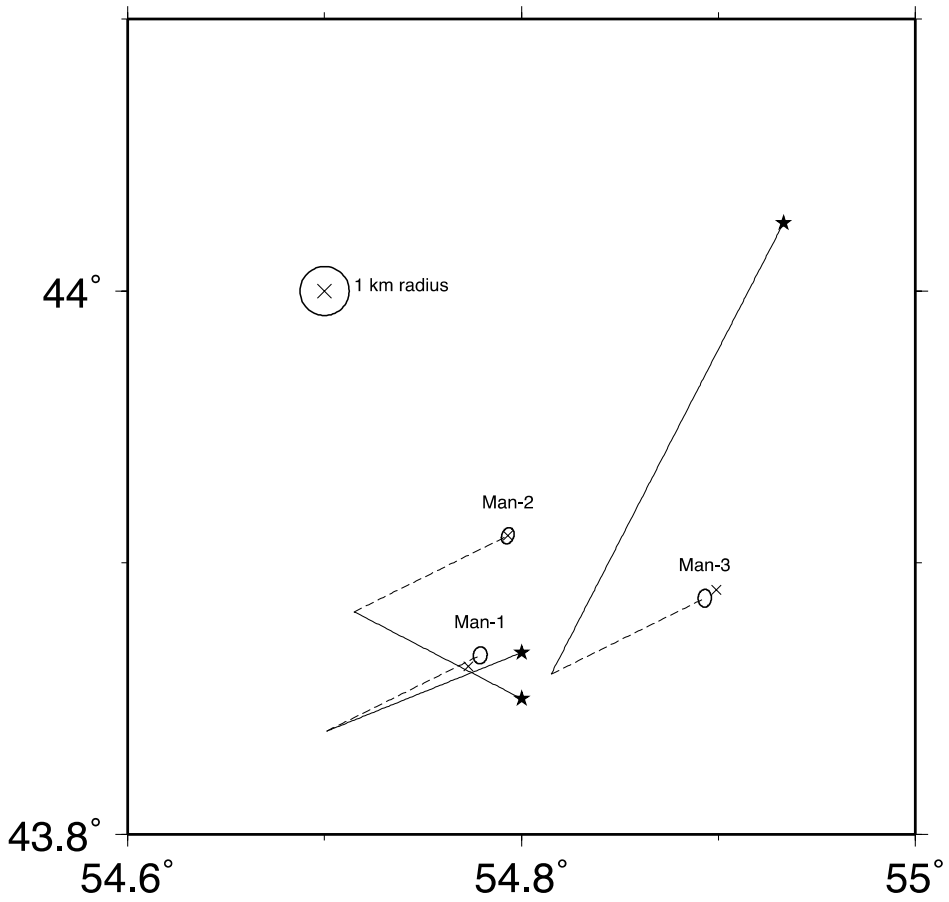

Figure 18. Relocations of the Mangyshlak PNEs. The original Sultanov et al. (1999) locations are indicated by stars and used as the starting locations in the relocation analysis. The solid black lines indicate the changes in relative locations in the relocation analysis. The absolute locations are biased because teleseismic P arrivals and a standard 1-D global travel time model were used to establish the absolute coordinates of the cluster. The dashed lines represent the single correction vector (7.0 km at N64E) needed to achieve the best fit of the cluster to the Man-1 and Man-2 collapse craters shown by the x's The ellipses represent the relative location uncertainty for each event, at the 90% confidence level. A circle of 1 km radius is shown for scale.

The relative locations allow us to say with certainty that the northern collapse crater is associated with Man-2, and the southern with Man-1. The association of the collapse craters allows us to assign GT-0 locations to both Man-1 and Man-2 with certainty (Table 1), and to ascribe errors to the Sultanov et al. (1999) locations. The error for the Man-2 location is 6.7 km, which is consistent with the Sultanov et al. (1999) confidence. However, the error for the Man-1 location, which was assigned a confidence of GT-1 or better, is actually 2.3 km.

The Sultanov et al. (1999) location for Man-3 is assigned a confidence of GT-1 or better, but does not fit with the new calculated location, which is significantly to the south. The fit to the seismic data and associated relative location with respect to the Man-1 and Man-2 locations restrict the location of Man-3 to be within one kilometer of the calibrated location. Based on apparent

disturbed ground that is similar to the appearance of other PNE detonation sites, we choose a location approximately 300 m east from the Man-3 calibrated location as a possible detonation site and a candidate site for field verification.

In July, 2013, an expedition was undertaken to field verify the three Mangyshlak PNE sites. The collapse craters from Man-1 and Man-2 are prominent in the field and both are surrounded by an extensive network of encircling fractures outside the collapse crater. The Man-1 site is quite clean and the specific borehole sites are not apparent in the bottom of the crater (Figure 19a). At the Man-2 site, the presumed central borehole is entombed in a concrete block about 3m square and one nearby instrument borehole is open. The borehole sites are surrounded by a rectangular trench and berm in the bottom of the collapse crater (Figure 19b). The Man-3 site was easily identified on the ground by the presence of several large boreholes. The borehole sites are surrounded by a rectangular trench and berm in the same manner as Man-2 (Figure 19c). Rocks dropped down one of the open instrument boreholes result in distinctive splash sounds, indicating that the instrumentation and likely the nuclear detonation was emplaced below the water table. The GPS coordinates taken in the collapse craters are essentially the same as the Google Earth determined coordinates. The location of Man-3 was coincident with the candidate site identified just east of the relative location determination. The actual error between the relative location coordinates and the GPS coordinates of the borehole is about 490m. The difference between the Sultanov et al. (1999) location and the GT0 location determined here is 15.7 km.

Figure 19. A. Collapse crater from Man-1. B. Collapse crater and infrastructure at the Man-2 site. C. Borehole locations for Man-3.

2.9. MAGISTRAL' - June 25, 1970

Dubasov et al. (2005) give explicit coordinates and a Cesium contamination sketch for Magistral', which formed a groundwater-proof cavity. The well mouth coordinates are given as 52.327°N x 55.723°E, and lie within a circular disturbed area, with similarities to that observed at the Sapphire sites (q.v.) in imagery from Yandex.ru (Figure 20) and Bing Maps (Figure 21).

The chosen site is located at 52.3265°N x 55.7238°E, about 14.2 km from Sultanov et al. (1999) location (Figure 22). This location, based on what appears to be the borehole visible on satellite imagery available from Yandex.ru and Bing Maps appears to be good and we are confident in a GT-0 location for this PNE. Additional small boreholes, perhaps for instrumentation, are visible to the north, west, and east. These coordinates are in a field to the southwest of a complex (Figure 22) labeled "gazopromysel Sovkhoznyi" (lit., Gas Scrubbing Agricultural Institute State Farm) on Soviet topographic maps (Figure 23); this PNE has been called Sovkhoznoe in other Russian papers.

Comparison of the older Yandex.ru and the newer Bing Maps images of the site show that the site is undergoing development. The newer image (Figure 21) shows an installed perimeter fence, concrete pads, possible building foundations, material storage, and a line of utility poles just south of the access road. There is also what appears to be a fluid waste pit in the southern portion of the fenced area, suggesting that drilling has occurred and/or that the explosion cavity has been re-opened. The utility poles trace back to the oil field development to the east. The overall character of the development of the site is consistent with the development and construction of a compressor station at the gas field a couple kilometers to the northeast (Figure 24). The utility poles installed to the Magistral' site also track back to the gas field. A comparison of older and more recent images of the gas field confirm development that is simultaneous with the Magistral' site.

Overall, the evidence is consistent with the Magistral site being redeveloped with the intent to use if for storage of either waste products from the gas field, or storage of gas condensate.

Figure 20. Yandex.ru imagery of Magistral' location as located by Dubasov et al. (2005). Note that there appear to be two instrument boreholes in the agricultural field, one to the north and one to the west. A third instrument borehole is visible on imagery off the figure to the east.

Figure 21. Bing Maps image of the Magistral' location. This is a more recent image and it shows that the site is under development. Note an installed perimeter fence, concrete pads, possible building foundations, material storage, and a line of utility poles just south of the access road. The utility poles trace back to the oil field development to the east.

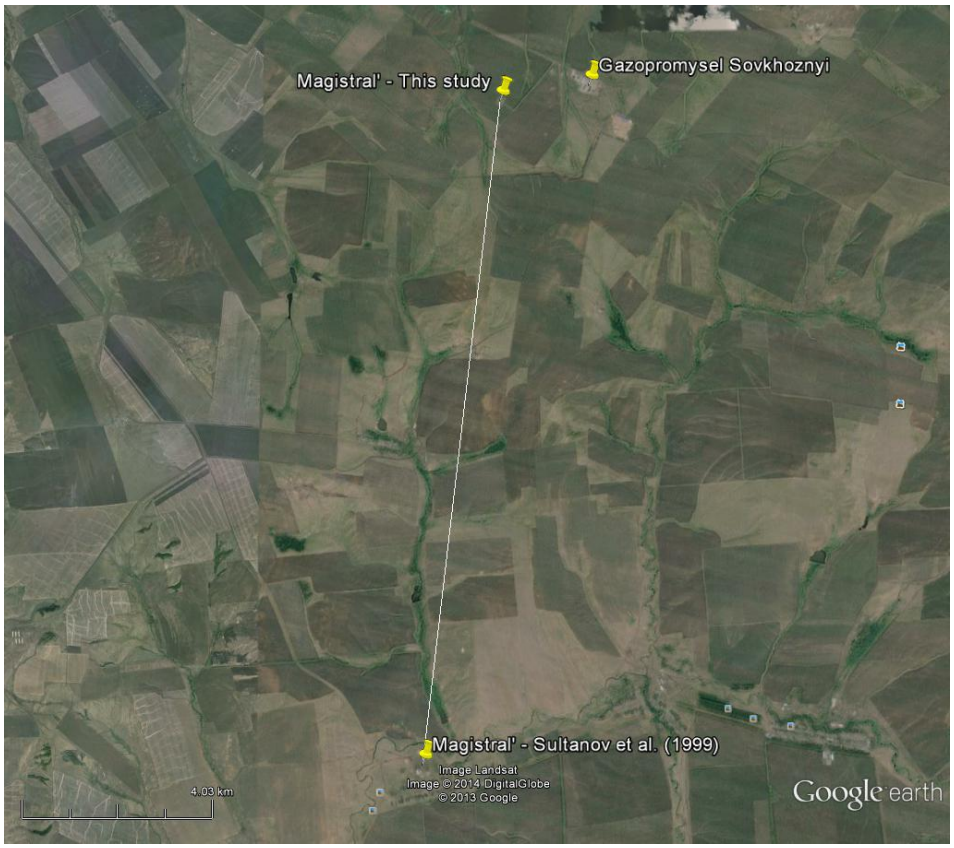

Figure 22. Google Earth image of the Magistral' locations and adjacent State Farm. Image © 2014 Digital Globe, Landsat.

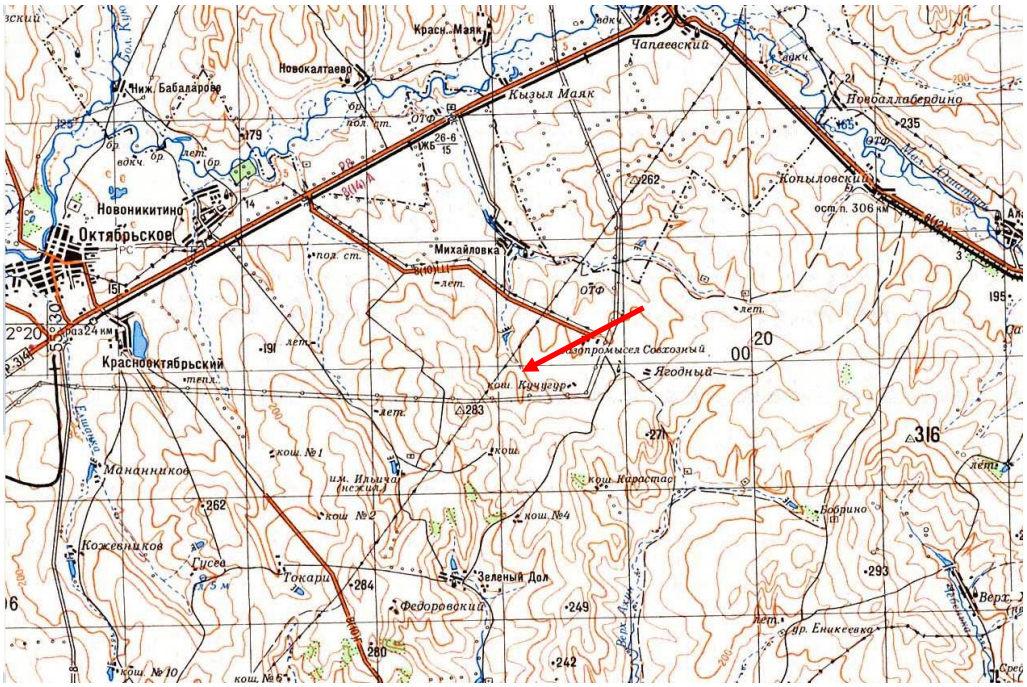

Figure 23. Fragment of Soviet 1:200,000 topographic map N-40-32 showing the Magistral' site (arrow).

Figure 24. Overview of the Magistral' site showing the PNE location at left, and the new gas compressor station at right. The older original "gazopromysel Sovkhoznyi" facility. Google Earth Image © 2016 Digital Globe.

2.10. TAIGA – 23 March 1971

The PNE 'Taiga' took place on 23 March, 1971, and was the simultaneous detonation of three 15 kt devices for the purpose of a canal building experiment. Sultanov et al. (1999) lists a location for Taiga in an isolated forest region with no apparent crater or nearby surface expression that would be expected from large excavation explosions. Ramzaev et al. (2011) and Ramzaev et al. (2012) have conducted radiological surveys of the Taiga PNE site. Both publications include maps and photos of the PNE site and an approximate location of the experiment. The excavation crater for Taiga is clearly visible on Google Earth satellite imagery as a north-south trending oblong lake approximately 600 m by 300 m in size (Figure 25).

From Google Earth imagery, the center of the lake is at 61.306°N x 56.599°E, which corresponds to the central of the three thermonuclear explosive devices. The other two devices were emplaced 165m north and 165m south of this point, based on notations in Sultanov et al. (1999). This location for Taiga, which we consider to meet GT0 criteria, is approximately 24 km southeast of the seismically determined location listed by Sultanov et al. (1999; Figure 26). A short Soviet era documentary film of the Taiga PNE was produced and is available on YouTube at http://www.youtube.com/watch?v=DV9OsftqDxw in Russian. The film shows preparation work for the experiment, the detonation, and after effects. A good aerial photo is in Figure 27.

Figure 25. Excavation crater of the Taiga PNE experiment. Three 15 kt explosions were detonated simultaneously to form this lake. Image from Google Earth.

Figure 26. Google Earth image showing the relative positions of the Sultanov et al. (1999) location for the Taiga PNE and the explosion crater.

Figure 27. Aerial photo of the Taiga crater and lake from Khamtsov et al. (2013).

2.11. GLOBE-1 – 19 September 1971

Like all Globe PNEs, Sultanov et al. (1999) lists Globe-1 as GT 1 or better, but there is no conclusive evidence on high resolution satellite imagery of the site. The problem is compounded by user photographs on Google Earth of the site showing a restricted zone sign and fenced area, and a capped wellhead. The photos are positioned about 2 km from the Sultanov et al. (1999), but it is not 100% clear that the photos are located properly. Globe-1 is therefore an example of a PNE where the Sultanov et al. (1999) GT 1 or better location cannot yet be verified and there is evidence that the error may, in fact, be larger.

Sultanov et al. (1999) coordinates are 57.508ºN x 42.643ºE; depth 610 m. Most authors cite the location as 30 to 40 km northeast (or east-northeast) of Kineshima (Nordyke, 2000; Yablokov, 2003; Short Characteristics...; Mikhailov, 1994), and Vasilyev and Kasatkin (2008) refer to canals to divert the Sacha River and contamination containment due to radiation leakage. Nordyke (2000) gives coordinates of 57.777ºN x 41.098ºE; these coordinates are clearly in error as they are 80 km NW of Kineshima and nowhere along the Sacha River. Yablokov (2003) also gives the location as 28 km northeast of Zavodsk (sic., should be Zavolzhsk) and Mir Novostei (2012) reported that the site was near the village of Galkino.

A picture labeled "Epicenter of Nuclear Explosion Test" (Figure 28) showing a 'Prohibited Zone' sign posted by isplash is located on Google Earth at 57.5163ºN x 42.6146ºE. isplash also has a photo labelling Galkino 4 km from explosion site. He has a second photo and location along the Sacha River claiming to be 50 m from the detonation site. A third photo is labeled 'Nuclear Glade' and shows part of a well casing. isplash's site is 3.4 km from Galkino, 30.3 km from Kineshma and 28.1 km from Zavolzhsk. The Sultanov site is 4.5 km from Galkino, 31.6 km from Kineshma, and 29.6 km from Zavolzhsk. Thus, based on distances alone, either site is reasonable. The area lies on a high-resolution image on Bing Maps. There is evidence of trails and/or fence lines crossing a grassy field on both the north and south sides of the river, and some possible areas of thinner grass (Figures 29). Unfortunately, a drill site cannot be distinguished. The isplash and Sultanov et al. (1999) sites are 1.95 km apart, thus either location could be used with a GT3 accuracy (Figure 30). The isplash site is on a track mapped on a Soviet topographic map and the sequence of photos by isplash make sense as the locations seem to lie on a reasonable path approaching the site. Vasilyev and Kasatkin (2008) report that the site has been restored and show a photo of the site as a grassy field with a fence (Figure 31). However, more recent imagery of the region around Globe-1 show clear evidence of remediation efforts, presumably consistent with downstream migration of radionuclides.

Overall, we cannot verify the coordinates listed by Sultanov et al. (1999) as being within their proposed 0.2-1.0 km error, and the possibility exists that the true location may be up to 2 km distant.

Given the radiation leakage, there should be more about this event in the radiation literature, thus additional research is warranted. However, it is our understanding in private discussion with researchers associated with the site that the contamination situation is significantly worse and more widespread than what is acknowledged in the open literature.

Figure 28. Sign legend ЗОНА ЗАПРЕТНАЯ (PROHIBITED ZONE) (isplash).

Figure 29. Bing maps image of the Globe 1 site as indicated by isplash.

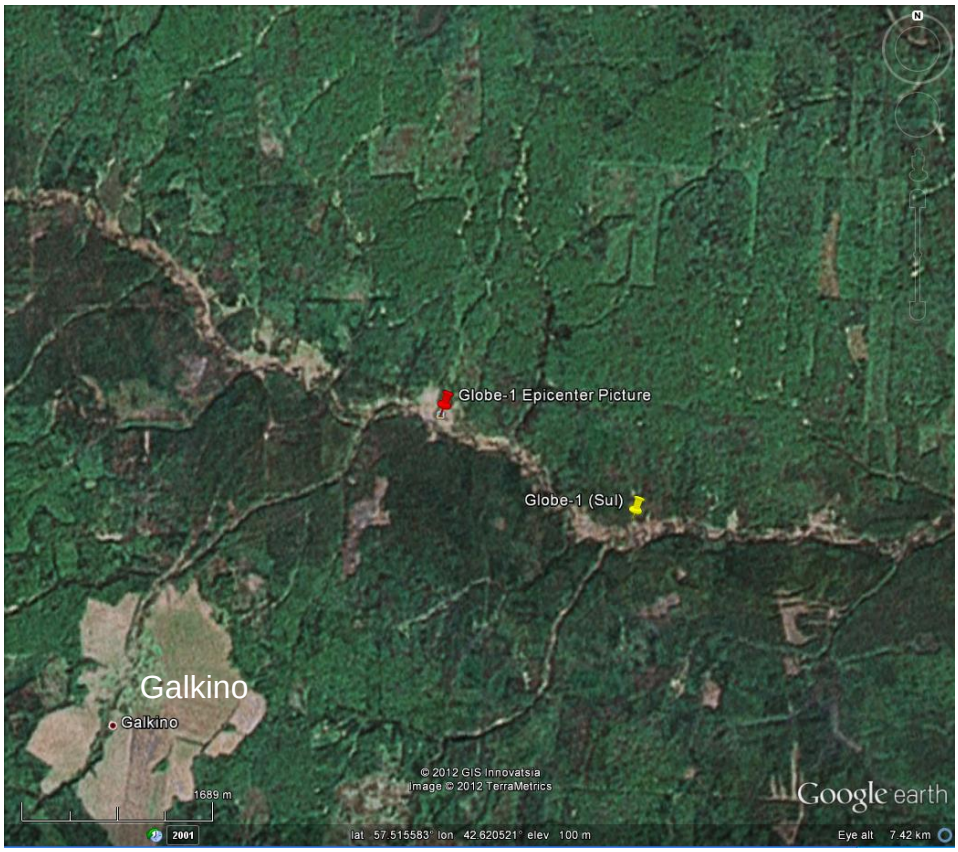

Figure 30. Google Earth image comparing the two locations, 2 km apart.

Figure 31. Restored Globe-1 area (2001) from Vasilyev and Kasatkin (2008)

2.12. GLOBE-2 – 4 October 1971 and RUBY-1 – 6 September 1989

The PNEs Globe-2 and Ruby-1 were both detonated as part of Deep Seismic Sounding (DSS) profiles conducted for geophysical research. The PNE are addressed here in the same section as they were detonated in close proximity to one another. A single discussion is warranted because the locations of each PNE trade places depending on the source making it difficult to separate the correct information for either event.

Sultanov et al. (1999) lists indicates that Globe-2 was a 2.3 kt device detonated at a depth of 595 m and Ruby-1 was an 8.5 kt device detonated deeper at 820 m. Khamtsov et al. (2013) lists the same depths, but indicates that both yields were 2.3 kt.

Both Globe-2 and Ruby-1 were detonated about 50 km ENE of the village of Koryazhma in the Arkhangelsk Oblast of Russia. However, sources differ as to the details of the locations. Sultanov et al. (1999) lists both events as having GT0-1 precision and lists them as being about 400 m apart and a couple hundred meters west of the Tombash River and in close proximity to a East-West trending dirt road (Figure 32).

.

Figure 32. Overview of possible locations as discussed in the text for the Globe-2 and Ruby-1 PNEs. Bing Maps image.

The Russian Wikimapia also catalogs locations for both Globe-2 and Ruby-1. Globe-2 corresponds to Location ‘A’ (Figure 34) while Ruby-1 corresponds to Location ‘B’ (Figure 35). Alternatively, a somewhat stylized map from Khamtsov et al. (2013) reverses the two positions, with Ruby-1 corresponding to Location ‘A’ and Globe-2 to Location ‘B’ (Figure 33). Khamtsov et al. (2013) also provides photographs of both boreholes (Figure 36). The sign at the borehole associated with Globe-2 appears rustier than the sign identified as associated with Ruby-2, which is consistent with one being 18 years newer. Unfortunately, none of the available information or

images allows the correct identification or association of any site with either PNE. Although Google Earth imagery is excellent for both sites, it is not sufficient to identify any remaining infrastructure. We suspect that both PNEs are in this vicinity, and perhaps one or both locations meet the Sultanov et al. (1999) GT0-1 criteria, though we are not confident considering either location to be verified.

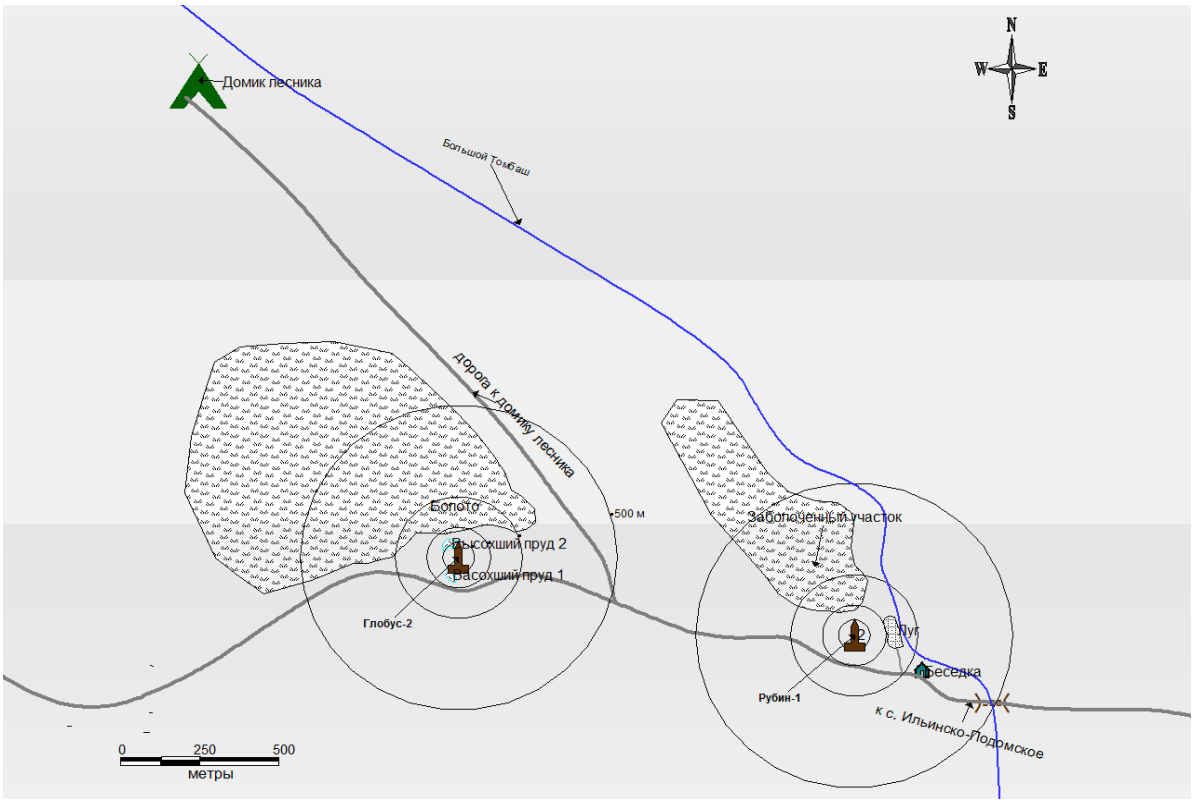

Figure 33. Schematic figure from Khamtsov et al. (2013) indicating the location of Globe-2 in the left circle and Ruby-1 in the right circle.

Figure 34. Location 'A' for which Russian Wikimapia identifies the site of Globe-2 and Khamtsov et al. (2013) identifies the site as for Ruby-1. Bing Maps image.

Figure 35. Location 'A' for which Russian Wikimapia identifies the site of Globe-2 and Khamtsov et al. (2013) identifies the site as for Ruby-1. Bing Maps image.

A. **B.**

Figure 36. Photos of radiation warning signs from Khramtsov et al. (2013) for the boreholes of: A. Globe-2. B. Ruby-1.

2.13. SAPPHIRE-1, -2 – 22 October 1971 and 30 September 1973

Coordinates and site descriptions are given in Dubasov et al. (2005). Both sites are currently fenced (Figures 37 and 38). Dubasov et al. (2005) give the well locations for Sapphire 1 as 51.5860°N x 54.6092°E. Sapphire-2 is given as 51.6053°N x 54.5987°E. These are 6-12 km from Sultanov et al. (1999) locations.

Clearly demarked areas are present in satellite imagery for both Sapphire locations (Figure 39), however the coordinates for Sapphire-1 are outside the clearly marked area. Based on Figure 37, the borehole should correspond to a Cesium peak near the center of circular region and better coordinates would be 51.5862°±0.0007°N x 54.6150°±0.0010°E. There has been activity at the Sapphire-1 site throughout the 2010's. The area at the northern edge of the circular fenced area with the high Cesium concentration is further fenced off. Coordinates reported here differ by those from Sultanov et al. (1999) by 11.5 km for Sapphire-1 (Figure 40).

The Dubasov et al. (2005) coordinates of Sapphire-2 within the fenced area are good, and need only a minor adjustment. The best fit Google Earth coordinates are 51.6052°±0.0004°N x 54.5991°±0.0005°E. Coordinates reported here differ by those from Sultanov et al. (1999) 6.0 km for Sapphire-2 (Figure 40).

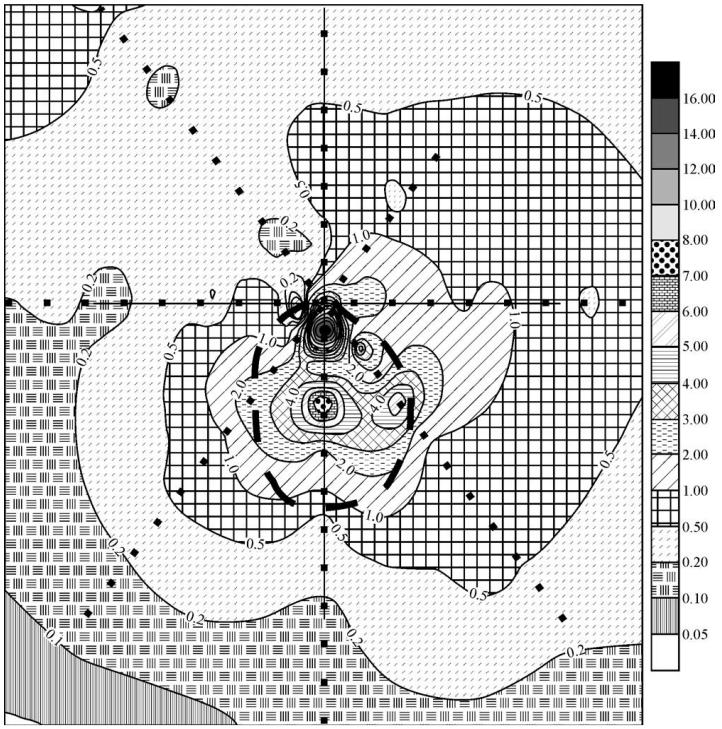

Figure 37. Cesium contamination area from Sapphire-1 (Dubasov et al., 2005). Black dashed line is fenced area.

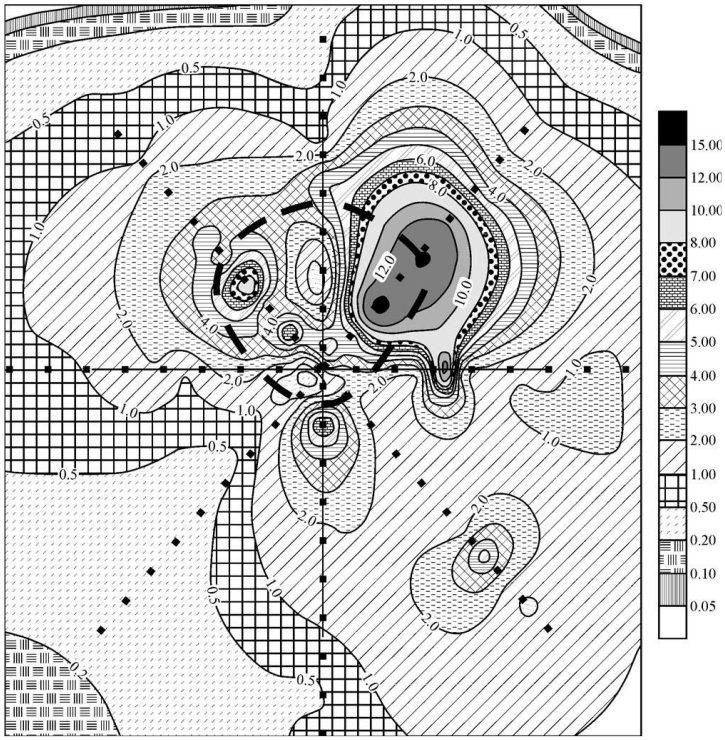

Figure 38. Cesium contamination area from Sapphire-2 (Dubasov et al., 2005). Black dashed line is fenced in area.

Figure 39. Google Earth image of Sapphire-1 and -2, showing fenced in areas (circular regions surrounding detonation sites). Google Earth Image © 2013 Digital Globe, Landsat Image.

Throughout the 2010's, several sequential images on Google Earth indicate that there has been near continuous activity at the Sapphire-2 site. Additional areas have been paved, excavations have been dug and filled, waste fluid containment reservoirs have been constructed and removed, and there is even a paved single lane construction with walls, which we speculate may be a decontamination facility for washing trucks and vehicles.

Figure 40. Relative locations of Sultanov et al. (1999) locations compared to this report. Google Earth Image © 2013 Digital Globe, Landsat Image.

2.14. CRATER – 11 April 1972

The PNE Crater is the only such event to have occurred in Turkmenistan. It was a 14 kt device detonated at a depth of 1720 m in an agrillite horizon at a location reported to be about 30 km SE of the city of Mary (Nordyke, 2000). The event was produced to seal a blown out gas well, which is reported to have been successful (Nordyke, 2000). Little other information seems available for this PNE. Seismologists at the Institute of Seismology of Turkmenistan indicate that they had no idea that a nuclear explosion had occurred in Turkmenistan.

The Sultanov et al. (1999) GT10 quality location for Crater falls on the edge of the desert about 33 km SE of Mary (Figure 41). There is no indication on imagery near this site of the PNE location. We attempted to include Crater in our cluster analysis and calculate relative locations with respect to Urtabulak and Pamuk, which were known. Unfortunately, Crater is over 275 km from these events and the cluster analysis produced a poor statistical result (Appendix B). The cluster event analysis gave a result about 7.5 km NE of the Sultanov et al. (1999) location in a region of agricultural fields surrounded by small villages. There is evidence of old oil/gas wells in the region, but there is no reason to choose any specific point near the cluster analysis result as the location of the PNE.

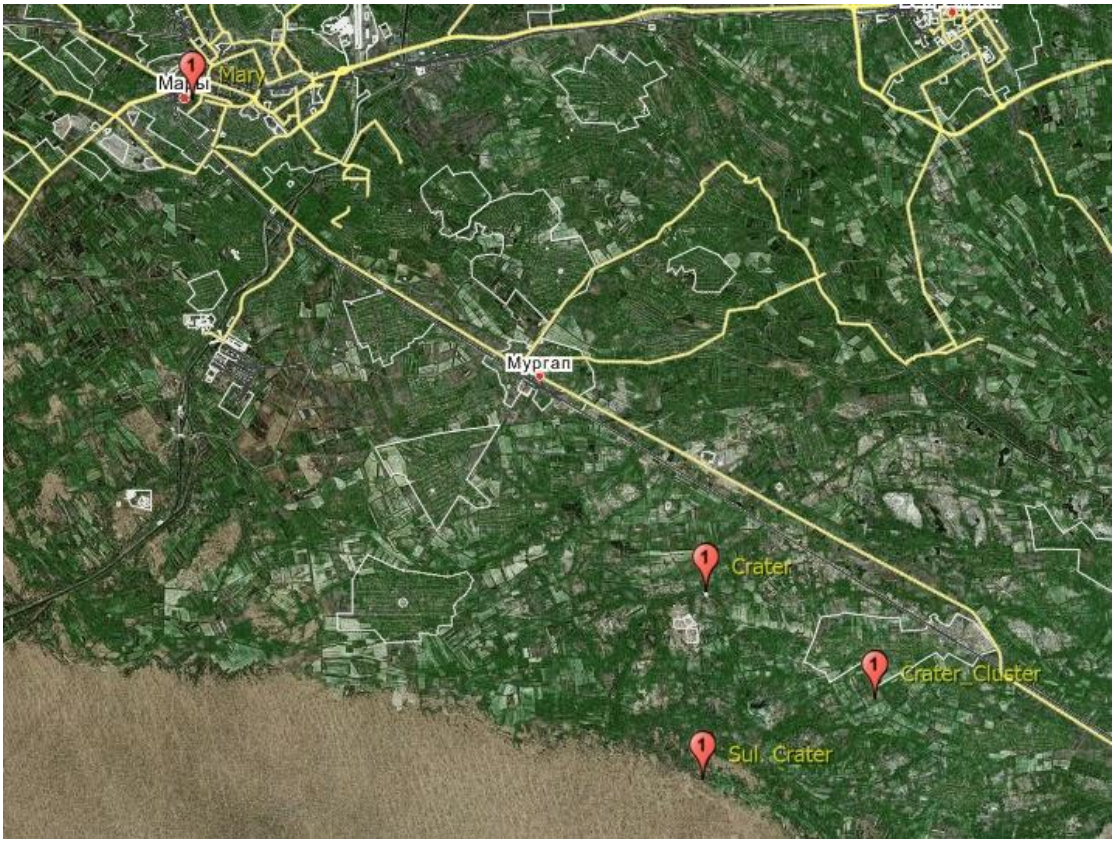

Figure 41. Location of the PNE 'Crater' relative to the town of Mary and locations determined by Sultanov et al. (1999) and our cluster event determination. Imagery is from Bing Maps.

A search of Russian Wikimapia identifies the site of Crater at what appears to be one of the local regions old drill pad, and includes the description "Gas well was blowing out for several years and then relieve well was drilled and nuclear bomb was blasted to close gas flare" (Figure 42). This site is about 7.5 km N of the Sultanov et al. (1999) location and 28 km SE of Mary. The apparent abandoned drill pad and location is consistent with the description of the event, thus we feel that it represents the correct location of the PNE. This location is within the GT10 accuracy of Sultanov et al. (1999).

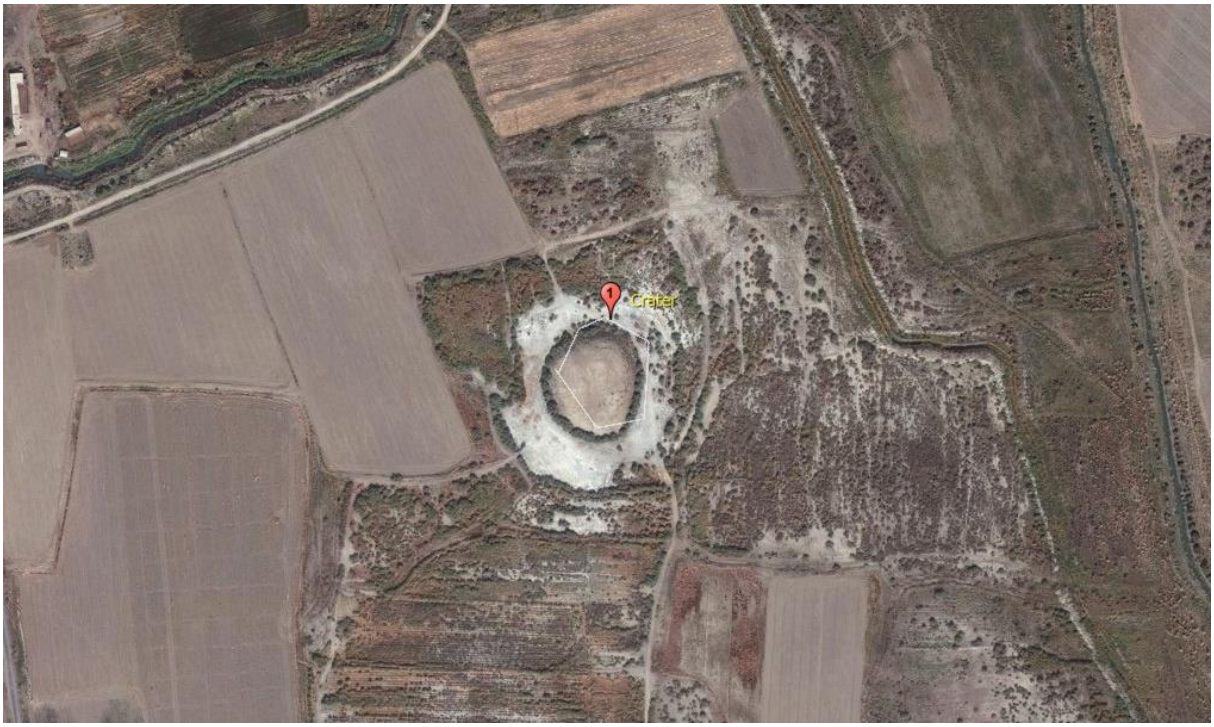

Figure 42. Site of the PNE 'Crater' as identified in Russian Wikimapia. Imagery is from Bing Maps.

2.15. FAKEL – 9 July 1972

The PNE 'Fakel' was a 3.8 kt detonation designed to extinguish a natural gas well fire. The PNE was located just north of the settlement of Pershotravneve, and approximately three km west of the village of Khrestyshche in northern Ukraine (Figure 43). The location was determined in the field following discussions with officials and geologists from the gas company that operates the wells in the area. A sketched map provided indicated that the PNE took place about mid-way between well numbers 258 and 181 (about 100m from each) and about 200m west of well number 303. We located well numbers 258 and 303 in the field. The number tag for well 181 was missing, but given its proximity to the other wells and the match to the sketch map provided we are confident in its identification. Figure 44 shows a ground view of well 258 with the PNE site behind. We note that there is no clear expression of the PNE, and the site has been redeveloped with new gas wells and a large compressor station a few hundred meters to the south. The immediate vicinity of the Fakel site is not farmed, though we are unsure if this is significant. We are also unsure if the location determined represents the surface point above the detonation, or the surface location of the borehole into which the bomb was emplaced. For general but independent

verification of the site, we asked people in the nearby (~1 km distant) settlement of Pershotravneve the location of the explosion, and we were told it took place just north of the east end of the new compressor station. The coordinates for the PNE Fakel are 49.552ºN x 35.471ºE, which is approximately 28 km south of the location given in Sultanov et al. (1999).

Various locally published newspaper articles and internet articles in Russian indicate that there was some level of radiation release following the detonation. In addition, the gas company geologists we spoke to questioned us as to whether we had dosimeters or other equipment for measuring radiation with us because there can or could be some contamination at the site. Collectively, this seems to suggest that the site should be formally surveyed for radionuclide contamination.

Figure 43. Left – Overview of the site of PNE Fakel in north-central Ukraine. Right – The location of Fakel as determined using referenced Gas wells. Image from Google Earth.

Figure 44. Left – Site of the PNE Fakel looking south. The compressor station is located in the background. Right – Gas well #258 used as a reference in locating Fakel. The PNE was approximately 100 m to the left (north) from this location. Photos by K. Mackey.

2.16. REGION-3 – 20 August 1972

The Region-3 PNE took place in northwestern Kazakhstan and was a seismic source for part of the Region DSS profile. Sultanov et al. (1999) lists the location of Region-3 as GT 0-1. Surprisingly, a field visit to the location did not reveal the borehole. Many surface features are apparent on satellite imagery in the vicinity of the Sultanov et al. (1999) location (Figure 45), though on-site inspection showed them to be generally related to agriculture or watering holes for livestock. We were fortunate that a local shepherd was able to lead us to the borehole. The shepherd was unaware of the site as that of a nuclear explosion, but immediately understood where we wanted to go once we asked him about 'a big metal pipe in the ground filled with concrete' (Figure 46).

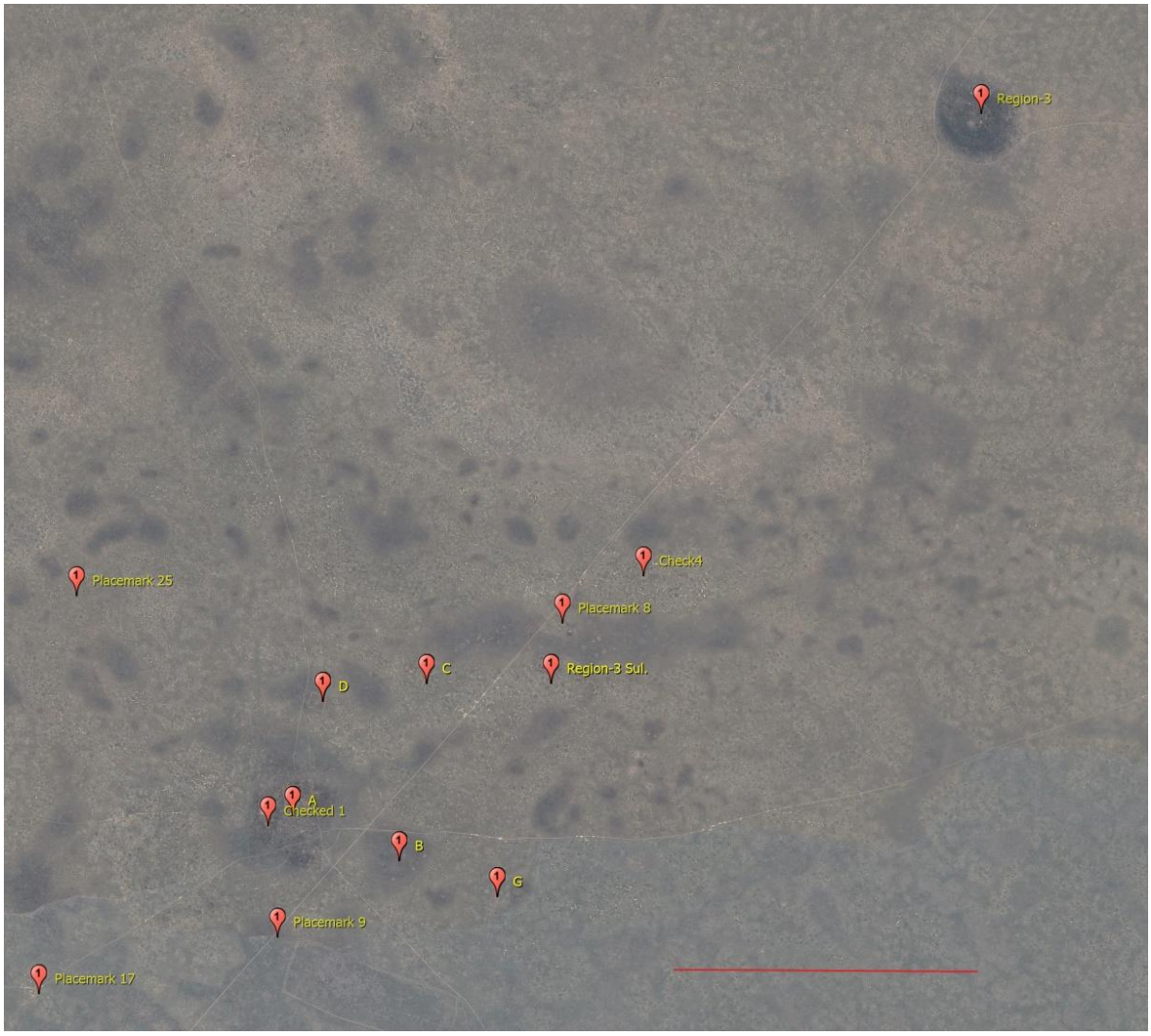

Figure 45. Overview of the Region-3 area. The Sultanov et al. (1999) location, just below the center of the image, is surrounded by many candidate sites that were checked. The borehole is visible in the upper right corner. The red scale bar is 1.0 km in length. Image is from Bing Maps.

The borehole is situated 2.53 km northeast of the Sultanov et al. (1999) coordinates in the center of a shallow depression that is about 280m in diameter (Figure 47). Visually on the ground and on satellite imagery, the depression appears to be a shallow collapse crater, though no ground cracks were observed.

Figure 46. The shepherd who led us to the Region-3 borehole. Photos by K. Mackey.

Figure 47. The location of Region-3 and associated possible collapse crater. Image is from Bing Maps.

The site is characterized by a considerable amount of rubble and appears to have undergone minimal clean-up following the detonation. The surface borehole expression consists of weathering concrete filling the well casings (Figure 48). There may be some minor radionuclide contamination at the site. The highest radiation measured was 22 uR/hr about 20m north of the main borehole. Although not significant, this is about two times what seemed to be the normal background.

Figure 48. The Region-3 borehole. Photo by K. Mackey.

2.17. DNEPR-1 and 2 (2-1, 2-2) – 4 September 1972 and 17 August 1984

Sultanov et al. (1999) gives coordinates for Dnepr-1 of 67.75°N x 33.10°E and for Dnepr-2 of 67.75°N x 33.00°E. These coordinates are located on an island in the middle of Lake Imandra about 24 km northwest of Apatity and 27.5 km from Kirovsk. A number of popular web sites and publications use these coordinates referenced to other towns in the area (e.g., Murmansk, Polyarnyy, etc.). Other sources giving distances use Kirovsk as a reference and place Dnepr 20-21 km to the north or northwest (Mikhailov, 1994; Myasnikov et al., 2004).

Several sources place both PNEs at the Kuel'porr apatite mine (variously transliterated; Nordyke, 2000) or in the Khibiny Range (Pavlov, 2011). Pochivalov (1998) reports the site as in the Novy ("New") Ore deposit in Apatity, but give coordinates of 67.8°N x 33.6°E. The location

of Kuel'porr mine (Figure 49) can be located through a series of photographs taken by tourists in the Khibiny Range (although often mislocated on Google Earth, the location can be recovered by using views from the mountains to the west).

The mine tailings and entrance work area are depicted on a photo posted to Google Earth by Siv1103 (Figure 50), which is mislocated on the east side of the ridge into which the mine entrance apparently goes. The location of the tailings pile and the mine entrance is shown on Figure 51 (Google Earth). The mine entrance region is shown on many photographs (e.g., Figures 50 and 52) and is located at 67.7907N x 33.6085E; this location is 21 km from Kirovsk. A view of the area prior to closure of the mine shaft in 1992 is shown in Figure 53.

It is unclear as to where in the mine the detonations were made. The relative locations of Dnepr-1 and Dnepr-2 are usually stated as differing by 1-2 km. The Sultanov et al. (1999) coordinates are 4 km apart (0.1° longitude). In appendix B of Nordyke (2000), Dnepr-1 is given as 67.689N, 33.445E and 20 km north of Kirovsk, while Dnepr-2 is given as 66.770N, 33.680E. Clearly the latitude for Dnepr-2 is in error, and the coordinates for Dnepr-1 would place the site on the opposite side of the valley and significantly father south. The coordinates for Dnepr-2, if adjusted by one degree latitude, falls in the same general area as the mine entrance, but approximately 4 km to the southeast. Dnepr-2 also consisted of two detonations 75 m apart (Nordyke, 2000).

Nordyke (2000) provides a sketch of the position of Dnepr-1 and -2 and the location of various shafts (Figure 54). If at least relative positioning is correct, Dnepr-2 is east of Dnepr-1. Although the sketch scale is difficult to determine, if the sketches are even to scale, and if the ore body is 60-80 m wide, the entire sketch is approximately 350-400 m across. This agrees within a factor of two with other distances given in the text. The lower diagram only shows one location. Also, Dnepr-1 was buried 44 m shallower than Dnepr-2 (Short Characteristics...), while Figure 54 shows them approximately at the same depth, with about 50 m further into the mountain (again, if a scale can be imposed).

Figure 54 shows the detonation sites on the left, presumably west or northwest, of the crest of the mountain. If we assume that the detonation occurred within the mountain into which the tailings and mine shafts seem to go, then the detonation sites are somewhere within the 600 m high mountain, which is about 1 km across. Thus an estimate of 67.782°N ± 0.005, 33.618°E ± 0.010 probably is a GT1 solution. These coordinates are approximately 1 km south from the mine entrance. Allowing for the detonation sites to be up to one additional kilometer south results in most of the mountain that contains the mine being within the error of a GT 1 location.

The proposed location is approximately 22 km east of the Sultanov et al. (1999) site for Dnepr-1 and 26 km east of the Dnepr-2 site.

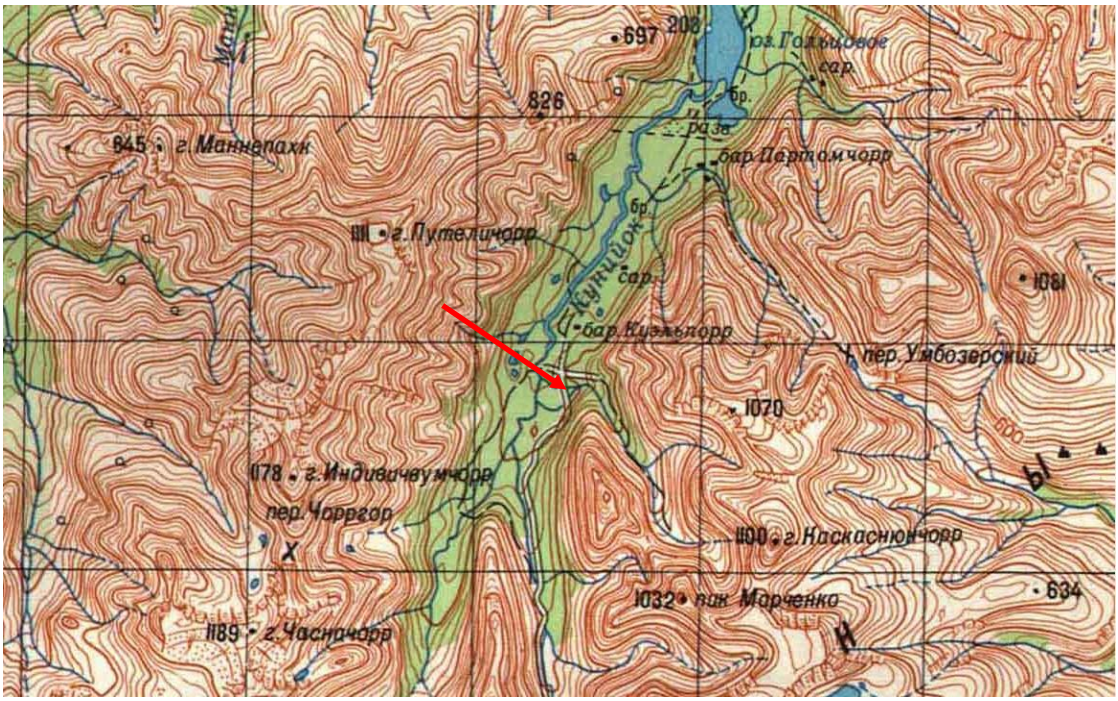

Figure 49. Detail of 1:200,000 base topographic map af the Dnepr PNE area.

Figure 50. Photo labeled Kuel'porr ore deposit sited at 67.786810ºN x 33.624575ºE on Google Earth by Siv1103. But location is off and is taken from the west.

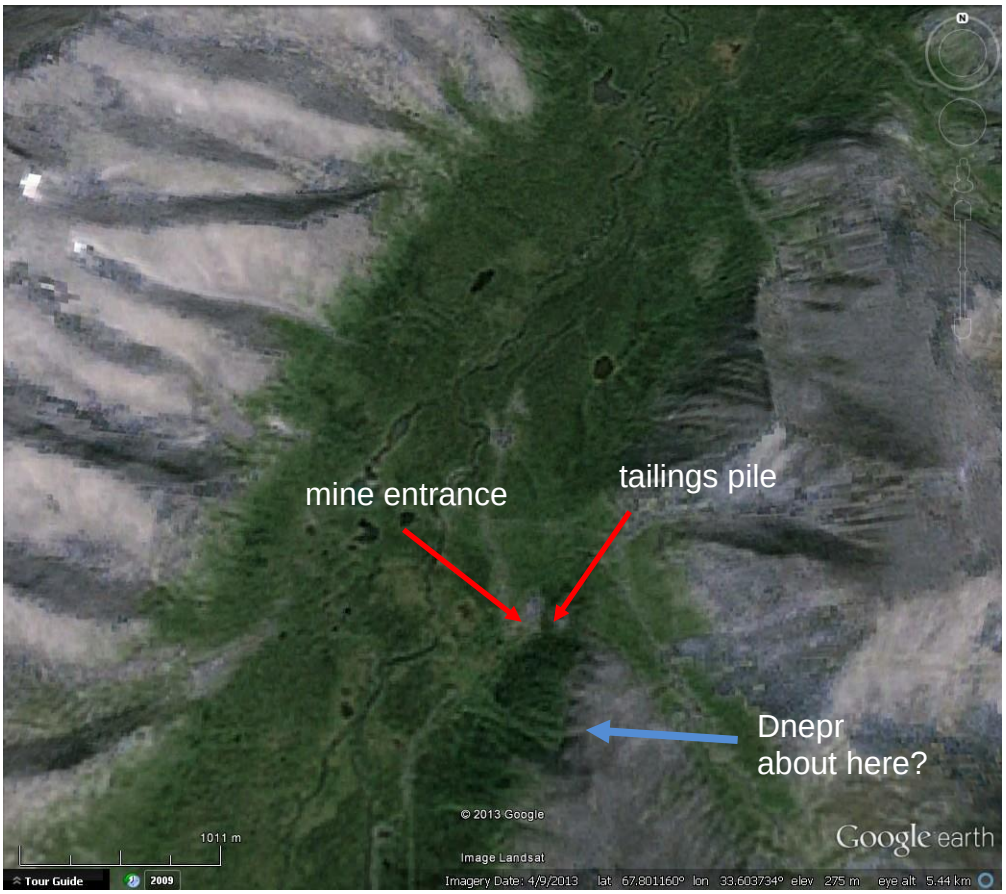

Figure 51. Google Earth (© 2013) image of area around Dnepr mine.

Figure 52. Photo labeled "at this concrete was the site of an atomic explosion" located at 67.7907ºN x 33.6085ºE. Photo located erroneously by Sityshooter at 67.8026ºN x 33.6592ºE

Figure 53. A view of the area (facing west) before the bridge to the closed gangway at the Dnepr facility taken in 2002 (Vasilyev and Kasatkin, 2008). This picture, as in the original source, is left-right reversed.

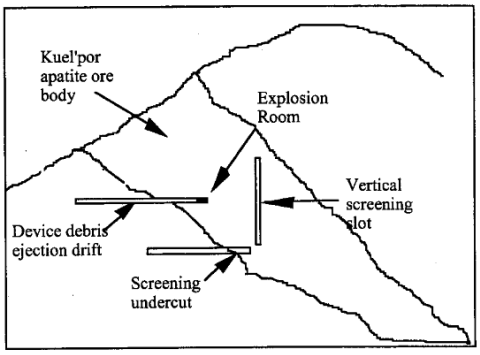

Figure 7a- Schematic of "Dnepr-1" Experiment

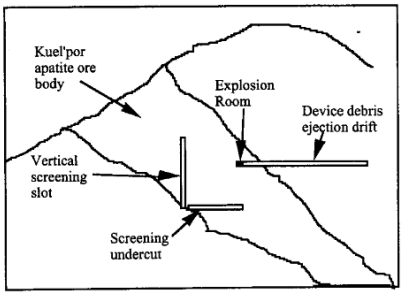

Figure 7b - Schematic of "Dnepr-2" Experiment

Figure 54. Relative position of Dnepr detonations Nordyke (2000). Ore body is described as 60-80 m thick.

2.18. REGION-1 – 21 September 1972

Region-1 was part of the Region DSS profile. Descriptive location gives the Region-1 detonation site as 70 km (Mikhailov, 1994; Dubasov et al., 2005; Yablokov, 2003) or 80 km (Short Characteristics...) south-southwest of Buzuluk at a depth of 485 m with a yield of 2.3 kt. Pochivalov (1998) cites north of Ural'sk. Interestingly, the Region-1 detonation point is only about 22 km from that of Region-2, a significantly closer spacing than is typical for PNE shots along DSS profiles. This spacing, in consideration with recent industrial development is suggestive that Region-1 may have been planned as dual-use, specifically to also create a material storage cavern.

Numerical coordinates cited are 52.1172°N x 52.0672 (Yablokov, 2003), 52.127°N x 51.994°E (Nordyke, 2000), and 52.118°N x 52.068°E (Sultanov et al., 1999). The ISC solution is at 52.1839°N x 51.9411°E, with a depth of 28 km. These are in generally close proximity, within a 6 km radius (12 km diameter) of each other (Figure 55). The Sultanov et al. (1999) location is in typical farmland for the area, and we were unable to identify any apparent infrastructure or visible site within 1 km of the listed coordinates on high resolution satellite imagery (Figure 56).

Mackey and Fujita (2014) identified two possible site locations based on satellite imagery. Newer Bing Maps imagery is available for their proposed 'Alternate B' site that clearly shows a borehole pad similar to other PNE locations. Region 1 was included as part of the Butane cluster event analysis (Appendix A). The calibrated location from the cluster event analysis locates Region 1 about 1.9 km WSW of the Alternate B location. In comparison, the Sultanov et al. (1999) location is about 3.0 km distant. We choose this location at 52.1414°N x 52.0929°E as the Region-1 detonation.

Several satellite images spanning several years clearly shows recent development of the Region-1 site. An earlier somewhat high resolution image is available from Geoportal Roskozmos (Figure 57) that shows the site as a visible square approximately 150 m on each side. A more recent image from Bing Maps shows the site with new development (Figure 58), including a road, concrete pad, new slightly smaller square earthen berm, and power lines and buried pipeline coming from the south. The pipeline is traceable on other imagery where the burying trench is open in places. The most recent image is available from Yandex and shows active development at the site as well as a small hydrocarbon facility and gas flare south of the site where the pipeline spur extending from Region-1 intersects the East-West trending pipeline (Figures 59 and 60).

Based on the development and connection of the site to the regional hydrocarbon infrastructure, we suggest that the site will be utilized as a storage facility, similar to the Magistral' site. This conclusion would also be consistent with the existence of an intact explosion cavern. This overall conclusion is somewhat puzzling as the host rock for the explosion is reported to be sandstone/shale by Sultanov et al. (1999). This host rock would not seem ideal for compressed gas storage as sandstone is usually permeable.

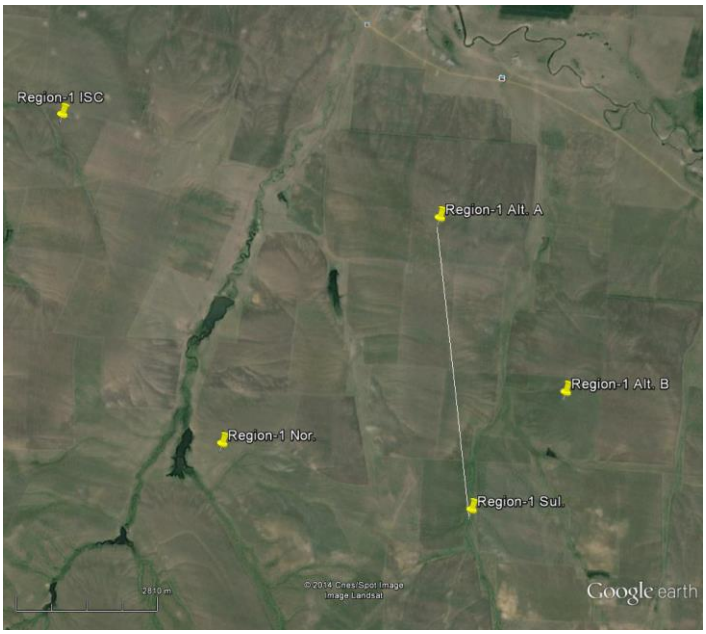

Figure 55. Area surrounding Region-1 showing various previously reported locations (ISC, Nordyke, 2000 Sultanov et al., 1999) and two possible sites (labeled Alt. A and Alt. B). Coordinates reported by Yablokov, 2003 are essentially the same as Sultanov et al. (1999). This image was originally displayed in Mackey and Fujita (2014). We here identify Alternate B as the correct location of Region-1. Google Earth Image © 2014 Cnes/Spot.

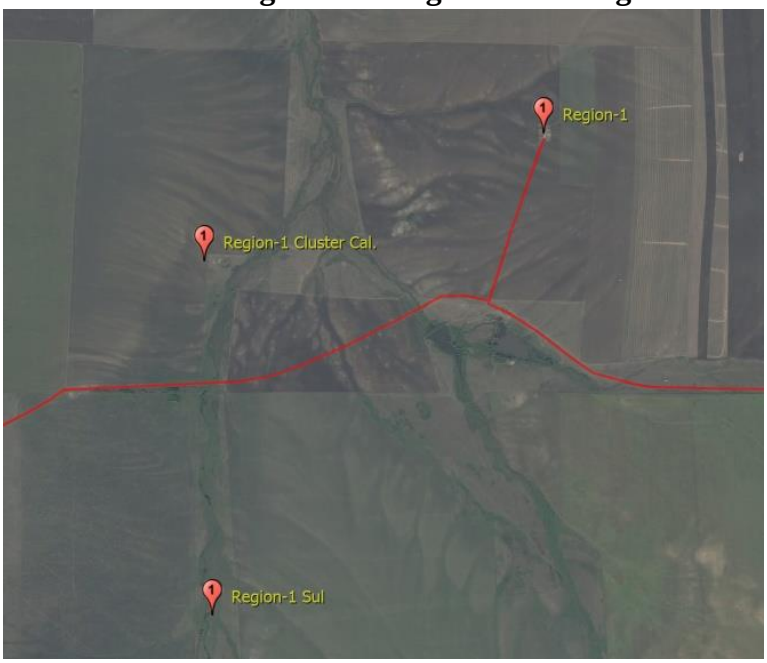

Figure 56. High resolution Bing Maps image of the area of Region-1 near Sultanov and Yablokov coordinates, 72 km from Buzuluk. The location of Region-1, Alternate B from Figure 55 is shown, as is the Sultanov et al. (1999) location and the calibrated location from the cluster analysis (Appendix A). The red line indicates the path of a new pipeline, generally running East-West, with a spur connecting to the Region-1 site. Note the lack of infrastructure near the intersection of the pipeline and spur.

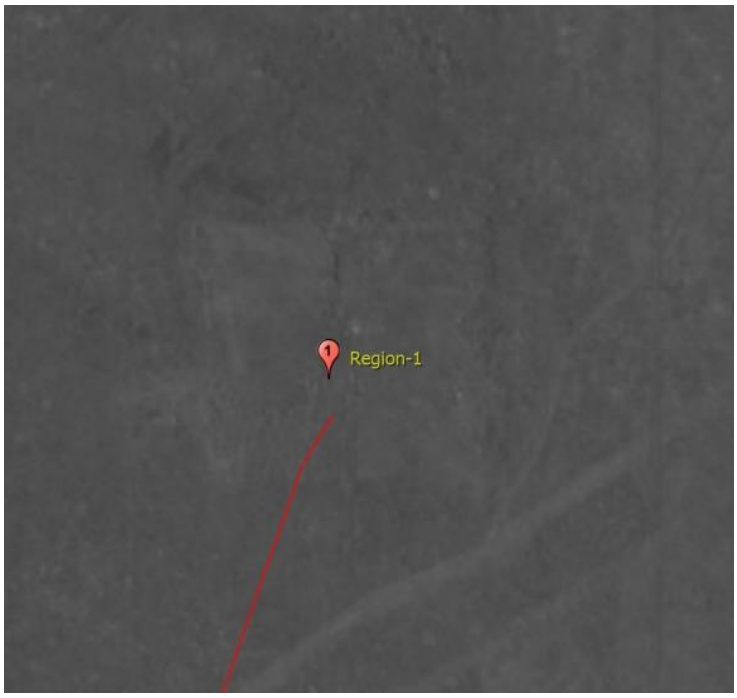

Figure 57. Geoportal Roskozmos image of the Region-1 site showing an overgrown square structure at the site. The square is approximately 150 m per side. A small white spot near the center would be consistent with the concrete plugged borehole. The red line indicates the future location of the connecting pipeline.

Figure 58. Newer high resolution image from Bing Maps of the Region-1 site. Fresh tracks and lack of vegetation around the borehole is indicative that the site has undergone recent development when comparing it to the Geoportal Roskozmos image in Figure 57. Utility poles and the trace of the pipeline are visible extending to the south. It is visually consistent with the Region-2 location.

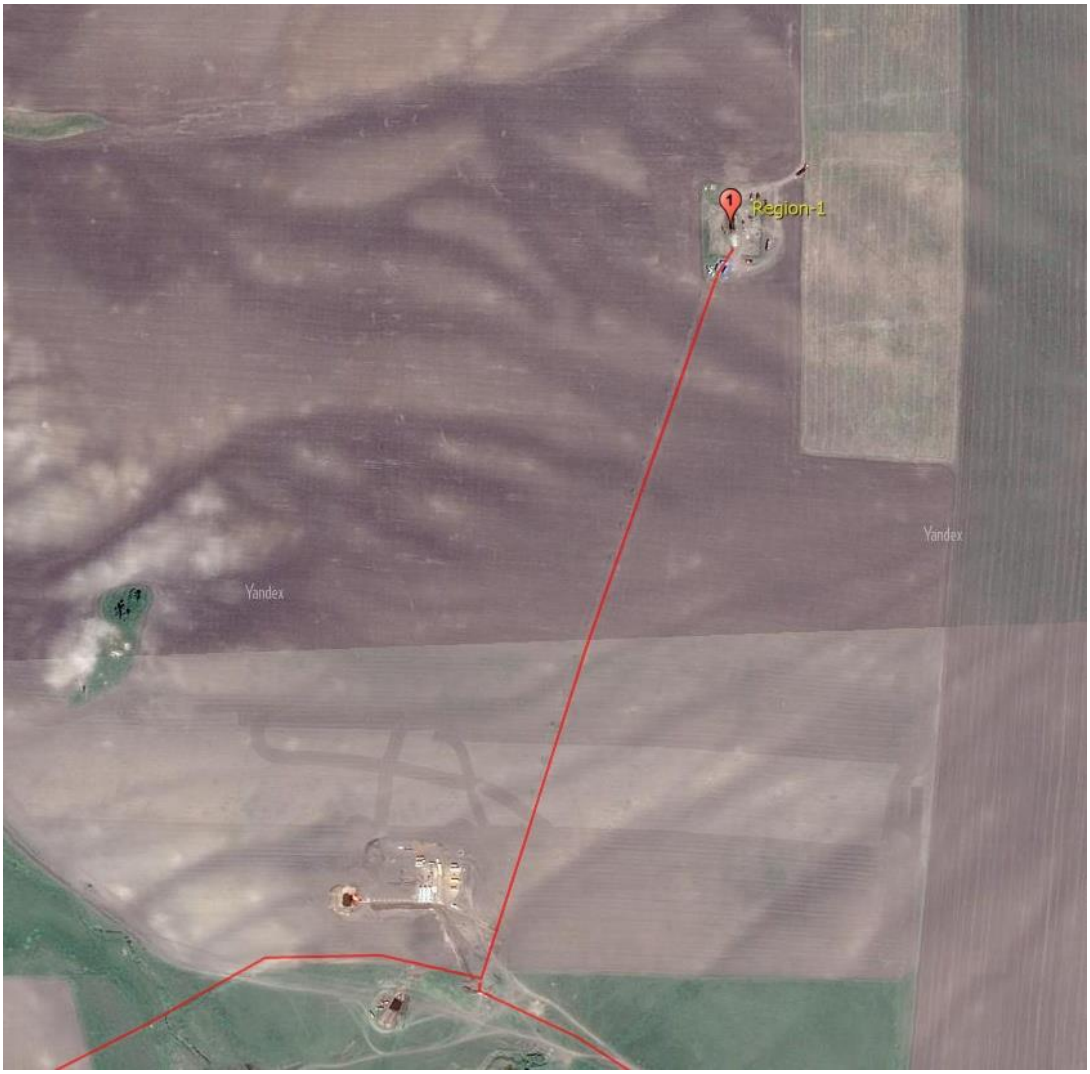

Figure 59. High resolution undated image from Yandex.ru showing active workings at the Region-1 site and a new pipeline facility with gas flare at the intersection of the East-West pipeline (red line) and spur connecting to Region-1. Based on infrastructure development, this is the most recent image available. The pipeline facility is not apparent on the Bing Maps image in Figure 56.

Figure 60. Close-up image from Yandex.ru showing activity and development at the Region-1 PNE site.

2.19. REGION-2 – 24 November 1972

Region-2 was part of the Region DSS line, and was detonated in relative close proximity to Region-1. The published coordinates are widely scattered. Nordyke (2000) gives coordinates of 52.779°N, 51.067°E, 90 km south-southwest of Buzuluk (actually 80 km west of Buzuluk). Norris and Cochran (1996) cite 52.179°N, 51.067°E (104 km southwest). Bulatov (1996, table 41) gives 52.140°N, 51.830°E (77 km), and Sultanov et al. (1999) give 51.990°N, 51.867°E (92 km south-southwest). This is a fairly wide set of coordinates, although the latitude of Nordyke (2000) or Norris and Cochran (1996) could be a misprint as both longitude values are the same. Yablokov (2003) gives coordinates that are too far south, 51.4839°N, 51.8675°E (147 km), and cites some uncertainty in terms of the depth (672 or 680 m) and whether it is south or west of Buzuluk. Pochivalov (1998) states northwest of Ural'sk.

Given that the Sultanov et al. (1999) locations have generally been good for DSS PNEs, and it fits the description of distance from Buzuluk, the area was surveyed for possible sites. Figure 61 shows a well pad similar to Region-1 with a circular structure immediately north. The location is centered at 51.9932°N, 51.8827°E, 1.1 km East from the Sultanov et al. (1999) coordinates. We included Region-2 in the Butane cluster event analysis (Appendix A). The

calibrated location from the cluster event analysis locates Region-2 about 1.4 km East of the apparent borehole, thus the chosen site is approximately midway between the Sultanov et al. (1999) and calibrated locations (Figure 62).

The close proximity of both the calibrated location and the Sultanov et al. (1999) coordinates give us high confidence in the identified borehole location. However, we note that other oil/gas workings are in close proximity about 3 km to the South. Positively, the chosen Region-2 site is somewhat offset from the oil wells to the south where many wells are in closer proximity to each other. Negatively, the circular region to the north resembles the drilling waste ponds near some of the oil wells, and the drill pads of the older wells are of a similar character. Using Google Earth imagery, the site was reconditioned in 2010 in a similar manner as some of the older wells to the south (Figure 63). It is unclear to us what the connection of the site is with similar wells to the south.

Figure 61. Bing Maps image of the identified Region-2 site.

Figure 62. Bing Maps image of the Region-2 site at 51.9932ºN x 51.8827ºE. This is 1.1km East from the Sultanov location and 1.4 km West of the calibrated location described in Appendix-A.

A. 3/31/2009

B. 8/12/2010

C. 6/26/2012

D. 5/19/2013

Figure 63. Historic imagery of the Region-2 site. All images Google Earth © 2016 Digital Globe. A. 2009 Older infrastructure. B. 2010 reconstruction of the site. C. Completion of reconstruction in 2012. D. 2013 post reconstruction.

2.20. REGION-5 – 24 November 1972

Region-5 was a PNE conducted for a DSS profile in northern Kazakhstan. Sultanov et al. (1999) reports the location as being of GT 0.2-1 quality. Google Earth and Bing Maps imagery of the site shows ground disturbance near the location of Sultanov et al. (1999) though it is not sufficiently clear to confirm the coordinates with confidence. The currently available imagery from Bing Maps is better than Google Earth. Figure 64 is an overview of the location.

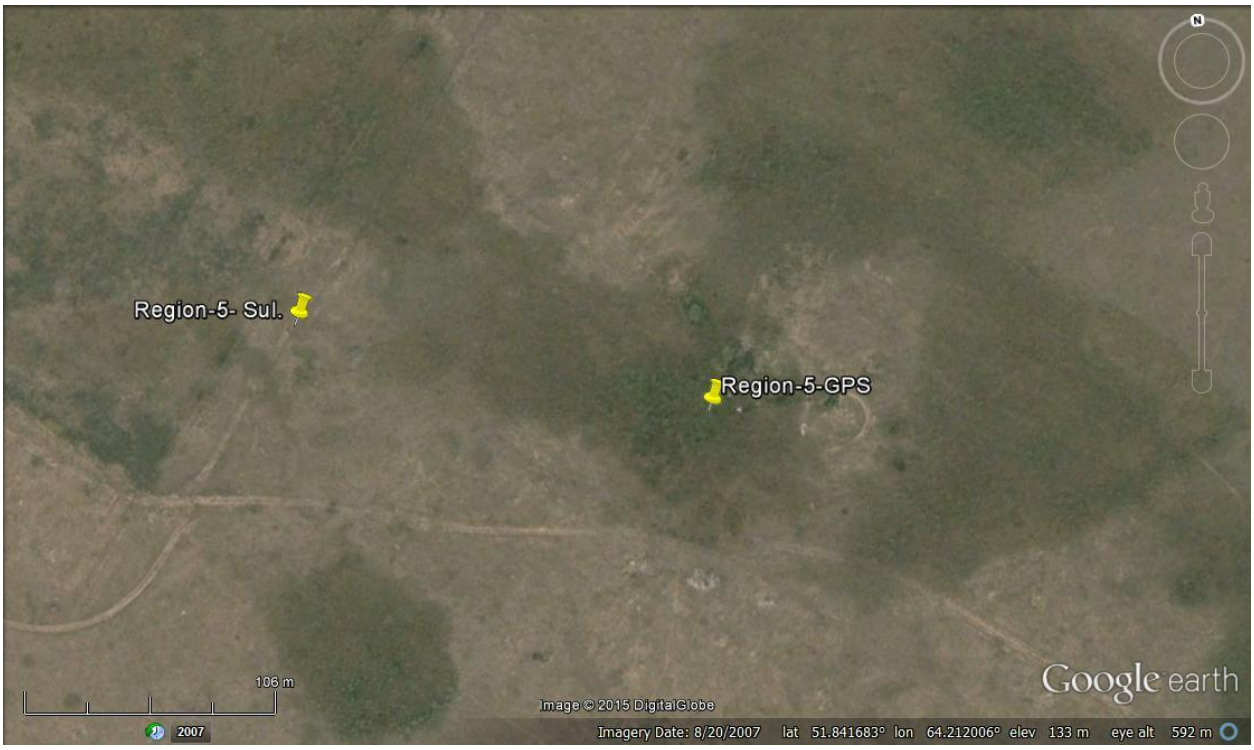

Figure 64. Google Earth imagery showing an overview of the Region-5 site. Both the Sultanov et al. (1999) and our GPS locations are shown.

We conducted a field inspection and verified the Sultanov et al. (1999) location of Region-5 as GT-0. A concrete encased and capped borehole with a single small pipe visible at the top characterizes the site (Figure 65). The main borehole location is 51.84151°N, 064.21248°E, which differs only a couple hundred meters from Sultanov et al. (1999). The GPS determined elevation of the top of the borehole is 131 m.

Three additional small diameter instrumentation or access boreholes, one borehole each to the north, west, and south, were noted around the main borehole at a distance of 25 meters of so. Each of these pipes angle slightly towards the main borehole. Coordinates of the instrumentation boreholes are in Table 2 and pictures in Figure 66.

One conctete pad with mounting hardware is at the site, though is in poor condition (Figure 66c). We presume that this pad was part of a tower mount for a drill rig or emplacement of the nuclear device. A large out-of-place broken concrete block is at the site. Part of the block seems to have the cast of a large pipe.

Figure 65. The capped borehole of Region-5

Table 2. Locations of objects at the Region-5 site.

Object	Latitude	Longitude
Main Borehole	51.84151ºN	64.21248ºE
Instrument or Access Borehole	51.84139ºN	64.21214ºE
Instrument or Access Borehole	51.84175ºN	64.21226ºE
Instrument or Access Borehole	51.84168ºN	64.21281ºE
Concrete Pad	51.84143ºN	64.21272ºE
Broken Concrete Block	51.84145ºN	64.21282ºE

A

B

C

Figure 66. A. Instrument borehole. B. Broken concrete block. C. Remains of concrete slab for tower emplacement.

2.21. MERIDIAN-3 – 15 August 1973

Meridian-3 is located in south-central Kazakhstan and is listed in Sultanov et al. (1999) as a GT0-1 located event. We confirmed the location as GT0 with an on-site inspection, finding the difference between the Sultanov et al. (1999) location and the GPS determination to be about 140 m (Figures 67 and 68). The Institute of Nuclear Physics of the Republic of Kazakhstan provided us with coordinates of Meridian-3 that were essentially the same as the GPS results.

The borehole is typical of many PNEs and consists of a large concrete filled pipe and a circular metal 'Forbidden Zone' warning sign welded to the top (Figure 69). There are four small diameter secondary boreholes angled towards the emplacement borehole. Additionally, a cut off borehole is in an adjacent concrete pad and the remains of a tower mount are evident. We did not identify any elevated radiation at the site.

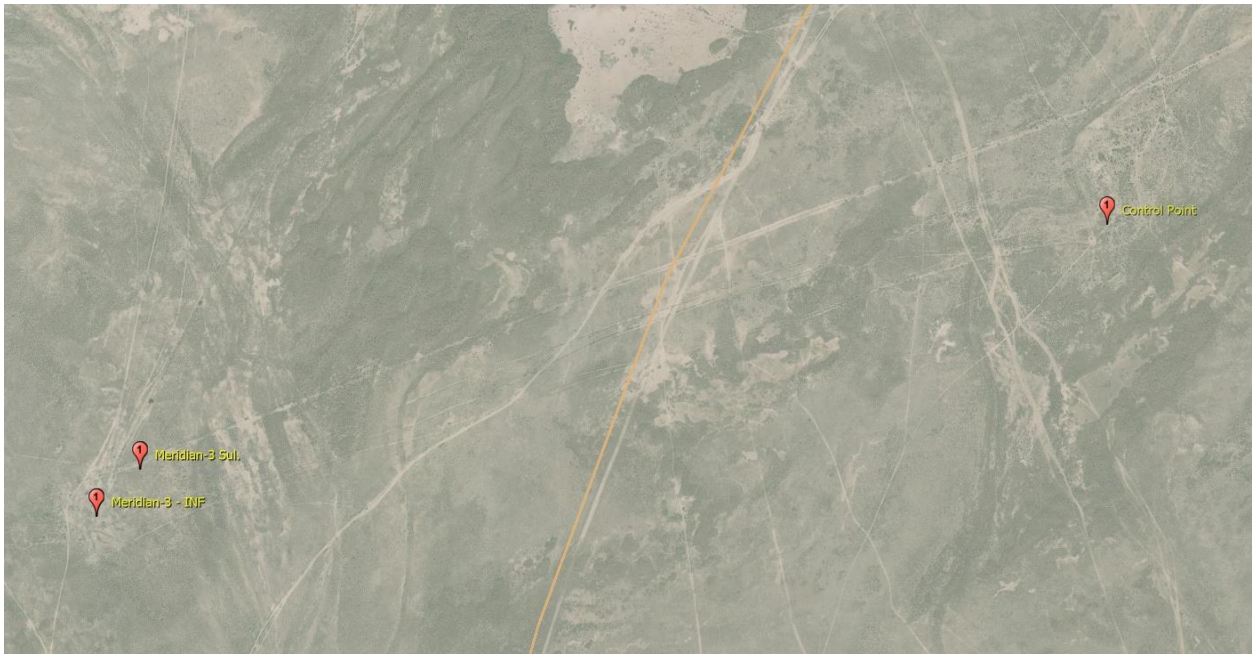

Figure 67. The identified borehole location and Sultanov et al. (1999) published location are shown at left. Cable lays are visible extending to the experiment control point identified at right. Image is from Bing Maps.

Figure 68. Close-up image showing the location of Meridian-3. Image is from Bing Maps.

Cable lays are visible on the satellite imagery that lead to the control base about 2 km east of the explosion site. The control base is characterized by disintegrated temporary wood and asbestos structures as well as cabling left from the experiment. (Figure 70).

Figure 69. Borehole of Meridian-3.

Figure 70. Remains at the control base of Meridian-3.

2.22. MERIDIAN-1 – 28 August 1973

Meridian-1 was a PNE conducted for a DSS profile in northern Kazakhstan. The location is reported as 100 km east of Arkalak, Kazakhstan (Nordyke, 2000). Sultanov et al. (1999) reports the location as being of GT 0.2-1 quality. Bing Maps imagery of the site shows ground disturbance near the location of Sultanov et al. (1999) though it is not sufficiently clear to confirm the coordinates with confidence. The currently available imagery from Bing Maps is better than Google Earth. Figure 71 is an overview of the location.

We conducted a field inspection and verified the Sultanlov et al. (1999) location as GT-0. The site is characterized by a concrete encased and capped borehole (Figure 72). The main borehole casing is visible for only a few centimeters under the concrete block cap. The main borehole is found at 50.52792°N, 068.32127°E, which differs only a couple hundred meters from Sultanov et al. (1999). Immediately adjacent to the device emplacement borehole is a smaller concrete pad with a presumed instrumentation or post-shot exploratory hole. Written on this pad is the number 100888 and the letters SPGO in Cyrillic (Figure 73). The meaning of the number and initials are not immediately clear, though could be a date from post-shot work at the site.

Figure 71. Overview of the Meridian-1 site from Bing Maps. The Sultanov et al. (1999) location is shown slightly to the southeast of the GPS coordinates obtained by field inspection if the site. The small white dot below the GPS location marker is the borehole. The two adjacent white dots are concrete pads probably used for erection of a support Extending southwest from the GPS location are two parallel lines which are probably cable trenches for signals to the experiment control site.

Figure 72. Capped borehole for the Meridian-1 PNE. The steel casing of the borehole is visible at the base of the concrete block. The smaller concrete bad and small borehole casing is highlighted in the next figure below.

Figure 73. Close-up of writing and instrument borehole.

Rough material incorporated in some of the concrete infrastructure consisting of medium grained greenish sandstone, medium and coarse grained brown sandstone, grey limestone, and soft friable grey shale that may be material extracted from the borehole. One piece of drill core of the greenish sandstone was found. One end of this drill core is polished and may represent a sample used in the geological characterization of the site.

Adjacent but several meters from the borehole are two concrete pads with threaded studs that we interpreted as mounts for a support tower. One additional instrument borehole angled slightly towards the main borehole was found. Additional concrete and other minor infrastructure are apparent at the site (Figure 74). There are no fences or warning signs indicating the nature of the site.

We found no evidence of radiation contamination at the site that was higher than regional background. Values across the site ranged between about 8-15 uR/hr

A **B**

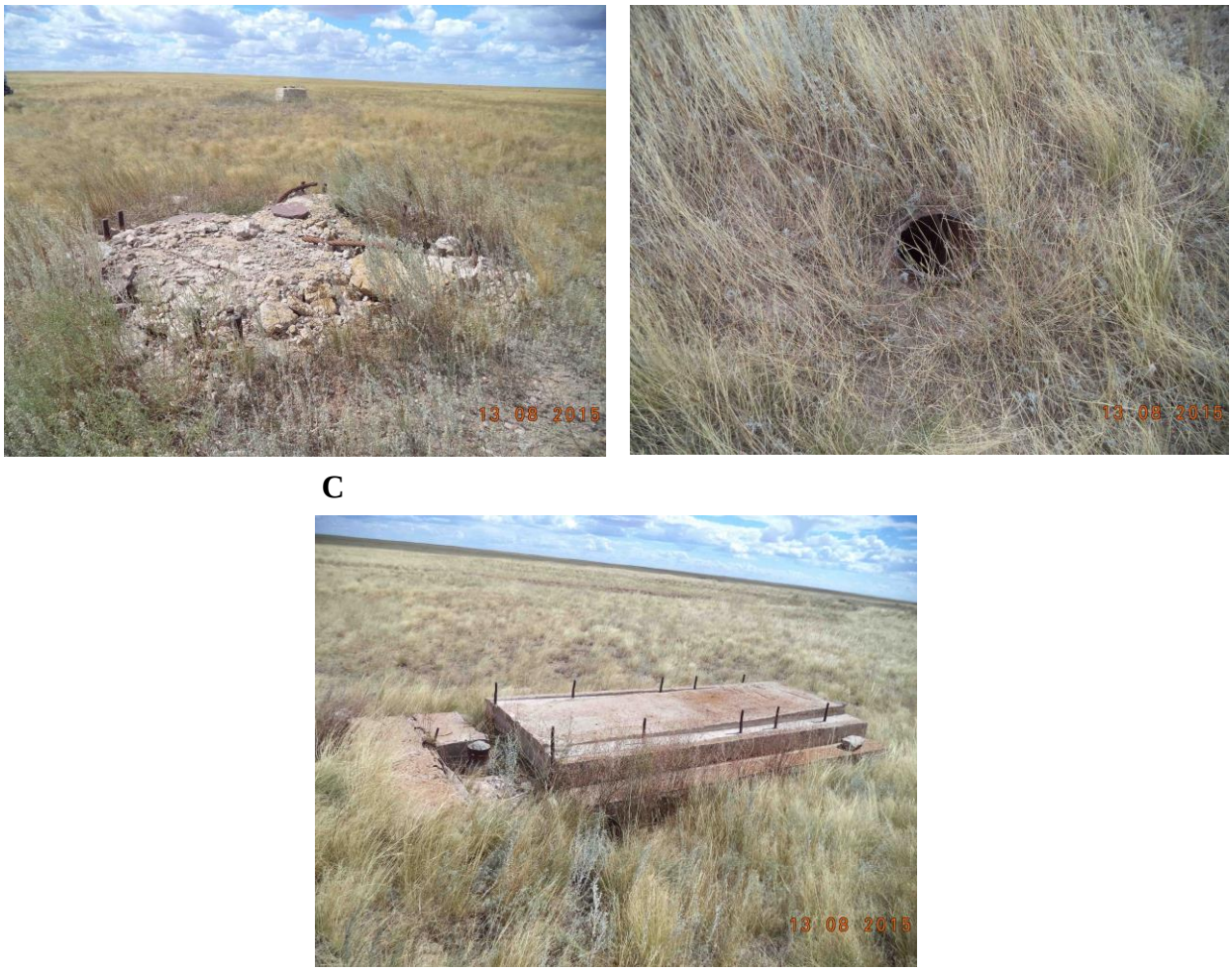

C

Figure 74. A. One of two concrete mounting pads in line with the main borehole and presumably used for a support tower. B. Instrument borehole casing. C. Concrete mounting pad of unknown use with an apparent borehole at one end.

Also visible in the Bing Maps image are two parallel lines extending from the region of the borehole to the southwest (Figures 71 and 75). We interpret these lines as old cable trenches used for control and instrumentation at the time of detonation. These lines extend 2.1 km and terminate

at approximately 50.5161ºN 68.29804ºE in another region of ground disturbance that appears to be an area previously occupied by structures based on apparent square foundations and trails. We interpret this as the control site for the Meridian-1 PNE. Ground inspection of the control site found a series of concrete piers (Figure 76), cable insulation consistent with that seen at other nuclear explosion sites, and evidence of light construction.

Figure 75. Bing Maps overview of the presumed PNE control site. The cable lays from the explosion site terminate here where the ghost of old infrastructure remain visible in satellite imagery. Several concrete piers are visible near the top of the image. On the ground at the site are the remains of light construction and asbestos panels.

Figure 76. Concrete piers at the control site for the Meridian-1 PNE.

2.23. MERIDIAN-2 – 19 September 1973

Meridian-2 is located in south-central Kazakhstan, about 200 km northeast of Kyzylorda, and is listed in Sultanov et al. (1999) as a GT0-1 located event. We confirmed the location as GT0 with an on-site inspection, finding the difference between the Sultanov et al. (1999) location and the GPS determination to be about 190 m (Figures 77 and 78).

Figure 77. The identified borehole location and Sultanov et al. (1999) published location are shown at left. Cable lays are visible extending to the experiment control point identified at right. Image is from Bing Maps.

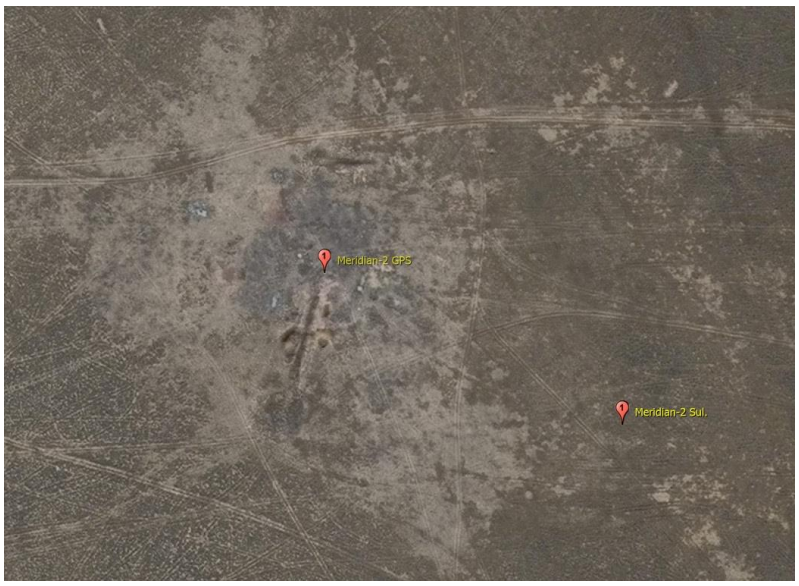

Figure 78. Close-up image showing the relative GPS and Sultanov et al. (1999) locations for Meridian-2. Image is from Bing Maps.

The borehole is typical of many PNEs and consists of a large concrete filled pipe and a circular metal 'Forbidden Zone' warning sign welded to the top (Figure 79). A second warning sign is installed in the ground adjacent to the borehole. One small diameter secondary borehole

was noted. Several concrete pads are at the site, one of which has the date '1973' written in it (Figure 80). We observed a slightly elevated radiation reading of 24 uR/h at one point near the borehole. Although not significant, this is about two times what seemed to be the normal background.

Figure 79. Borehole of Meridian-2.

Figure 80. Concrete pad at the Meridian-2 site. The year of the explosion is written into the concrete, which is highlighted with small stones for clarity. Additional writing on the pad is no longer visible due to deterioration of the concrete.

Cable lays are visible on the satellite imagery that lead to the control base about 2 km east of the explosion site. The control point is characterized by a circular artificial mound of dirt about 2 m in height with a depression on the top, resembling a miniature volcano. The mound is

surrounded by disintegrated temporary wood and asbestos structures as well as cabling left from the experiment (Figure 81).

Figure 81. Artificial mound at the Meridian-2 control point.

2.24. KAMA-2 – 23 October 1973

Kama-2 was conducted to create waste-disposal facilities 30 km west of Sterlitamak (53.656°N x 55.375°E) at a depth 2026 m; waste was pumped from Sterlitamak Soda Factory into the chimney through three holes from 1976-1993 (Nordyke, 2000). The same coordinates are given in (Norris and Cochrane, 1976). Mikhailov (1994) also states it was at 30 km west of Sterlitamak.

The region is in low-resolution in Google Earth (Figure 82). The correct location was identified by the site being labeled in a Wikimapia layer available in the SAS Planet GIS software. A high resolution image of the site is available from Geoportal Roscosmos (Figure 83) showing industrial infrastructure and enclosed areas. The site is about 5 km southeast of Maksimova, and ~30 km west of Sterlitamak (Figure 84) as visible on Soviet Military topographic maps. We can't determine exactly where within the complex the borehole is. The site is approximately 300 m across, thus we assign a GT-0 quality location to the center with a presumed maximum error of 150m. The Kama-2 site is about 12.4 km from the location published in Sultanov et al. (1999). A video about the site can be found at http://www.ria-bashkiria.com/video/517.html, where the entrance is shown (Figure 85).

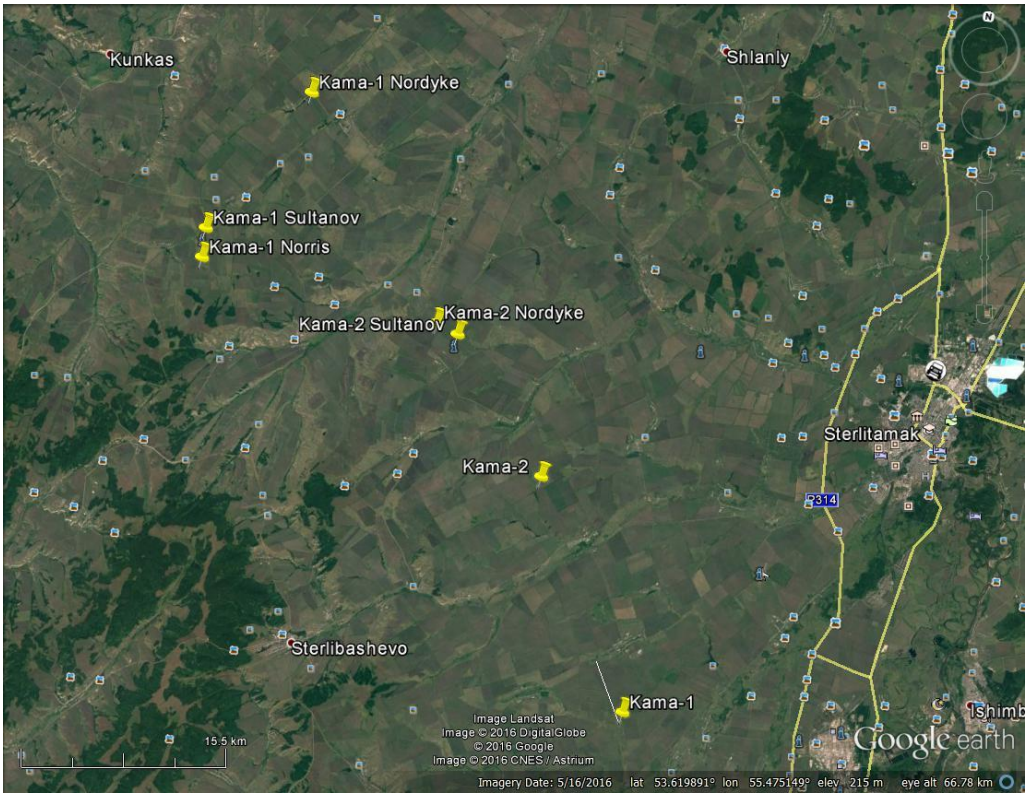

Figure 82. Google Earth image of region west of Sterlitamak showing various published locations and our determinations for both Kama-1 and Kama-2. Google Earth image © 2016 Digital Globe, © Google, © CNES/Astrium, and Landsat

Figure 83. Satellite image of the Kama-2 site. Image from Geoportal Roskosmos.

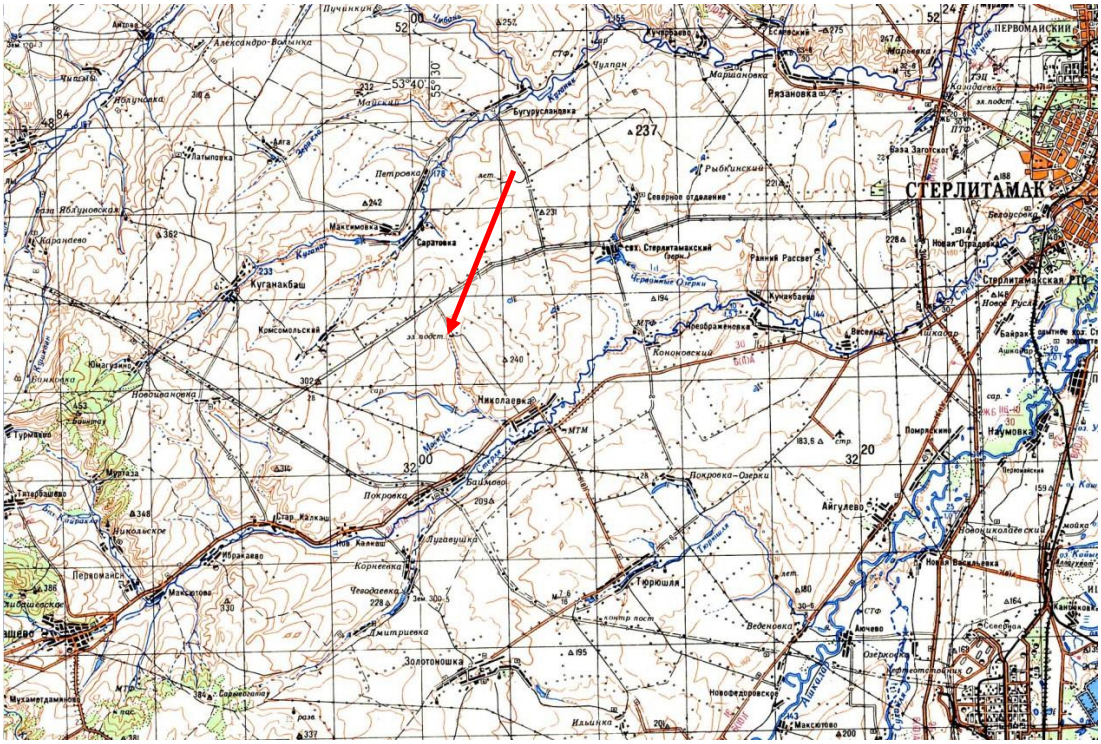

Figure 84. Soviet 1:200,000 topographic map N-40-20. Sterlitamak is at right edge. Figure 82 is in the center of the upper half of the map. The red arrow indicates the location of Kama-2.

Figure 85. Screenshot of the Kama-2 facility from a YouTube video found at https://youtu.be/X7aZ7HWhVFY. The video is embedded in the webpage at http://www.ria-bashkiria.com/video/517.html.

2.25. KAMA-1 – 8 July 1974

At the Kama-1 site, waste from the Salavat oil refinery was injected in 1983-1993, reportedly 30 km west of Sterlitimak (53.80°N x 55.20°E) at a depth of 2123 m (Nordyke, 2000). Norris and Cochrane (1996) gave coordinates of 53.68°N x 55.10°E. Mikhailov (1994) places it 20 km west of Salavat. Sultanov et al. (1999) lists coordinates as 53.70°N x 55.10°E.

Russian Wikipedia on the event states Kama-1 was detonated 18 km from Salavat, near the village of Il'inka (Figure 86). Residents were evacuated and it was felt with intensity II. Radioactivity was discovered in area in 2011.

Vasilyev and Kasatkin (2008) report that an improvised surface burial area for polluted soil and equipment was formed. A suspicious dark brown area (Figure 87) at 53.4020°N x 55.6343°E is identified in a low resolution Google Earth image 20 km west of Salavat. A high resolution black and white image is available from Geoportal Roscosmos (Figure 88). On this image, the village of Il'inka is abandoned and structures are removed. This would be consistent with a contaminated site. The identified brown spot from Figure 87 is apparent, and could be interpreted as a large burial mound. There are three small square fenced areas that could be borehole sites, either primary or for instruments or monitoring. These small square fenced areas are not typical for the region outside this site. In the north part of the image, there is a complex of buildings and a large fenced area. The building complex site is on the map in Figure 86, and shown in close-up on Figure 89. To the east of the buildings, there appears to be a small area enclosed with an earthen berm of fence with two large tanks and possibly pipes. The Kama-1 complex is verified by comparison of a recently found site plan in Shaybakova et al. (2013; Figure 90). We assign a GT0 location at 53.4097°N x 55.6387°E to the center of the large fenced area, which corresponds to the injection site at the facility (Shaybakova et al., 2013). This location is 48.1 km from the Sultanov et al. (1999) seismically determined location.

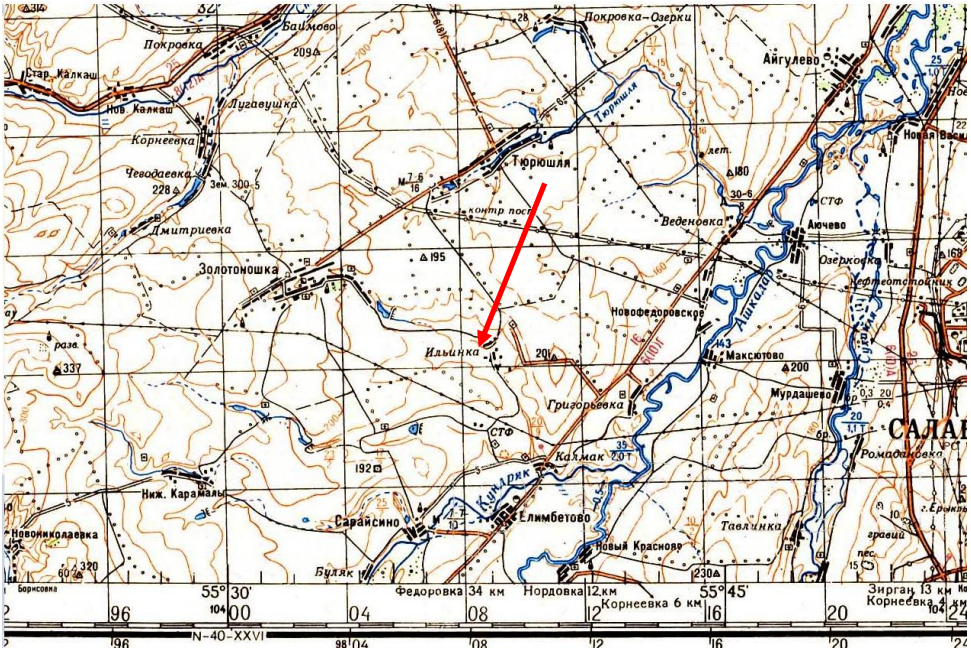

Figure 86. Soviet 1:200,000 topographic map N-40-20 (rescaled). Arrow points to Il'inka. Salavat is at right edge.

Figure 87. Il'inka and vicinity with possible burial site of contaminated material (arrow).

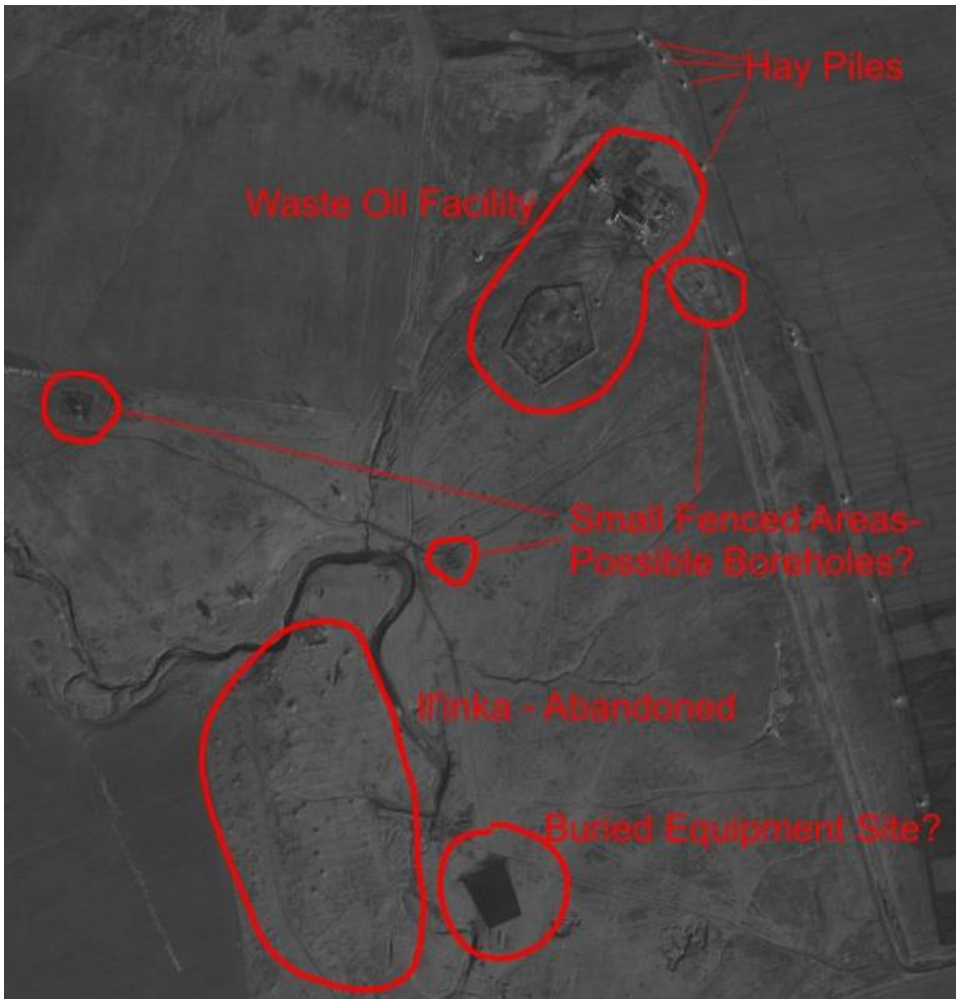

Figure 88. Interpretation of the Kama 1 PNE site. Imagery from Geoportal Roskosmos.

Figure 89. Interpretation of the Kama 1 PNE site waste oil injection facility showing storage tanks. Imagery from Geoportal Roskosmos.

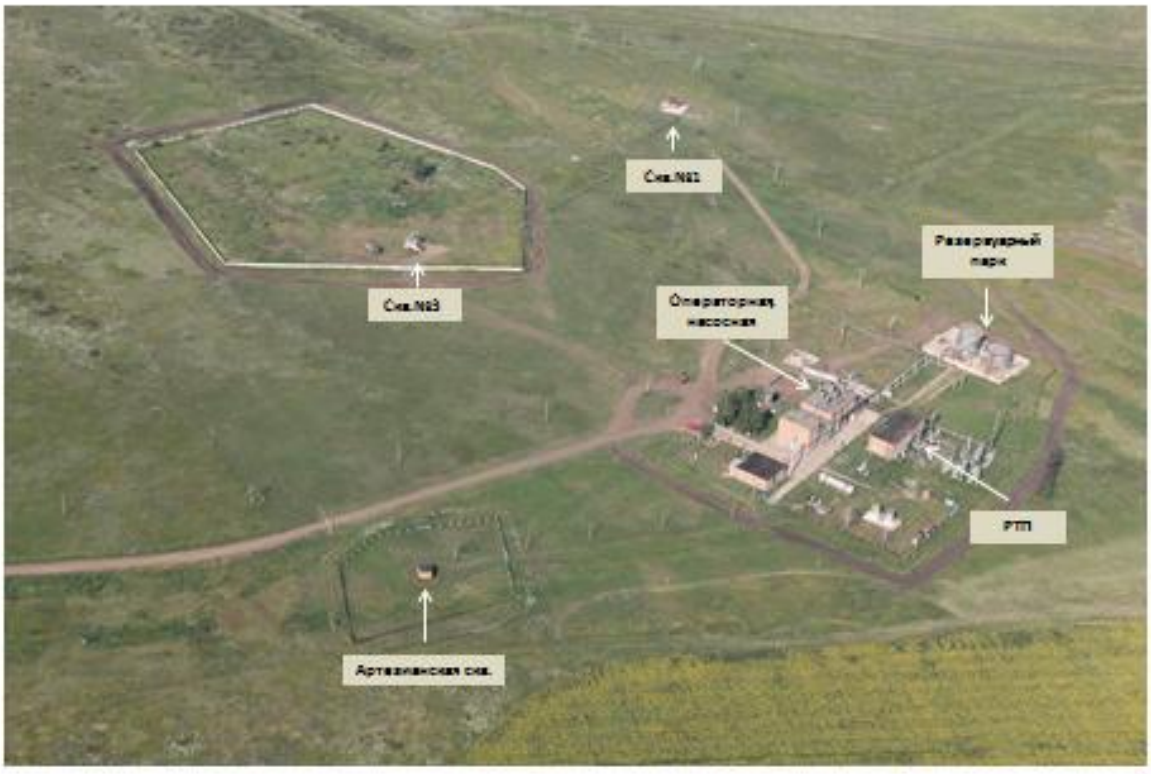

Figure 90. Plan of the Kama-1 facility (Shaybakova et al., 2013).

2.26. CRYSTAL – 2 October 1974

Crystal was a small (1.7 kt) explosion that occurred near the Udachnyi diamond mine in Yakutia to create the foundation for a tailings storage pond dam. The GT location for the Crystal PNE is presented in Fujita et al. (2013) and not revised here, though we present some additional information.

The Google Earth image of the Crystal PNE site as presented in Fujita et al. (2013) was taken 6/9/2004. The Bing Maps and Yandex.ru images both appear to be newer as they show that the shield covering the site has been expanded to the north, east, and south. This may suggest that radiation leakage may continue to be a problem and that the original shield did not contain the site. Figure 91 compares the two images.

Figure 91. Satellite imagery showing the expansion of the shield covering the Crystal PNE site. The older image on the left is from Google Earth while the newer image, on the right, is from Bing Maps and shows that the shield is considerable expanded.

A time-lapse series of photographs of the Crystal PNE was available at the site www.newpk.ru, though this site now seems linked to unrelated content. The time lapse series is shown below as Figure 92. Ramzaev et al. (2007) reports an initial mound was created that was 14 m high, and 180 m in diameter. Alekseev et al. (1993), Tsyganov (1993), and Gedeonov et al. (1997, 2002) indicate that a final crater 6 m deep and 60 m in diameter resulted. Analysis of the time-lapse photos indicates that there was essentially no ejecta expelled to form a true crater. It appears in the latter photos that uplifted material is collapsing back down into explosion cavity. If this is the case, then it would seem that the diameter of the uplifted dome should be approximately the same as the final collapse crater. If this is 60 m, than the scale markers visible in the images are about 10 m apart (the center markers appear to be somewhat closer together). This would also indicate that the uplifted dome reached a height of about 30 m. These measurements do not seem consistent with those reported by Ramzaev et al. (2007). If the scales determined above are correct, additional measurements, such as uplift rate, can be calculated as time scales are available with the photos.

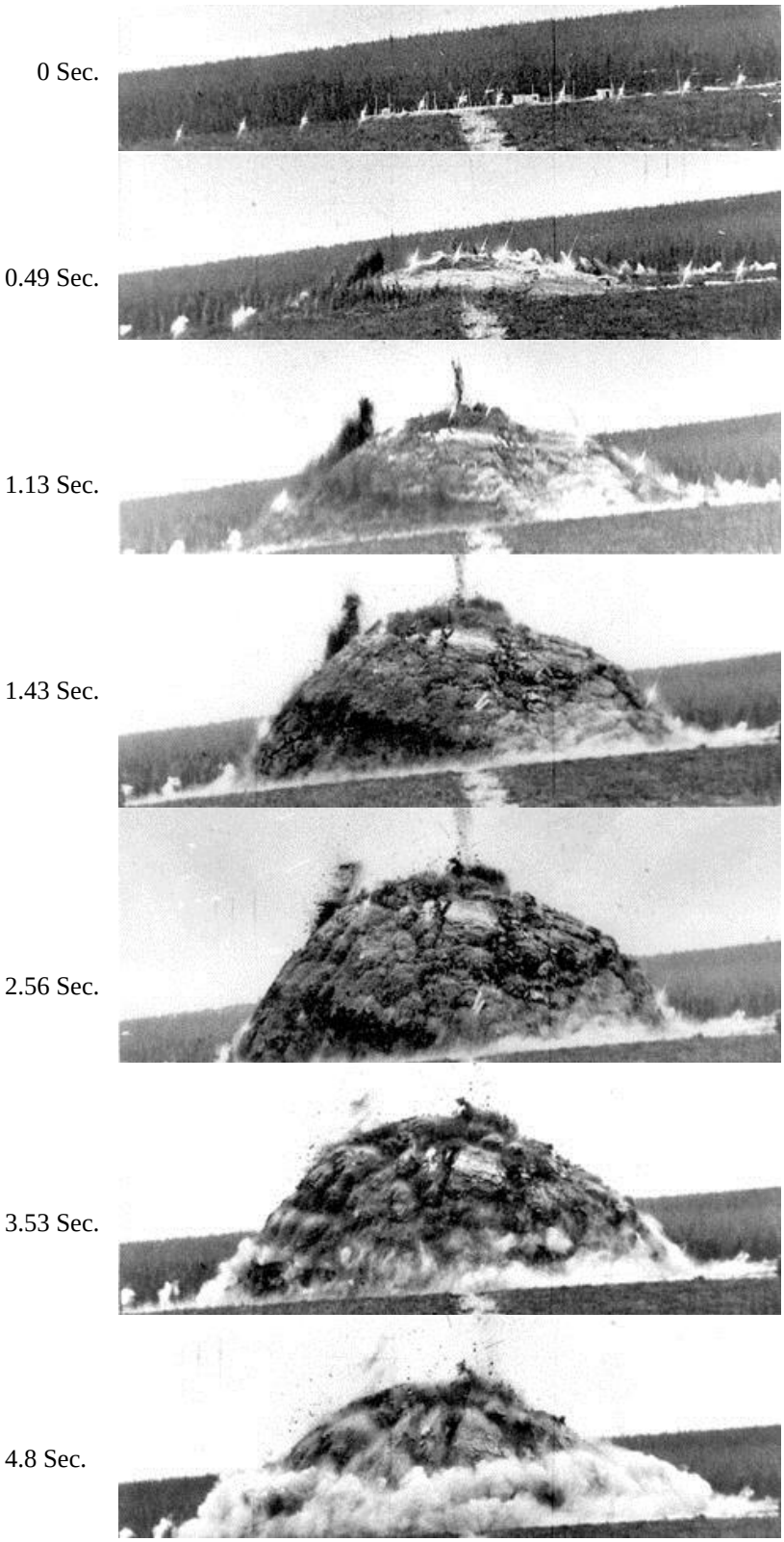

Figure 92. Time lapse sequence of the Crystal PNE from www.newpk.ru. View is looking to the northeast.

Some additional photographs and information on the Crystal explosion site are available at http://www.atomic-energy.ru/articles/2011/12/21/29710.

Sultanov et al. (1999) lists the coordinates for Crystal as 66.10°N x 112.65°E, 41.4 km from our previously reported coordinates in Fujita et al. (2013) at 66.4573°N x 112.3989°E.

2.27. HORIZON-4 – 12 August 1975

The site of the Horizon-5 PNE is described in Fujita et al. (2013) where the location was determined using low resolution imagery of the site. More recently, a higher resolution satellite image has become available on Here.com the resolves the site and shadow of the emplacement tower (Figure 93). Based on this, we have revised the coordinates about 50 m north from those published in Fujita et al. (2013). Two photos of the site have been published on the Yakutian site www.vecherka.ykt.ru, though the web address no longer seems valid. One photo is looking at the site across the Eekit River and shows the tower (Figure 94), and the second is a close-up of the tower (Figure 95). The tower was constructed for drilling the borehole and emplacing the bomb and survived the detonation.

Figure 93. Satellite image from Here.com that shows the Horizon-4 PNE site and remaining infrastructure. The shadow of the emplacement tower is visible extending to the north. A slight collapse crater having a diameter of about 130 m appears visible at the site.

Figure 94. View of the Horizon-4 PNE site as seen looking to the north across the Eekit River.

Figure 95. The emplacement tower for the Horizon-4 PNE.

2.28. HORIZON-3 – 29 September 1975

The Horizon-3 PNE was a part of the Horizon DSS profile. The explosion occurred north of Lake Lama in the northern part of the Krasnoyarsk Region, Russia. Meteorite-2 was detonated about 1 km NE of Horizon-3.

The best imagery for the site is found on Here.com, with identical imagery found on maps.ovi.com. An overlay of Wikimapia locations onto the Here.com imagery (Figure 96) indicates a site about 1 km NW of the Sultanov et al. (1999) location. No infrastructure or obvious candidate for the borehole is apparent in the satellite imagery. However, Ermite Z posted a photo of the borehole (Figure 97) on Google Earth and has additional photos in a Picasa Web Album at: https://picasaweb.google.com/118329769552267714082/3. Photos in this album are tagged with coordinates of 69.5831°N x 90.3179°E that place the borehole within 100 m of the Wikimapia location. Ermite Z has also posted photos from the nearby Meteorite-2 site taken on the same date. Tagged coordinates for the photo of the Meteorite-2 emplacement tower correspond exactly to those taken from the Here.com imagery. This indicates that coordinates tagged to Ermite Z's imagery are correct. Please see the section on Meteorite-2 below. Figure 98 shows the relation of the Horizon-3 location to the coordinates published in Sultanov et al. (1999) and to the location of the Meteorite-2 PNE.

Figure 96. Here.com imagery overlain with Russian Wikimapia locations for Horizon-3.

Figure 97. Photo of the Horizon-3 borehole. Photo from Ermite Z posted at https://picasaweb.google.com/118329769552267714082/3.

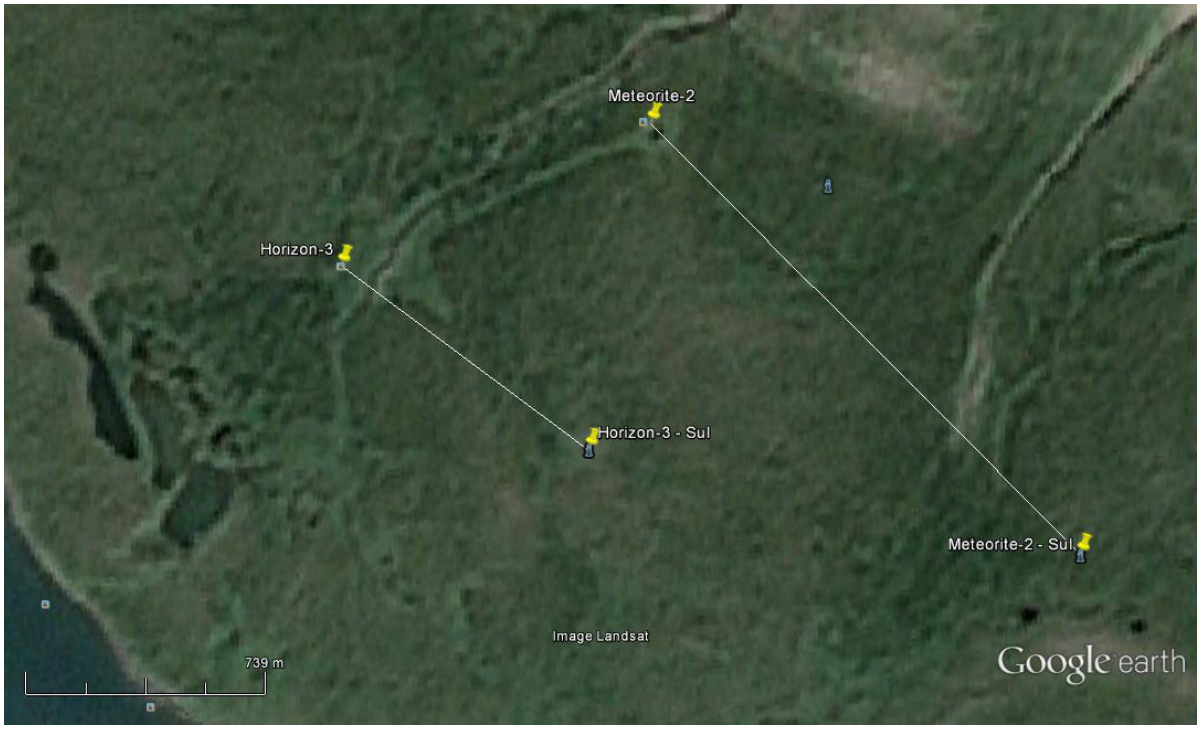

Figure 98. Google Earth (Landsat) image showing the shows the relation of the Horizon-3 and Meteorite-2 locations to the coordinates published in Sultanov et al. (1999).

2.29. METEORITE-2 – 26 July 1977

The Meteorite-2 PNE was a part of the Meteorite DSS profile. The explosion occurred north of Lake Lama in the northern part of the Krasnoyarsk Region, Russia. The PNE Horizon-3 was detonated about 1 km SW of Meteorite-2.

The Sultanov et al. (1999) location falls in a forested area about 2 km SE of the source area as identified in Wikimapia. The best imagery for the site is found on Here.com, with identical imagery found on maps.ovi.com. An overlay of Wikimapia locations onto the Here.com imagery mutually correlate the emplacement tower for Meteorite-2 (Figures 99 and 100). Both Wikimapia and Google Earth associate photos with the site that show the standing emplacement tower and remaining infrastructure (Figure 101). Ermite Z, one of the posters of photos on Google Earth, has additional photos in a Picasa Web Album at: https://picasaweb.google.com/118329769552267714082/202?amp;feat=directlink. Photos in this album are tagged with coordinates, which correspond exactly to coordinates obtained from the imagery. This album has several photos of the Meteorite-2 site, including a borehole and toppled radiation warning sign (Figure 102). Figure 98 shows the relation of the Meteorite-2 location to the coordinates published in Sultanov et al. (1999) and to the location of the Horizon-3 PNE.

Figure 99. Here.com imagery overlain with Russian Wikimapia locations for Meteorite-2. The gray area under the cross is vertical emplacement tower and surrounding ruins of infrastructure. The shadow of the tower can be seen faintly extending to the north. Figure 100 shows a zoomed image the location.

Figure 100. Close-up of Here.com imagery of the Metworite-2 site showing the remaining surface infrastructure. The shadow of the standing emplacement tower extends to the north.

Figure 101. Photo of the Meteorite-2 emplacement tower posted by Ermite Z on Google Earth.

A. **B.**

Figure 102. A - Toppled radiation warning sign at the Meteorite-2 site. B – Borehole and dosimeter at the Meteorite-2 site. Photos from Ermite Z posted at https://picasaweb.google.com/118329769552267714082/202?amp;feat=directlink.

2.30. KRATON-4 – 9 August 1978

The Kraton 4 PNE was previously located as described in Fujita et al. (2013). With the subsequent availability of higher resolution satellite imagery available on Bing Maps, we feel that the location should be moved about 300m south to approximately 63.6773°N x 125.5266°E where there are several sites with disturbed ground. There is no apparent ground disturbance at the Fujita et al. (2013) site. We cannot tell which of the points of disturbed ground represent the borehole, though all are within 100m of the new location. Figure 103 is a high resolution image of the site. The new location is about 200m east of the Sultanov et al. (1999) location.

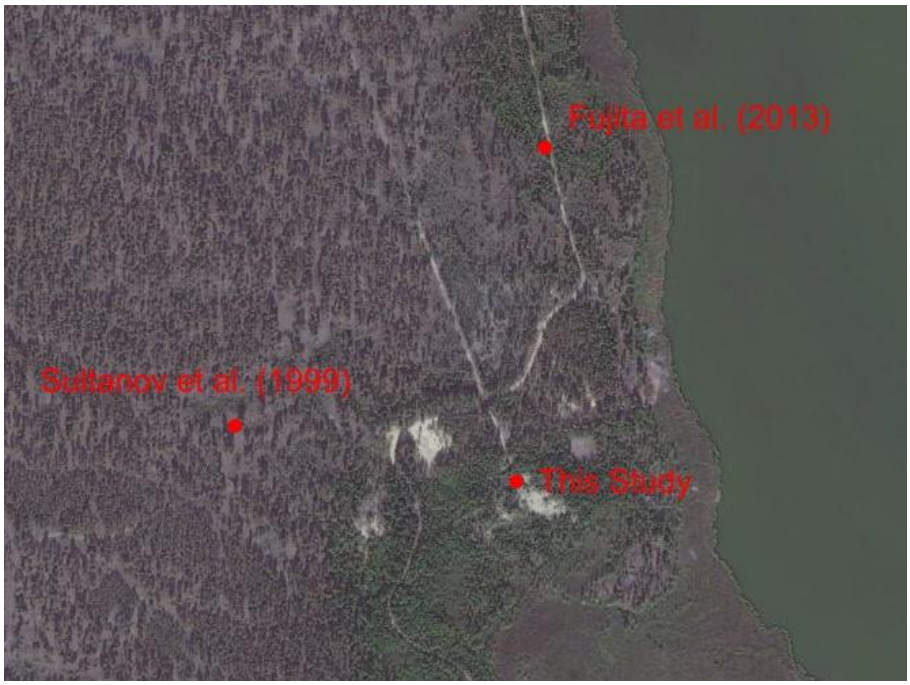

Figure 103. Revision of the location for the Kraton-4 PNE.

2.31. KRATON-2 – 21 September 1978

Kraton-2 was one of the PNEs used for the Kraton DSS line. The explosion took place within the long abandoned Ermakovo Gulag Camp located along the Yenisei River. The abandoned ruins of the camp extend several kilometers along the river and the hundreds of identifiable ruins presented a difficulty to confirm the location. However, the location is identified in the Russian Wikimapia. The best imagery of the site is from Bing Maps. An overlay of Wikimapia locations onto Bing Maps imagery clarifies geographic relationship to nearby ruins, placing the borehole about 50 m ENE from the camps abandoned train depot (Figure 104). One pair of photos posted on Wikimapia shows the borehole with the ruins of the train depot in the background (Figure 105), which compares identically with a photo of the depot posted on Google Earth by Sergei Metik (Figure 106). A comparison of different photos from Wikipedia indicate that the site is becoming overcome with vegetation (Figure 107).

The distance between the Sultanov et al. (1999) location and that found here is 1.59 km (Figure 108), thus the location error in Sultanov et al. (1999) slightly exceeds their stated GT0-1 quality.

The circular radiation warning sign atop the borehole (Figure 109) is typical to those found at other PNEs sites.

Figure 104. Bing Maps imagery overlain with Wikimapia sites. The approximate borehole location is indicated with the radiation symbol and the abandoned train depot is the large building just left of center. Dashed lines indicate abandoned rail lines. Note that the geo-referencing of the Wikimapia sites is about 10m off from the imagery.

Figure 105. Photos of the Kraton-2 PNE site and borehole posted on Wikimapia. The ruins of the train depot are visible in both photos. These photos appear rather old as ruins in the foreground are not thoroughly vegetated.

Figure 106. Photo of the old train depot as posted in Google Earth by Sergei Metik. This building and the Kraton-2 borehole is visible in the background of Figure 105.

A. **B.**

Figure 107. A- Older photo of the Kraton-2 borehole situated among ruins and. Note the lack of vegetation and the railroad tracks in the foreground. B- Newer photo of the Kraton-2 borehole surrounded by vegetation. Photos were taken from opposite directions as indicated by the light pole visible in both photos. Both photos were posted on and obtained from Wikimapia.

Figure 108. Google Earth image (© 2016 Digital Globe) showing the relation between the Sultanov et al. (1999) Kraton-2 location in the upper right and the location identified here at the lower left. The difference between the locations is 1.59 km.

Figure 109. Photo of the Kraton-2 radiation warning sign from Wikimapia. The sign says to not come within 350 m as radiation may be present.

2.32. KIMBERLITE-4 – 12 August 1979

The Kimberlite-4 PNE was located by Fujita et al. (2013) and there is no reason to change those published results. What is interesting to note is that the high-resolution satellite imagery now available on Bing Maps shows significant activity at the site. The Bing Maps satellite image is undated, though it is clearly winter as the lake to the north is frozen and covered with vehicle tracks. It seems that a series of roads or excavations have been constructed radiating from the Kimberlite-4 site (Figure 110). The confluence of the radiating spokes is within meters of the Kimberlite-4 identified by Fujita et al. (2013). Considering how remote the area is, it seems that there can be no question that the recent activity is connected to the Kimberlite-4 detonation site. It appears that a base consisting of small buildings, bulldozers, and trucks has been set up about 200-300m to the west. A few tens of meters to the north of the Kimberlite-4 site there appears to be a series of parallel-parked tanker trailers, or perhaps a series of parallel-bulldozed earthworks (Figure 111). It is difficult to tell with the resolution of the satellite image although they certainly seem to have some elevation as there appears to be snow on the north side indicating that it is in a shadow.

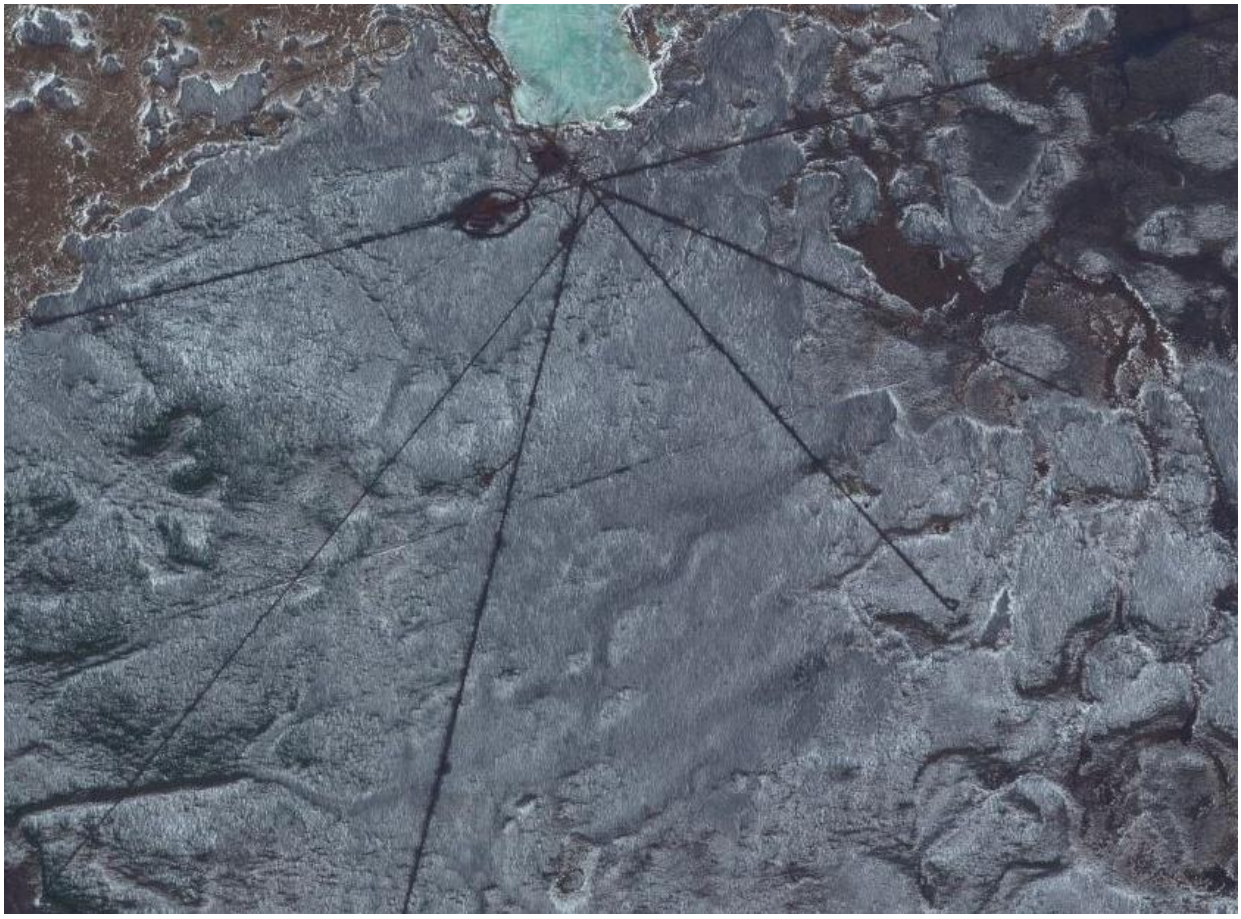

Figure 110. Bing Maps satellite image showing roads or excavations radiating out from the Kimberlite-4 PNE site. The purpose of the work is unknown, but seems clearly associated with the site.

The satellite images appear to be relatively recent and they do not look like the older Soviet Era aerial photographs. If this were an older aerial photograph, it could be interpreted as showing preparatory work for the PNE detonation back in 1979. The new roads visible in the photographs are not visible in the lower resolution Google Earth imagery. What appear to be older structures and roads are visible in both the low resolution Google Earth Imagery and the high resolution Bing Maps images. The radial spoke that strikes at about 070^{o} is traceable on high resolution imagery for about 70 km, at which point it is lost in a low resolution area. This strike is also not consistent with the original DSS profile which extended to the west.

We can only speculate as to why recent activity is taking place at the Kimberlite-4 PNE site. The possibility exists that radiation has been discovered and a crew has been working to clean and contain the site. The bulldozed roads may be for survey work. If one compares the Craton-3 site, most radiation damage to trees also falls along a strike of about 070^{o}, which may represent the dominant wind direction in the area, and may explain the longest new road extending from the Kimberlite-4 site. The presumed tanker trucks or earthen works may be the borehole site and what we are seeing is a constructed sarcophagus. We have not uncovered any literature about radiation leakage at the site.

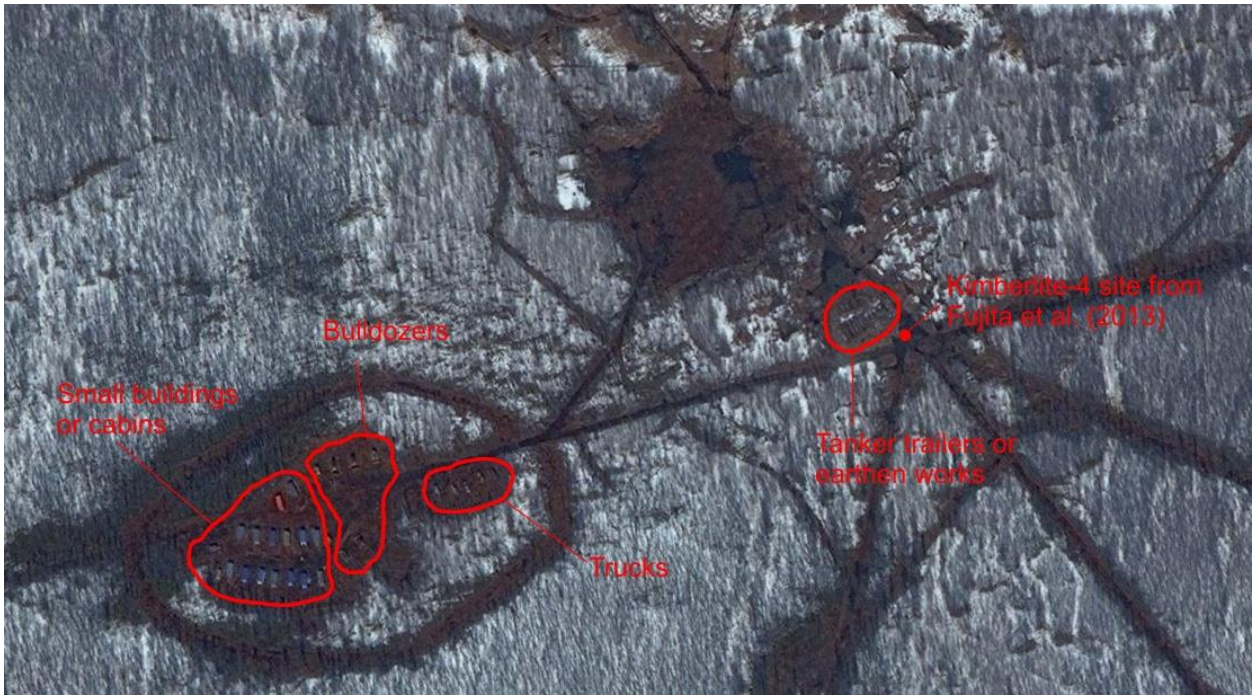

Figure 111. Close up Bing Maps satellite image of the Kimberlite-4 PNE site. The image date is unknown, but recent activity is clearly evident. Interpreted infrastructure is labeled. The small buildings or cabins are probably temporary and were probably towed to the site, which is typical for remote sites in eastern Russia.

2.33. CLEAVAGE – 16 September 1979

Cleavage was a small 0.3 kt explosion that took place in the Yunokommunarsk coal mine, about 5 km east of Yenakijeve in eastern Ukraine (Figure 112). The location of Cleavage was determined by a site visit to the mine and a discussion with mine's chief engineer. The explosion took place about 600m south of the mine's shaft house and approximately below the southeastern edge of the mine's tailings pile at the surface (Figure 113). The coordinates for the PNE Cleavage are 48.214ºN, 38.284ºE, approximately 2 km northwest from those given in Sultanov et al. (1999). The mine is no longer in possession of most information regarding the explosion, though the depth is confirmed as being between the 826 and 936 m levels, consistent with the 903 m reported by Sultanov et al. (1999).

Cleavage was not well recorded and there is no seismically determined epicenter. It was recorded at weakly NORSAR but not recognized as a nuclear explosion due to its small size until after the collapse of the Soviet Union when more information became available (Ringdal and Richards, 1992). From our discussions at the mine, seismographs were in-place and operating in other nearby coal mines when the explosion occurred. The explosion was preferentially recorded by stations to the east, while weakly visible on stations to the west. The reason for this is unclear. It is unknown if any of the mine seismograms still exist or if they are obtainable.

The mine is currently closed though being kept dewatered. Mining and government officials are unsure if or how radioactive contaminants may migrate if the mine is allowed to flood.

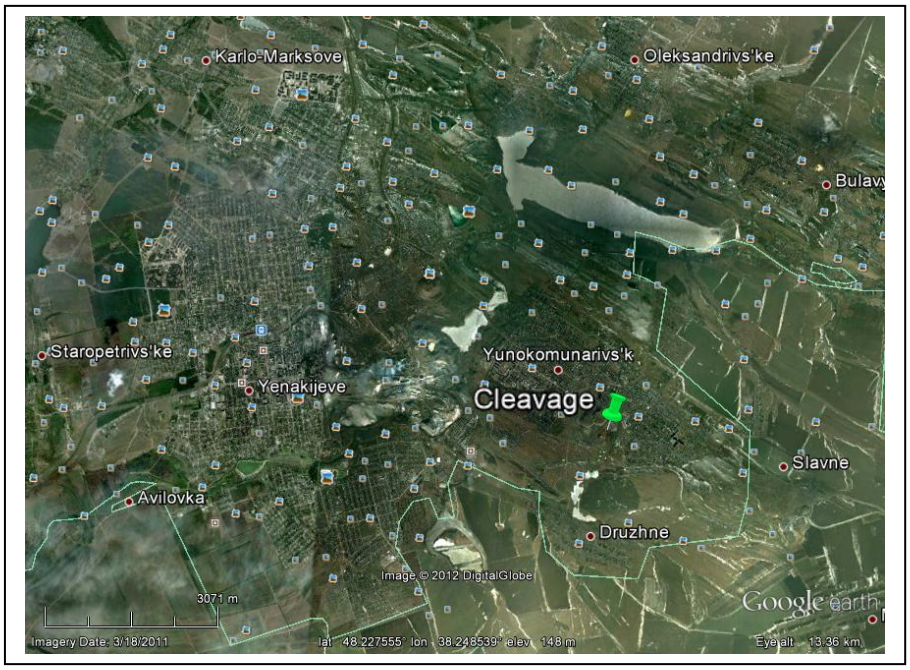

Figure 112. Location of the PNE Cleavage in eastern Ukraine, about 5 km east of Yenakijeve. Image from Google Earth.

Figure 113. Left – Location of the PNE Cleavage showing the relation to the mine shaft house and tailings dump. Image from Google Earth. Right – On-site photo of the mine tailing dump. The explosion took place at depth just to the left of the tailings. Photo by K. Mackey.

2.34. BUTANE 2-1 and 2-2 – 16 and 25 June 1980

The Butane 2-1 (borehole 1) and 2-2 (borehole 3) PNEs were 3 kt blasts at depths of 1400 and 1390 m respectively that occurred 15 km NW of Meleyz, Bashkiria, near 53.10°N, 55.87°E ("based on description of site"; Nordyke, 2000). It is reported that some gas is polluted with Tritium, and water from burning gas is polluted (Vasilyev and Kasatkin, 2008).

The Butane 2 PNEs are also reported west of Magnitogorsky near the village of Irgizly (Pochivalov, 1998). Note: Irgizly is located east of Meleuz and west of Magnitogorsk. This is 36 km east of the Sultanov et al. (1999) location and 74 km east of Meleuz. Other sources (e.g., Yablokov, 2003; Mikhailov, 1994) give the location as 40 km east of Meleuz. The Sultanov et al. (1999) coordinates are 38.6 km east of Meleuz.

Travel time analysis for Butane-2 are, like Butane-1, unclear, but could yield solutions either near the Sultanov et al. (1999) coordinates or those proposed for Butane-1 (q.v.). Both stations ARU and SVE had impulsive Pn arrivals, but they are essentially at the same azimuth. All other arrivals are emergent or questionable. A relocation of Butane 2-1 may provide useful information. See Section 2.2 and Appendix A.

Most likely the Butane-2 PNEs were detonated in close proximity to those of the Butane-1 sequence, and all authors give the same description for the detonation site for both, although they differ as to whether it was east or west of Meleuz. Based on the analysis for Butane-1, most likely the sources was northwest of Meleuz. Additional work is needed to identify the exact location.

There is a short Soviet Era documentary on the Butane explosion found at http://ludiwosleaeskotlov.1bbs.info/loc.php?url=http://www.youtube.com/watch?v=fmGnLRd_UnA.

2.35. VEGA SEQUENCE – 8 October 1980 – 27 October 1984

The Vega sequence consisted of 15 PNEs detonated to create caverns in rock salt for storage of gas condensate. All but the last two of the Vega PNEs are reported as GT0-1 locations in Sultanov et al. (1999). The last two, Vega 5-1 and 5-2 are listed with seismically determined locations. All the Vega PNEs took place in the vicinity of, or intermingled with, gas wells of the Astrakhan gas condensate field (Figure 114).

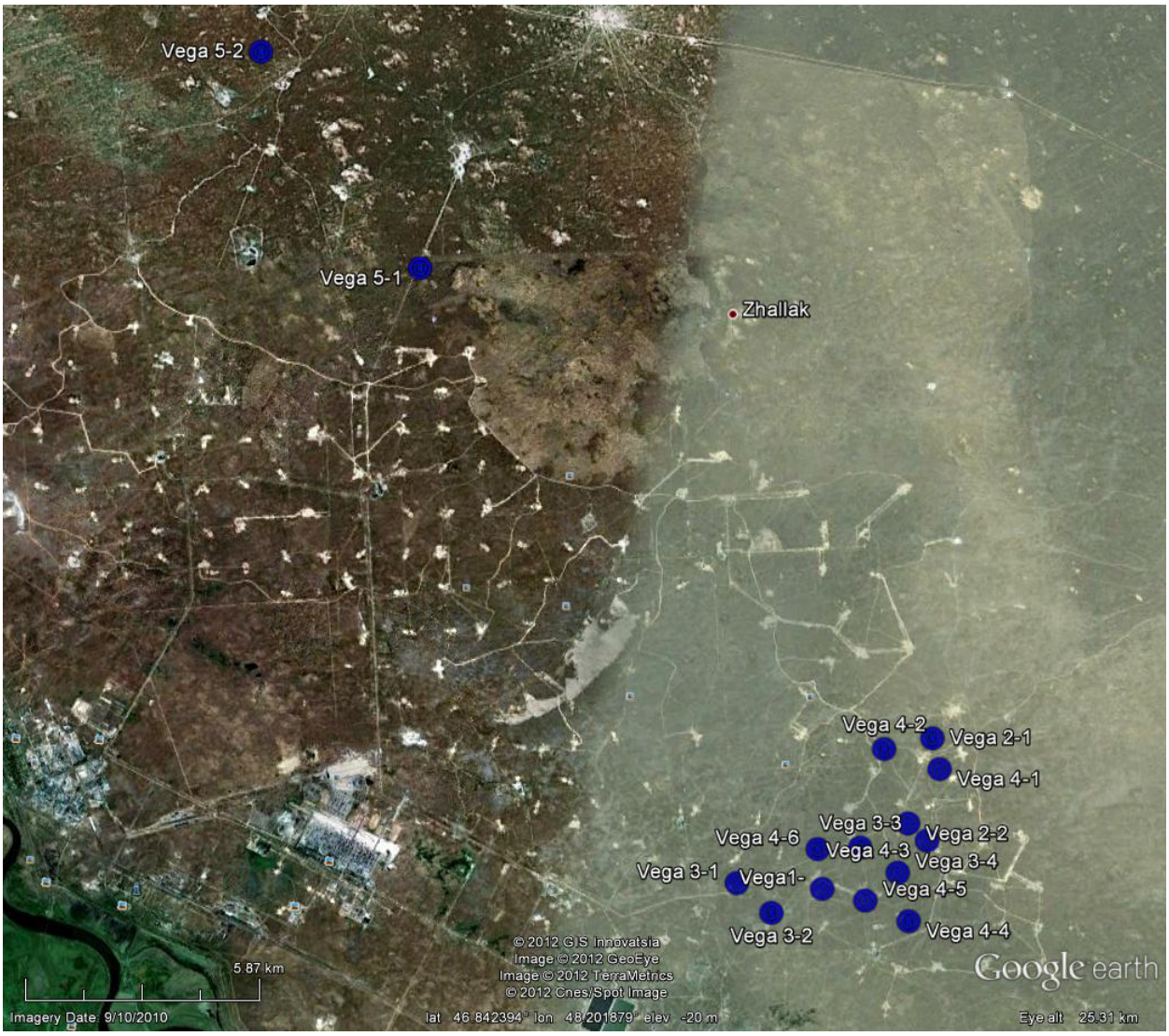

Figure 114. The Vega PNE region. Blue points represent locations from Sultanov et al. (1999). See Table 1 for coordinates. Image from Google Earth.

From analysis of satellite imagery using Google Earth and BingMaps, the Sultanov et al. (1999) locations of Vega 1 and the Vega 2 through 4 sequences appear good, and no errors exceed 0.6 km. Within a couple hundred meters of each Sultanov et al. (1999) location, there is generally a square, probably fenced or with a poured concrete pad. Figure 115 shows a couple examples, and the satellite imagery appears consistent with photos published photos by Nekhoroshev et al. (2011; Figure 116). The PNE sites are easily distinguished from the intermingled gas wells that

appear to have their own unique configuration in arrangement of infrastructure (Figure 117). The Vega 5 sequence is listed with seismically determined coordinates in Sultanov et al. (1999). We were unable to track down independent locations or satellite imagery features identical to the earlier Vega tests, though several sites are possible. Slightly revised coordinates from Sultanov et al. (1999) are shown in Table 3.

Figure 115. Google Earth image of the Vega 4-2 site (left) and the Vega 4-5 site (right). All the identified Vega PNE sites are characterized with a similar square concrete pad surrounding the site.

Figure 116. Photographs of Vega PNE sites (Nekhoroshev et al., 2011).

Figure 117. Typical configuration of the gas wells that are intermingled with the Vega PNE sites.

Table 3. Coordinates of the Vega PNEs.

#	PNE Name	Date MM/DD/YYYY	Coordinates – This Paper	Coordinates – Sultanov et al. (1999)	Difference in km
1	**Vega-1**	10/08/80	46.7565ºN 48.2738ºE	46.757N 48.275E	0.11
2	**Vega-2-1**	09/26/81	46.7936ºN 48.3088ºE	46.790N 48.313E	0.52
3	**Vega-2-2**	09/26/81	46.7760ºN 48.3012ºE	46.771N 48.304E	0.59
4	**Vega-3-1**	10/16/82	46.7582ºN 48.2447ºE	46.759N 48.247E	0.20
5	**Vega-3-2**	10/16/82	46.7494ºN 48.2569ºE	46.752N 48.258E	0.30
6	**Vega-3-3**	10/16/82	46.7688ºN 48.2858ºE	46.766N 48.288E	0.36
7	**Vega-3-4**	10/16/82	46.7597ºN 48.2987ºE	46.760N 48.300E	0.10
8	**Vega-4-1**	09/24/83	46.7812ºN 48.3197ºE	46.783N 48.315E	0.41
9	**Vega-4-2**	09/24/83	46.7872ºN 48.2966ºE	46.788N 48.297E	0.92
10	**Vega-4-3**	09/24/83	46.7671ºN 48.3079ºE	46.767N 48.310E	0.16
11	**Vega-4-4**	09/24/83	46.7500ºN 48.3006ºE	46.749N 48.303E	0.21
12	**Vega-4-5**	09/24/83	46.7538ºN 48.2877ºE	46.754N 48.289E	0.16
13	**Vega-4-6**	09/24/83	46.7657ºN 48.2740ºE	46.766N 48.274E	0.03
14	**Vega-5-1**	10/27/84		46.90N 48.15E	
15	**Vega-5-2**	10/27/84		46.95N 48.10E	

Text from online sources:

The Russian language Wikipedia document on the Vega PNEs has some interesting history and information. The reference and text below is from this site.

http://ru.wikipedia.org/wiki/%D0%92%D0%B5%D0%B3%D0%B0_(%D0%BF%D1%80%D0%BE%D0%B5%D0%BA%D1%82)

Vega" project - a series of 15 underground nuclear explosions ranging from 3.2 to 13.5 kilotons, implemented in 1980 - 1984 in the territory of the Astrakhan region to create a reservoir for the needs of the gas production . Currently, only two stores are used as intended , and the rest are in the pre-emergency condition, which causes criticism of environmentalists.

History

By analogy with the bombings "Highway" and "Sapphire", being made in the early 1970s, in the Orenburg region , the Soviet government decided to create a reservoir in the salt-dome uplifts near the Astrakhan gas condensate field . Most of them should have become repositories of gas condensate , and a broad fraction of light hydrocarbons , two more tanks to be used to purge gas production wells. For these purposes in 1980-1984 at 40-50 km from Astrakhan were carried out 15 nuclear tests at a depth of 1 kilometer 13 for storage in Aksaraysk Utigenskoy-ridge, the other two, to create a rascally reservoirs, Sarah-Sora and Aydikskom domes. Putting into operation of tanks has been slow, and many have not yet been used, when in 1986 all 13 stores Aksaraysk-Utigenskoy ridge for an unknown reason began to decline in volume. A year later, seven of them were in operation, the remaining use was impossible. According to calculations, the boundaries of tanks were glass, but some of them entered the water, which was dissolved radioactive residues and began to ascend to the surface of the earth. In June 1991, radioactive brine from the 5th hole broke through the wellhead valve [1] . In the early 1990s Rosatomnadzor inspected the stores, recognizing 13 of them pre-emergency. Operation of vessels engaged in branch " Gazprom "," Astrakhangazprom "until 1998 had no license to work with radiation sources. A few years of his employees were engaged in discharging radioactive brine and cleaning of contaminated rocks, unaware of radioactivity repositories.

In 1998, the Committee on Environmental Protection of the Astrakhan region said about exceeding the natural background radiation at the site 265 times, and was troubled neohranyaemostyu territories. This led to the theft of 800 meters of pipes that were previously in the well, leading to one of the repositories. Learning about the real situation at the facility, the workers' Astrahangazproma "began to demand compensation from the employer, and were fired. In 1999, the tanks were transferred to another subsidiary company "Gazprom", "Podzemgazprom." In November 2003 the euro last Solovyanov Alexander announced the tender for the liquidation of the "Vega", which was planned to completely shut down in 2006. Solovyanov announced that the store does not represent a real threat kilometer monoliths of rock salt to protect groundwater from ingress of radionuclides, the prosecutor's office confirmed his words. The method of conservation storage was chosen filling cement in the hole [2] . In August 2011 has been declared a regular tender for the radiation protection of wells. Most competitions have won a limited liability company "Volgaburvod" and "PKF Eurasia", the latter of whom had engaged in trade and baking bread. Some scientists, including well-known environmentalist Alexei Yablokov , show concern about the safety of the object. Much of the information about the "Vega" is in the closed access "Gazprom", two tanks are still used as the storage of gas condensate.

Notes

1. ↑ *V. Mikhailov* Technology USSR nuclear tests. The impact on the environment. Measures to ensure safety. Nuclear test sites and platforms . - New York: Begell-House, Inc., 1998. - (Soviet nuclear tests).
2. ↑ Astrakhan region. Object "Vega" is being prepared for preservation at the regions.ru

References

- Astrakhan underground Hiroshima online newspaper " Top Secret "
- "Gazprom" is trying to prevent an ecological disaster near Astrakhan on the marker.ru

AV Yablokov The myth of the safety and efficacy of peaceful nuclear explosions . - M ., 2003. - S. 60-61. - 175 p. - (Atomic mythology).

2.36. ANGARA – 10 December 1980

Angara was an oil stimulation experiment in Yesi-Yegovskii oil field. Containment and disposal efforts completed in 2002. Photo of decontamination facilities in 2001 (Figure 118) shown in Vasilyev and Kasatkin (2008).

Sultanov et al. (1999) give coordinates of 61.75°N, 66.75°E. Cited as 140 km NW Khanti-Manslysk, Khanti-Manslysk Autonomous Okrug (61.713°N x 67.018°E) with 15 kt blast at 2485 m depth (Nordyke, 2000). Earlier, coordinates were reported as 61.686°N x 66.999°E (Norris and Cochran, 1996). Alternatively described as southeast of the city of Niagan in Khanty-Mansi AO in Tyumen Oblast (Pochivalov, 1998).

Positive identification based on site photo (Figure 119). Google Earth and topographic coordinates of 61.7088°N±0.0016, 67.0710±0.0010°E (Figures 119 and 121) are 18 km from the Sultanov et al. (1999) location.

There is a documentary video visiting the site available at: **https://www.youtube.com/watch?v=gGW49QX5pCE.** Figure 121 shows the borehole in a screen capture from this video.

Figure 118. Angara site in 2001, view to south. Vasilyev and Kasatkin (2008). Note that the river is at flood stage in this photo and looks different than the river in Figure 62.

Figure 119. Site location on Google Earth based on Figure 118.

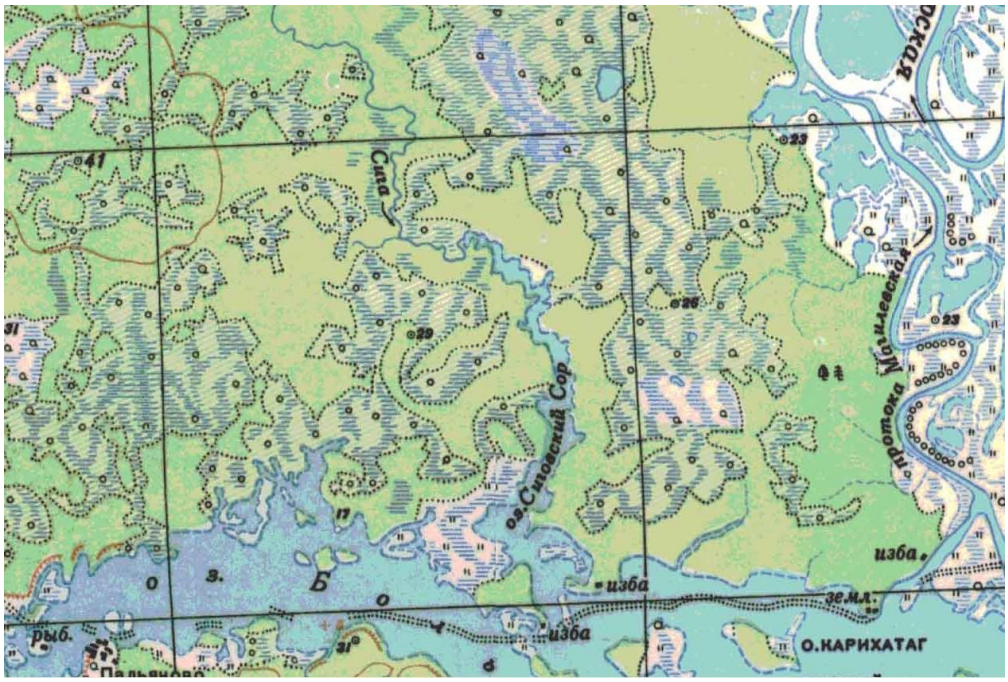

Figure 120. Site location on 1:200,000 Soviet topographic map.

Figure 121. The Angara borehole site. Screen capture taken from https://www.youtube.com/watch?v=gGW49QX5pCE.

2.37. HELIUM SEQUENCE – 2 September 1981, 28 August 1984, and 19 April 1987

The Helium sequence of PNE occurred in the Gezhskoe oil field, whch is about 25 km southeast of the town of Krasnovisbersk. The locations of the 5 detonation wells for Helium were interpolated in Google Earth from borehole in Utkin et al. (2007; Figures 122 and 123) in an article on radiation contamination of the Gezhskoe oil field. No coordinates or scale are given, but the borehole numbers are plotted. These sites range between 11 and 95 km from the seismically determined coordinates found in Sultanov et al. (1999). Helium 2-1 has the closest coordinates. Bing Maps has a better image of the site and each PNE location is marked by a characteristic square of grass surrounded by an embankment and with a linear concrete pad in the center (Figure 124). Only the 5 PNE boreholes have this character and all of the fields oil infrastructure is different.

According to Mikhailov (1999), Helium 1 was in shaft 401, 2-1 was in shaft 402, 2-2 was in shaft 403, 3-1 was in shaft 404, and 3-2 was in shaft 405. According to Kalmykov et al. (1999), however, the fifth detonation was in well 406 to the east of the others instead of hole 404 (note that this could be a typo for 405). The high resolution Bing Maps image does not show another characteristic grass square that could be interpreted as hole 406, thus we are confident in the hole 405 identification. The coordinates are approximately GT0 and difference with respect to Sultanov et al. (1999) are summarized in Table 4. These sites range between 11 and 95 km from the seismically determined coordinates found in Sultanov et al. (1999). Helium 2-1 has the closest coordinates.

Table 4. Summary of the Helium sequence PNEs.

PNE and Date	Latitude and Longitude	Depth and difference from Sultanov et al. (1999)
Helium 1 1981.09.02	60.2751±0.0008°N, 57.2991±0.0015°E	h = 2088 m; 95 km
Helium 2-1 1984.08.28	60.2695±0.0006°N, 57.2838±0.0014°E	h = 2065 m; 11 km
Helium 2-2 1984.08.28	60.2840±0.0006°N, 57.2840±0.0009°E	h = 2075 m; 48 km
Helium 3-1 1987.04.19	60.260±0.002°N, 57.263±0.003°E	h = 2015 m; 39 km
Helium 3-2 1987.04.19	60.2609±0.0006°N, 57.2981±0.0011°E	h = 2055 m; 61 km

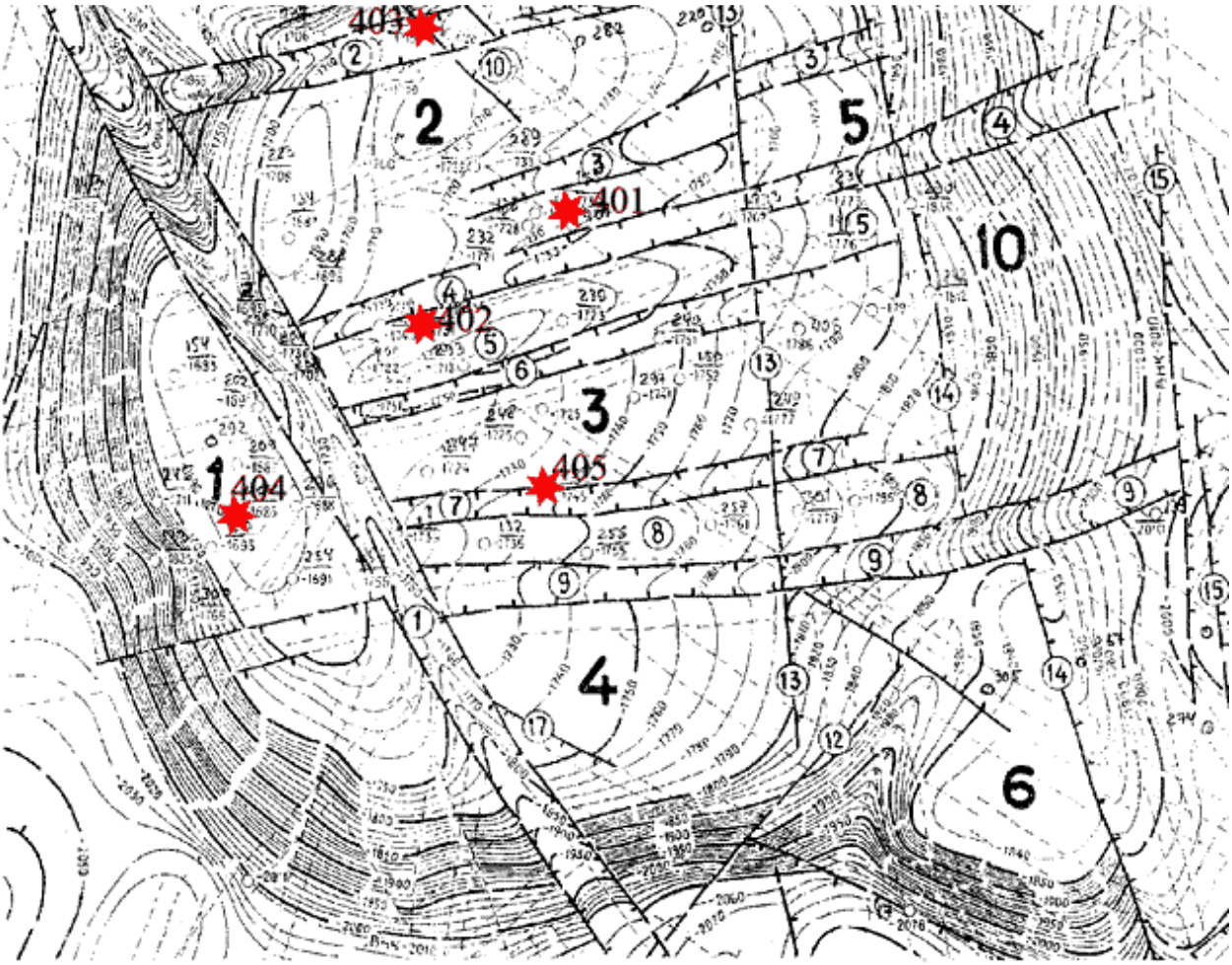

Figure 122. Map from Utkin et al. (2005) showing the borehole locations and numbers of the Helium PNE sites.

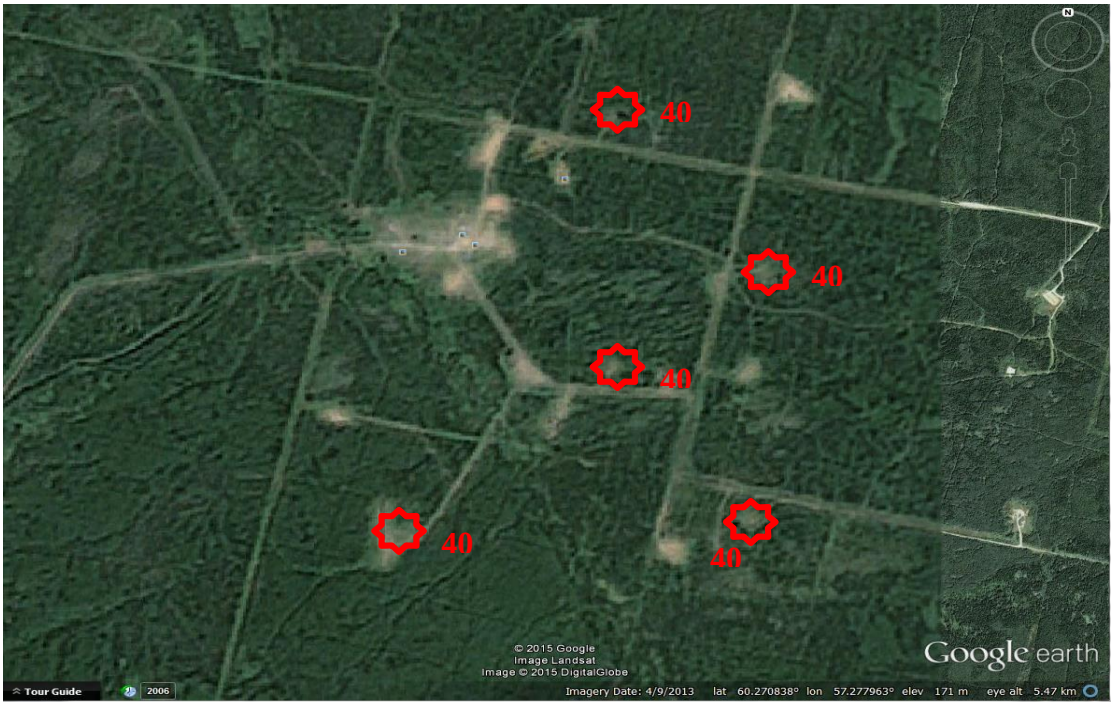

Figure 123. Google Earth image of the Helium PNE sites with borehole numbers indicated.

Figure 124. Bing Maps image of the Helium 3-2 site (grass square at right) and other oilfield infrastructure at left.

2.38. RIFT-3 – 31 July 1982

Rift-3 was one of the PNEs detonated for the Rift DSS seismic profile. It was detonated in the Irkutsk region of Russia about 170 km north of the city of Irkutsk. Rift-3 was located through a combination of sources. In particular, a news article on the explosion by Ulybina and Ignatenko (2005; http://baikal-info.ru/sm/2005/09/004001.html) has a photo of the borehoe with mountains in the background. The borehole location can be verified by matching the mountains and vegetation in the background with a 3-dimensional ground perspective view of topography from Google Earth (Figure 125).

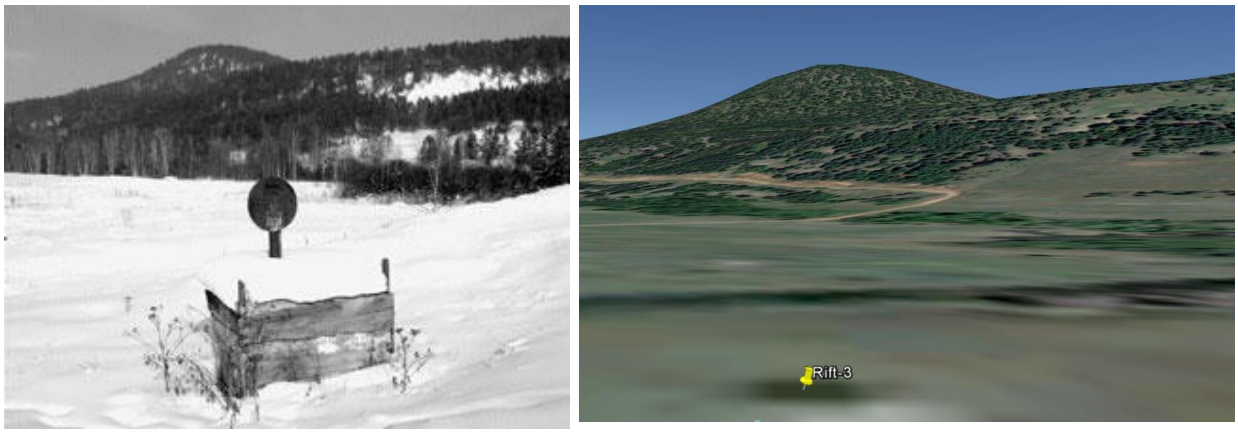

Figure 125. Photo (Ulybina and Ignatenko, 2005) of the Rift-3 borehole at left compared with a Google Earth ground perspective view. The perspectives match allowing the verification of coordinates.

Additional photos and discussion of potential radiation contamination in the area of Rift 3 are provided in Startsev (2012; https://travel.drom.ru/19390/). In particular there is a large water tank visible in close proximity to the borehole (Figure 126). Startsev indicates that the tank was used for water storage during the drilling of the borehole used for Rift-3. The tank is visible in Bing Maps imagery, further correlating the borehole location (Figure 127). The true location of Rift-3 is 4.5 km southwest from the Sultanov et al. (1999) coordinates (Figure 128).

Figure 126. Photo of the Rift-3 location from Startsev (2012) showing the water tank at center-left and borehole top in the snow at far right (arrow).

Figure 127. Bing Maps image of the Rift-3 site where the borehole and associated water tank are visible.

Figure 128. Google Earth image showing the location of the Rift-3 borehole to that determined by Sultanov et al. (1999).

2.39. LIRA SEQUENCE – 10 July 1983 and 21 July 1984

The Lira sequence of PNE consisted of two sets of three explosions, for a total of six, near the Karachagansk oil and gas complex in northwestern Kazakhstan. All six explosions took place within salt domes to create storage tanks for gas condensate. The Sultanov et al. (1999) locations all correspond closely to circular fenced structures visible in satellite imagery (Figures 129 and 130), and are also consistent to a location map in Ageyeva et al. (2008). A ground level photo of the Lira 2-2 site is posted in Google Earth by timn.harrison (Figure 131).

We also investigated the lira sequence in the cluster analysis presented in Appendix A. The cluster analysis identifies some discrepancies in the associations of borehole to event. Specifically, in the cluster analysis, all 6 Lira PNEs align in in a trend parallel to the Sultanov et al. (1999) and satellite image visible borehole locations, though offset about 7 km to the southwest (Figure 132). Relative positions of the three northern events in the cluster analysis correspond almost exactly to the northern three events from Sultanov et al. However, the specific events are in different order (Figure 133). Lira 2-2 shifts from the southern location to the northern end within this cluster and Liras 2-3 and 1-3 each shift one position lower. In the cluster analysis for the southern three events, Lira 1-2 and 2-1 plot close to the Sultanov et al. (1999) 1-2 position, and Lira 1-1 shifts to be near the Sultanov et al. (1999) 2-1 position. In general, most of the positions calculated from the cluster analysis plot close to borehole locations, but the transposed locations indicates that Sultanov et al. (1999), and perhaps other researchers or documentation, is suggestive that there may be documentation errors on the correlation of events to boreholes within the cluster. Because of this,

we have assigned larger errors or GT criteria numbers on the Sultanov et al. (1999) such that they could associate to the cluster analysis location. With respect to the Lira sequence, it may be necessary to go back to original material in Kazakhstan to verify the correct event identification with each borehole. See Appendix A for additional discussion.

Figure 129. Google Earth image showing an overview of the Lira PNE locations. Labels with 'Sul.' are Sultanov et al. (1999) locations while other markers are from this study.

Figure 130. Typical view of the Lira PNE sites. This Google Earth image is of the Lira 2-2 location.

Figure 131. Photo of the Lira 2-2 site as posted on Google Earth by timn.harrison.

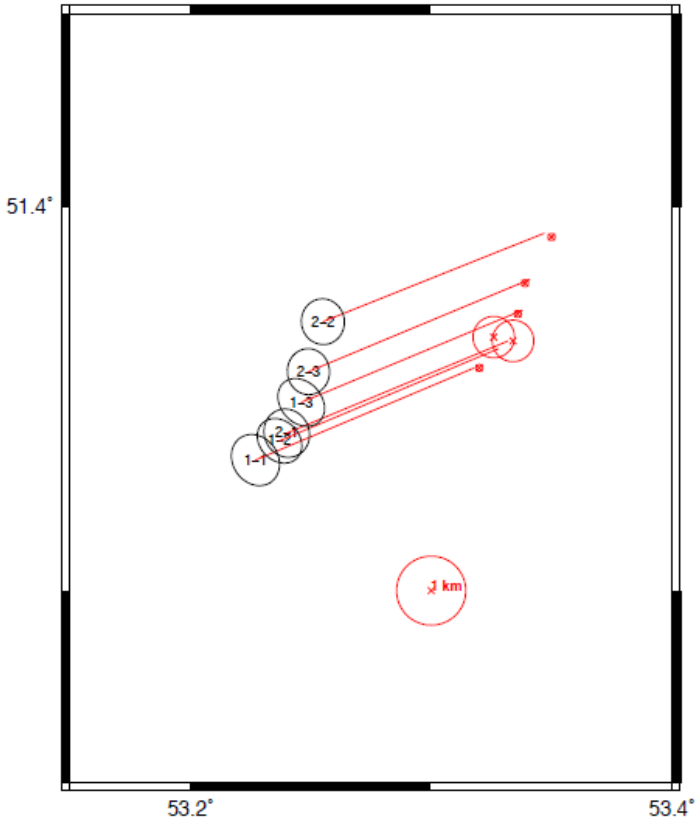

Figure 131. Relative locations of the Lira PNEs and the shift (red vector) required to bring them into concordance with the assumed shot sites. The confidence ellipses (90% confidence level) for relative location (cluster vectors) are shown in black. The locations of the reference locations that were used to calculate the calibration shift of the cluster as a whole are shown as red x's, and a circle around each site represents a measure of the uncertainty in the location. A circle of 1 km radius is shown for scale.

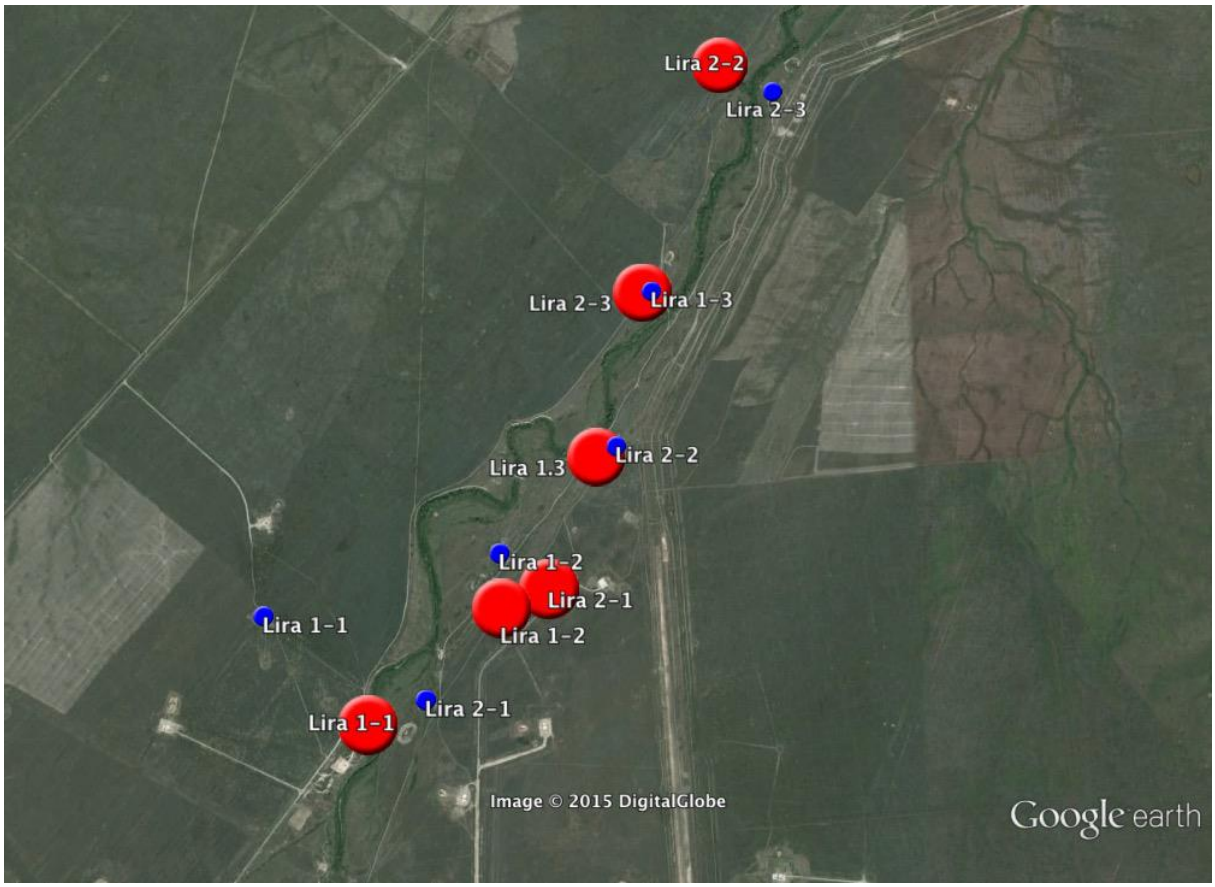

Figure 132. Satellite imagery of the source region of the Lira PNE sequence (*Google Earth, 2015*). Large red icons are the locations from the cluster analysis in Appendix A. Smaller blue icons are the borehole locations that correlate with the Sultanov et al. (1999) reported explosions.

2.40. QUARTZ-4 – 17 September 1984

The Quartz-4 PNE was a part of the Quartz DSS profile and occurred in the Kemerovo region of Siberia.about 25 km south of the village of Upper Chebula. The Sultanov et al. (1999) location is in the northeast corner of a large field (Figure 133). There is nothing characteristic in the available satellite imagery that could verify the Sultanov et al. (1999) location.

There is a YouTube video posted by Wind Strangers (2015; https://www.youtube.com/watch?v=9rmdUTQyGeA) summarizing a trip to the Quartz-4 PNE site. In the video, they mention that the site is across the field (they came in from the east), which would put it on the west side. At the borehole site, a considerable amount of time is spent investigating the wreckage, and then the narrator walks about 100 m down a slope to a ford across a stream. The segment of road that was hiked and stream was identified on satellite imagery, thus verifying the borehole location, which is near the southwest corner of the field (Figures 133 and 134). A screenshot from Wind Strangers (2015) shows the view from near the borehole location towards the stream (Figure 135). The borehole itself is being overgrown by vegetation (Figure 136).

Figure 133. Google Earth image showing the relationship between the Sultanov et al. (1999) location and the site identified in this report.

Figure 134. Close-up of the Quartz-4 detonation site. The stream is highlighted in blue and the road hiked in the Wind Strangers (2015) video is shown in yellow. The screenshot in Figure 135 was taken from the red arrow location. Image is from Google Earth.

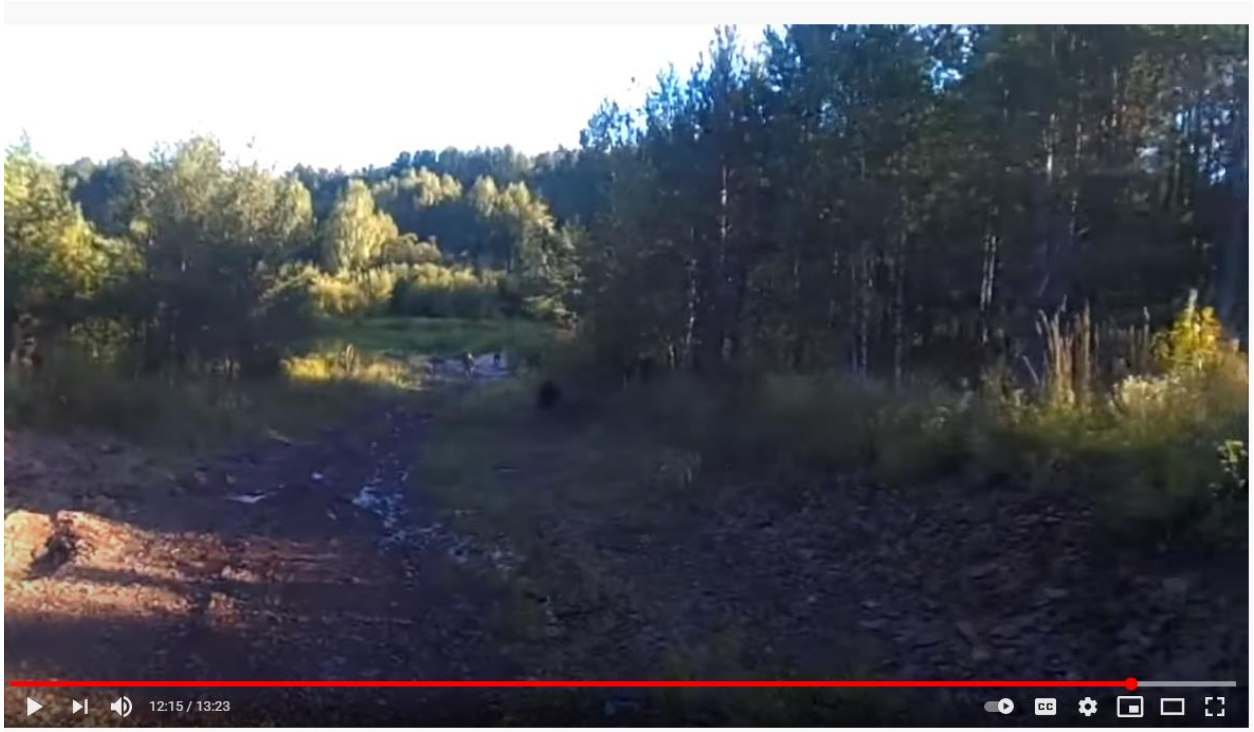

Figure 135. Screenshot from Wind Strangers (2015) showing the road connecting the Quartz-4 borehole location to the stream.

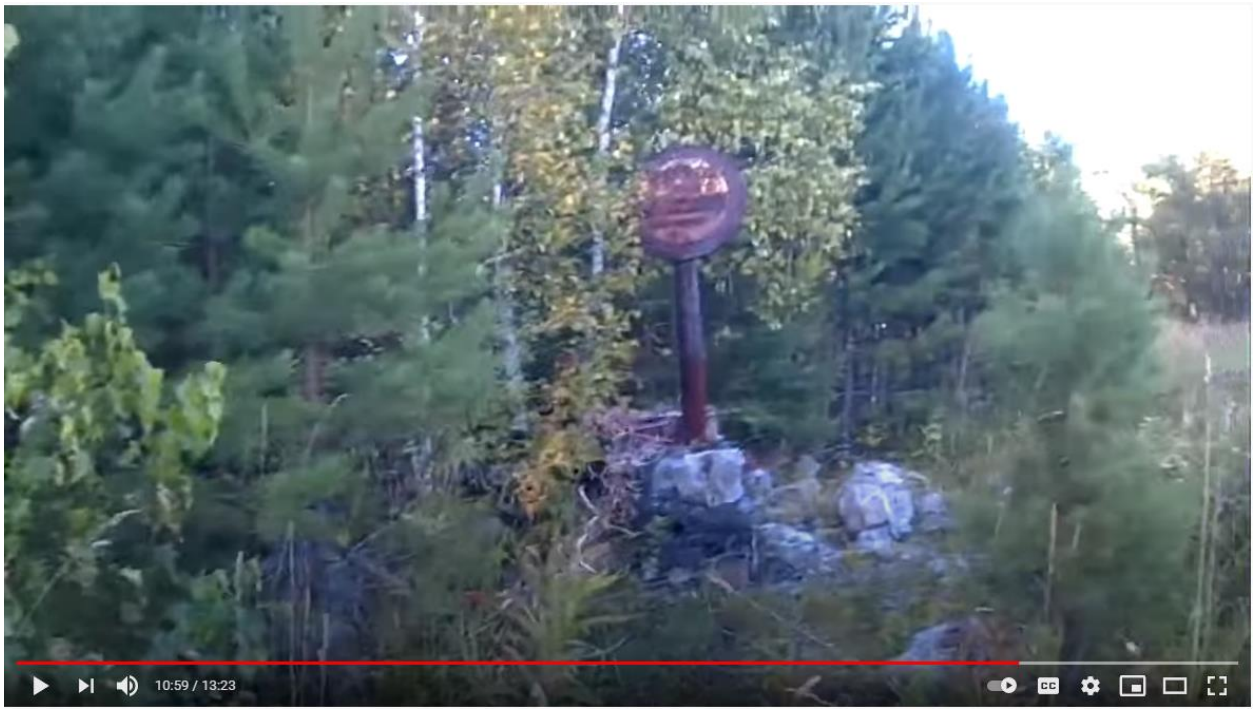

Figure 136. Screenshot from Wind Strangers (2015) of the Quartz-4 borehole.

2.41. BATHOLITH-2 – 3 October 1987

The Batholith-2 PNE was part of a DSS profile and is reported by Nordyke (2000) to have been detonated 320 km SE of Aktubinsk, Kazakhstan. Sultanov et al. (1999) reports the location of Batholith-2 as meeting GT-10 criteria.

We conducted a site visit to the vicinity of Batholith-2 to verify the location. After two days of investigation in the region, we were unable to locate the borehole. We did identify several landmarks in the region, including livestock and hydrocarbon infrastructure (Figure 137). We can state with certainty that the location is not at the Sultanov et al. (1999) coordinates, though the published GT-10 quality location may still be valid. Figure 138 focuses on the region surrounding the Sultanov et al. (1999) location. Two additional locations were provided by the Institute of Nuclear Physics of Kazakhstan, labeled GIS Location A and B, though no evidence of the borehole was found at either site.

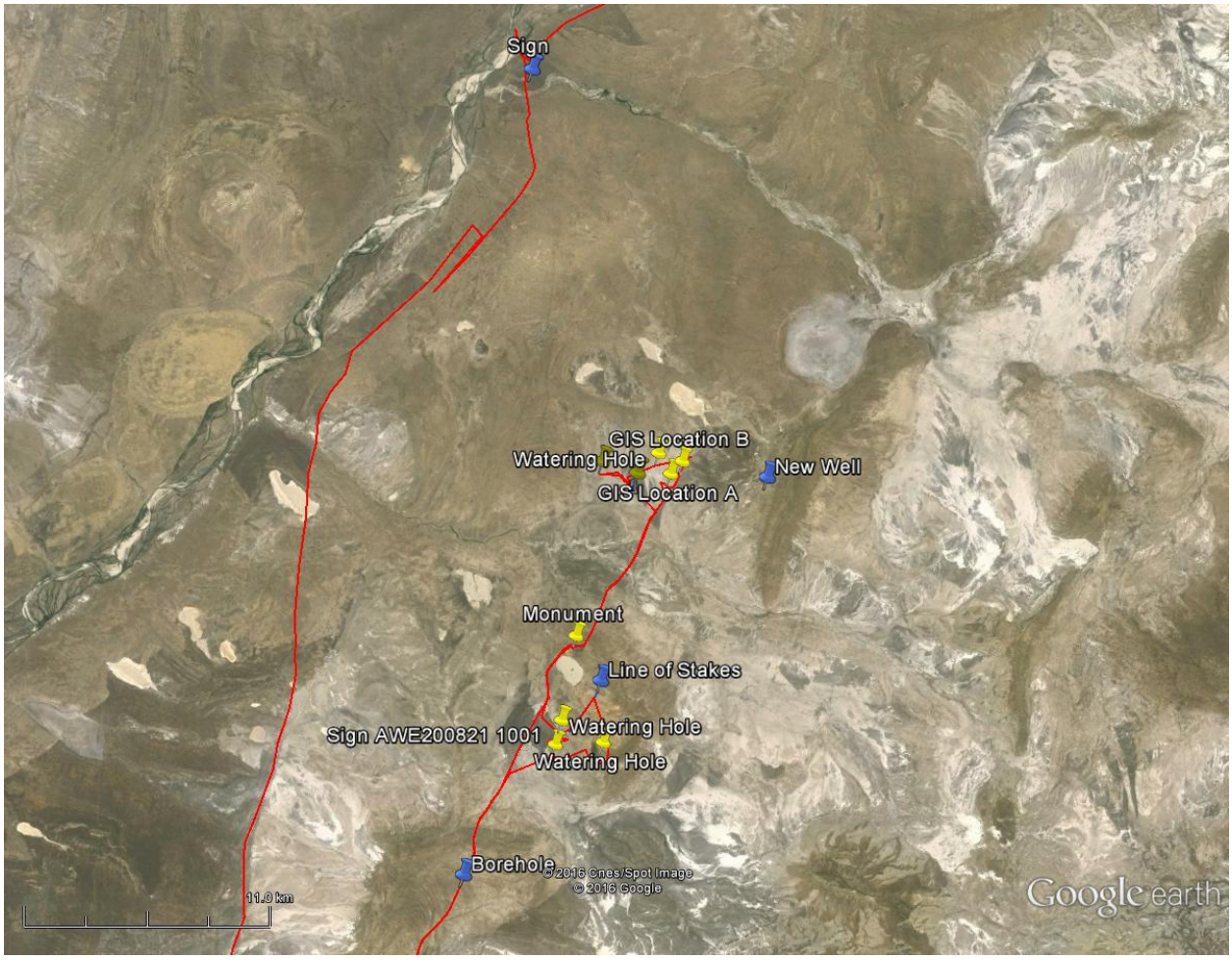

Figure 137. Regional overview of the Batholith-2 PNE site indicating locations visited and approximate driving routes. Image is from Google Earth (© 2016 Cnes/Spot Image).

Figure 138. Localized overview of the reported Batholith-2 PNE site indicating locations visited and approximate driving routes. The borehole was not found at the reported Sultanov et al. (1999) location, labeled 'Sul.' or either GIS location proposed by the Institute of Nuclear Physics. Image is from Google Earth (© 2016 Cnes/Spot Image).

There is evidence that there has been relatively recent exploration in the region, probably related to oil and gas fields to the north. A line of wooden steaks was observed over a couple km, terminating at a sign that read 'AWE 200821 1001' that aligns with a small diameter borehole found in the southern portion of the region and a new drill pad in the north visible on newer Bing Maps imagery (Figure 137). A similarly lettered sign was found in the northwest that also indicated a possible 2008 date.

Verification of the location of the Batholith-2 PNE will require additional research. We spoke with people in two of the local villages who told us that they were aware of the site and that there were a few people who worked on the emplacement crew. They also indicated that there was some scientific investigation by foreigners at the site following the fall of the Soviet Union. With additional field time, we are certain that the location is verifiable. Alternatively, the location may be obtained through other investigation or the DSS data from the experiment, though the waveforms available from IRIS are missing the metadata that would contain the source location.

2.42. RUBY-2 – 22 August 1988

The Ruby-2 PNE was part of the last Soviet DSS profile that utilized nuclear explosion sources. The Sultanov et al. (1999) location appears accurate at the GT0-1 level based on imagery available on Google Earth where the emplacement tower is still standing (Figure 139).

Figure 139. Google Earth (© 2016 Digital Globe) image of the Ruby-2 site showing the apparent emplacement tower about 120m north of the Sultanov et al. (1999) location. The image date is 5/5/2004, though only recently became available on Google Earth.

There are additional photos and information of the Ruby-2 site found in Kryukov et al. (2015; Figure 140). In 2012 the emplacement tower was scheduled to be demolished due to deterioration and the site cleaned.

Figure 140. Photo of the Ruby-2 emplacement tower and borehole warning sign from Kryukov et al. (2015).

3. CONCLUSIONS AND RECOMMENDATIONS

The explosions of the Soviet PNE program represent a large dataset of GT events that are useful to the nuclear explosion monitoring community as well as seismologists in general. This project has determined or verified 85 of 122 Soviet PNE locations at a GT 0-1 level. The work presented in this report should be expanded to verify the remaining 37 Soviet PNE Locations.

4. ACKNOWLEGMENTS

This project was sponsored by the U.S. Department of State under Order No. SAQMMA11M2465. We thank Konstantine Chalyy for field assistance, and the administrations of the Yunokommunarsk coal mine and Khrestyshche gas field for discussions and information on their respective PNE sites in Ukraine. The Institute of Geophysical Research, the Kazakhstan National Data Center, and Alec Abishev were essential and are thanked for generous help and field assistance in Kazakhstan.

5. REFERENCES CITED

Ageyeva, T.I., Tuleushev, A.Zh, and Podenezhko, V.V. 2008. Reduction of Risks from Lira Underground Nuclear Facilities at Karachaganak Oil-And-Gas Complex, *in* Nuclear Risks in Central Asia, Springer, Netherlands, doi:10.1007/978-1-4020-8317-4_11, Ch. 11, p. 115-123.

Alekseev, A. A., V. E. Stepanov, V. E. Ushnitsky, G. I. Borisov, V. I. Buturlin, S. V. Maleev, G. A. Nezhdanov, and B. V. Odinov (1993). Investigations of radiation conditions in the Bulun region (lower course of the Lena River) Sakha Republic (Yakutia), in *Radiation Contamination of the Territory of the Sakha Republic (Yakutia): Problems of Radiation Safety*, Burtsev, I. S. (Editor), Ministry of Public Health of the Sakha Republic (Yakutia), Yakutsk, 199-214. (in Russian)

Bulatov, V. I., 1996. Russia – Radioactive: TsERIS, Novosibirsk, 266 pp. (in Russian)

Dubasov, Y. V., Trifonov, V. A., Smironov. E. A., and Arshanskii, S. M., 2005. Underground nuclear explosion sites in Orenburg oblast: Current radiation situation. Radiochemistry. v. 47, p. 605-613.

Fujita, K., K. G. Mackey, K.G., and Hartse, H.E. (2013). Ground truth determinations of Peaceful Nuclear Explosions in the Sakha Republic (Yakutia), Russia, *Bull. Seismol. Soc. Am.*, v. 103 #2A, p. 730-740. doi: 10.1785/0120120176

Gedeonov, A. D., I. N. Kuleshova, E. R. Petrov, M. L. Savopulo, V. Y. Shkroev, B. N. Shuvalov, V. G. Alexeev, V. I. Arkhipov, and I. S. Burtsev (1997). Plutonium in soils, bottom sediments and lichen near peaceful nuclear explosion sites in the Republic of Sakha (Yakutia), *J. Radioanal. Nucl. Chem.*, **221**, 85-92.

Gedeonov, A. D., Petrov, E.R., Alexeev, V.G., Kuleshova, I.N., Savopula, M.L., Burtsev, I.S., Shroev, V.Y., and Arkhipov, V.I., 2002. Residual radioactive contamination at the peaceful underground nuclear explosion sites "Craton-3" and "Crystal" in the Republic of Sakha (Yakutia), *J. Environ. Radioactiv*, **60**, 221-234.

Grek, A., 2006. Blow up for Peace: Explosions for us – Ahead of the Rest: Popular Mechanics (Moscow). December, 2006. http://www.popmech.ru/article/999-vzorvat-po-mirnomu/. (in Russian)

GS RAS, 2001. Calibration of the Seismic Stations of the Russian Academy of Sciences for the CTBT Seismic Monitoring Purposes, Annual Technical Report, Geophysical Survey of Russian Academy of Sciences, 30 pp. + 6 Appendices.

Jordan, T.H., and Sverdrup, K.A., 1981, Teleseismic location techniques and their application to earthquake clusters in the South-Central Pacific: *Bull. Seismol. Soc. Am.*, v. 71, no. 4, p. 1105–1130.

Kalmykov, S. A., Sapozhnikov, Yu. A., and Goloubov, B. N., 1999. Artificial radionuclides in oils from underground nuclear test site (Perm region, Russia), *Czechoslovak Journal of Physics* #49, p. 91-95 doi: 10.1007/s10582-999-0011-x.

Khamtsov, E.B., Repin, V.S., and Ramzaev, B.P., 2013. Radiation-hygienic characteristics of areas adjacent to the places of peaceful nuclear explosions: Presentation at the round table discussion "Formation of ecological culture in societe: regional and municipal experience" Nevsky International Ecological Congress, 21-22 May, 2013, St. Perersburg, Russia (in Russian).

Kolpakov, D., and Momot, Z., 2008. Time "Ch". 20 years ago in Bashkiria curtailed the program of nuclear explosions: Mediakorset 3/31/2008. http://www.mkset.ru/news/today/8524/ (in Russian).

Kryukov O. V., Abramov A. A., Tikhonova A. A., Dorofeev A. N., Ivanov K. V., Komarov E.A., Zakharchev A.A. Linge I. I., Antipov S. V., Savkin M. N., Biryukov D. V., Drozdov V. V., Utkin, S. S., Obodinsky, A. N., Samoilov, A. A., and Ivanov, V. K., 2015. Liquidation of Nuclear Heritage: 2008-2015: Rosatom, Moscow, 159 pp.

Mackey, K.G., and Bergman, E., 2014. Ground Truth Locations for the Mangyshlak Peaceful Nuclear Explosion Sequence, Western Kazakhstan, *Bull. Seismol. Soc. Am*., v. 104(4). Doi: 10.1785/0120130330.

Mackey, K.G., and Fujita, K., 2014. Improvement of GT Classification of Soviet PNEs, Final Report for contract SAQMMA11M2465, 282 pp.

Mikhailov, V. N., ed., 1994. Nuclear Explosions in the USSR, issue. 4, Mimoe ispol'zovanie podzemnykh yadernykh vzryvov, VNIPIpromt ekhnologii, Moscow.

Mikhailov, V.N., 1999. Catalog of Worldwide Nuclear Testing, Begell-Atom, LLC, New York, 129 pp.

Myasnikov, K. V., Kasatkin, V. V., and Kharitonov, K. V., 2004. Underground nuclear explosions in the Arctic for peaceful purposes: Nuclear Explosions in the USSR: The North Test Site Reference Material, version 4., International Atomic Energy Agency, Vienna, p. 93-98.

Nekhoroshev, G., Florin, D. and Radovskii, A., 2011. Atomic Underground "Gazprom" Underground gas storage sites became uncontrollable high-level waste, www.compromat.ru/page_31285.htm.

Nordyke, M. D., 2000. *The Soviet Program for Peaceful Uses of Nuclear Explosions*: Lawrence Livermore National Laboratory, UCRL-ID-124410 Rev 2, 74 pp. + appendices.

Norris, R. S., and Cochrane, T. B., 1996. Nuclear Weapons Tests and Peaceful Nuclear explosions by the Soviet Union – August 29, 1949 to October 24, 1990. Draft – October, 1996. National Resource Defense Council, Washington DC, 31 pp. + tables.

Pavlov, A., 2011. Former nuclear blast sites in Russia's Murmansk Region to become a national park. www.bellona.org/articles/articles_2011/khibiny_testrange. (in Russian)

Pochivalov, L., 1998. Russia – Country of hundreds of Hiroshimas: Russian Social Science Review, v. 39(2), p. 70-80.

Podvig, P., ed., 2001. *Russian Strategic Nuclear Forces*: MIT Press, Cambridge, xxi + 692 pp.

Ramzaev, V., Mishine, A. Golikov, V., Brown, J.E., and Strand, P., 2007. Surface ground contamination and soil vertical distribution of 137Cs around two underground nuclear explosion sites in the Asian Arctic, Russia, *J. Environ. Radioactiv.*, **92**, 123-143.

Ramzaev, V., Repin, V., Medvedev, A., Khramtsov, E., Timofeeva, M., and Yakolev, V., 2011. Radiological investigations at the "Taiga" nuclear explosion site: Site description and in situ measurements, *Journal of Environmental Radioactivity*, v. 102:7, p. 672-680. doi:10.1016/j.jenvrad.2011.04.003

Ramzaev, V., Repin, V., Medvedev, A., Khramtsov, E., Timofeeva, M., and Yakolev, V., 2012. Radiological investigations at the "Taiga" nuclear explosion site, part II: man-made γ-ray emitting radionuclides in the ground and the resultant kerma rate in air, *Journal of Environmental Radioactivity*, v. 109:7, p. 1-12. doi:10.1016/j.jenvrad.2011.12.009

Ringdal, F., and Richards, P. G., 1992. The Ukrainian event of 16 September 1979, *in* NORSAR Scientific Report No. 1-92/93, Semiannual Technical Summary 1 April – 30 September 1992, p. 120-124.

Shaybakova V. R., Shaybakov, R. A., Abdrakhmanov, N. H., Shavaleev, D. H., 2013. Control Systems for Industrial Effluents and Industrial Waste, *Oil and Gas Business*, #1, p. 498-509 (in Russian).

Short Characteristics of Underground Nuclear Explosions conducted for Requirements of the Peoples' Economy in the territory of the USSR in 1965-1988. No date, photocopy.

Startsev, V., 2012. Travel on a Ford Ranger to the site of the Rift-3 underground nuclear explosion in the Irkutsk Region, *Online resource* https://travel.drom.ru/19390/. (in Russian)

Sultanov, D.D., Murphy, J.D., and Rubinstein, K.D., 1999. A seismic source summary for Soviet peaceful nuclear explosions: *Bull. Seismol. Soc. Am.*, v. 89, p. 640-647.

Tsyganov, A. S. 1993. Report on the results of studying the effects of underground nuclear explosions on the radiation situation in the Mirny rayon of the Yakut-Sakha SSR, in *Radioactive and Other Environmental Threats to the United States and the Arctic Resulting From Past Soviet Activities: Hearing Before the Select Committee on Intelligence of the United States senate, One Hundred and Second Congress, 2nd Session, August 15, 1992*, United States Senate, Washington, 351-378.

Ulybina, J., and Ignatenko, 2005. Nuclear testing in the Ust-Orda district left their mark on the century, *Online resource* http://baikal-info.ru/sm/2005/09/004001.html . (in Russian)

Utkin, V.I., Rybakov, Ye. N., and Shchapov, V.A., 2007. Ecological consequences of underground nuclear explosions on petroleum deposits of the Perm region, NNC_RK Bulletin, Issue 2(30), pp. 56-62.

Vasilyev, A., and Kasatkin, V., 2008. Peaceful Nuclear Explosions in the USSR: Hopes and Realities, in Ion, C., editor-in-chief, 2nd Russian National Dialogue on Energy, Society and Security: Green Cross Russia, St. Petersburg, p. 318-341.

Walker, R. T., Bergman, E. A., Szeliga, W., and Fielding, E. J., 2011. Insights into the 1968-1997 Dasht-e-Bayaz and Zirkuh earthquake sequences, eastern Iran, from calibrated relocations, InSAR and high-resolution satellite imagery. *Geophys. J. Int.*, no–no. doi:10.1111/j.1365-246X.2011.05213.x.

Wind Strangers, 2015. Internet Resource video from YouTube, https://www.youtube.com/watch?v=9rmdUTQyGeA.(in Russian)

Yablokov, A. V., 2003. Myths About Hazards and Effectiveness of Peaceful Underground Nuclear Explosions: Center for Ecological Politics of Russia, Moscow, 174 pp. (in Russian)

6. APPENDICIES

6.1. APPENDIX A - Calibrated Relocations of Peaceful Nuclear Explosions in the former Soviet Union

6.1.1. Introduction

Along with an extensive set of weapons tests at a handful of testing sites, the former Soviet Union conducted 122 Peaceful Nuclear Explosions (PNEs) across its territory in the period 1965-1988. Due to their wide geographic distribution (thus wide sampling of the crust and upper mantle across the region) and the prospect that the source locations could be knowable to very high accuracy, the seismic recordings from these explosions form a potentially valuable resource for seismological research. It has therefore been of great interest to seismologists to know the hypocentral parameters of these explosions as accurately as possible.

Unfortunately, the records on the locations of PNEs are not as complete as those for weapons tests and the uncertainties of the locations of many of the PNEs are large enough to discount their usefulness as "Ground Truth" seismic sources. The standard reference work on the locations of the PNEs is the publication by Sultanov et al. (1999), which also includes an estimate of the uncertainty in the provided parameters. Mackey and Bergman (2014) have shown, however, that even some of the locations assigned high accuracy by Sultanov et al. (1999) are in fact significantly in error.

In cases where PNEs are located near one another or in regions where there is a population of natural earthquakes, there is an opportunity to test the consistency of the proposed source parameters of PNEs in either a relative or absolute sense through a calibrated relocation analysis. An example of this process is found in Mackey and Bergman (2014), where the relative locations of three PNEs in western Kazakhstan are investigated, leading to new associations with shot sites determined from ground observations and remote sensing. We use the same relocation program in this report, a program called *mloc* that is based on the Hypocentroidal Decomposition (HD) algorithm introduced by Jordan and Sverdrup (1981). It has been developed and extensively tested for research on calibrated locations, that is, locations for which systematic errors (bias) from unknown earth structure and unbalanced network geometry are minimized. Moreover, the calculated uncertainties of the source parameters are considered to be substantially unbiased because they are based on estimates of the uncertainties of the arrival time data that are derived from the data itself and the algorithm contains checks on the internal consistency of the estimated uncertainties of both data and parameters. Other recent investigations utilizing *mloc* in a variety of circumstances include Aziz Zanjani et al. (2013), Hayes et al., (2014) and McNamara et al. (2015).

In this study, we are primarily concerned with calibrated epicenters of the events. The type of data necessary to independently constrain focal depths and origin times (i.e., readings at very short epicentral distances) does not exist in these arrival time datasets. It is possible, however, to make certain checks of consistency between multiple PNEs that can provide confidence in the reported origin times. The focal depths of the PNEs are reliably known to be quite shallow; they are held at the borehole depths reported by Sultanov et al. (1999), corrected for surface elevations, which are only a few hundred meters in this region. Focal depths of earthquakes included in this cluster are set to a reasonable default value, 10 km. Calibrated relocation analyses was carried out for a clusters of seismic events, comprised of Peaceful Nuclear Explosions (PNEs), and natural earthquakes in the territory of the former Soviet Union. The primary purpose of the relocation analysis was to validate reported locations of PNEs and, in cases where no reliable estimates of location are available, to provide high-quality seismic estimates of location for comparison with

ground-based or remote-sensing observations that are indicative of shot sites. The methodology used for the analysis has been developed and thoroughly tested for applications in which it is desired to minimize systematic location bias due to unknown earth structure and unbalanced seismic network geometry. Two specific PNE sequences, Butane and Urtabulak, which occurred in different regions, are addressed here.

The "Butane" cluster lies near the Russia-Kazakhstan border north of the Caspian Sea, but most of the events are in southern Russia. The "Urtabulak" cluster lies dominantly along the Uzbekistan-Turkmenistan border, but most of the events are in southern Uzbekistan.

For the Butane cluster, ground-truth quality hypocenters with less than 1 km of location uncertainty for thirteen PNEs were validated and in some cases slightly improved from previous estimates. Of the four PNEs belonging to the Butane sequence, only one (Butane 2-1 on June 16, 1980) could be reliably relocated with seismic data, about 10 km north of the city of Meleuz, but no clear shot site has been identified in the source region from satellite imagery. Based on calibrated relocation results, new associations of some of the Lira sequence PNEs with specific boreholes are proposed.

Within the Urtabulak cluster, reported epicenters and origin times for two PNEs (Urtabulak and Pamuk) were validated and slightly improved. The location of the third PNE (Crater) cannot be confirmed at a useful level of accuracy, but the reported origin time is likely as accurate as those of the other PNEs, to 0.1 s or less. Nineteen events in the cluster were identified as chemical explosions, probably related to construction of irrigation canals. Additional events in the cluster may also be explosions.

6.1.2. Relocation Methodology

6.1.2.1. Overview

The preferred method for obtaining calibrated hypocenters for a cluster relies on the existence of arrival time readings at relatively short epicentral distances; in particular, less than the distance at which Pn becomes the first-arriving P phase. In the case of these clusters, that distance is about 1.2° (~135 km). The arrival time dataset contains no readings in this distance range, so we employed an alternative method of calibration ('indirect calibration') in which the location of one (or more) event is assumed to be known *a priori*.

The relative locations of all events in a cluster are strongly constrained by the HD analysis, but the absolute location in space and time can be biased by the influence of unmodeled earth structure convolved with unbalanced geometry of observing stations (red box in Figure A-1). By shifting the cluster as needed to match the independently known hypocenter of the calibration event(s), however, the entire cluster can be brought into "calibrated" status (green box in Figure A-1).

6.1.2.2. Velocity Model

To obtain the most reliable results in the HD analysis, or any other location method, it is important to calculate theoretical travel times with an appropriate model. For this purpose *mloc* uses a flat-layered crustal model that is adjusted to fit the observed arrival times of direct (Pg and Sg) and refracted (Pn and Sn) crustal seismic phases, based on preliminary relocations. The crustal model is only used for these phases. For teleseismic arrivals, the *ak135* global travel-time model (Kennett et al., 1996) was used. The arrival time dataset for the clusters have no readings at epicentral distances less than about 1.2° where Pg and Sg would be the first-arriving P and S phases, but they do contain Pg and Sg readings as secondary arrivals that help constrain the average crustal velocities. The overall thickness of the crust is constrained by times of Pn and Sn

arrivals and the upper mantle velocity is constrained by the slopes of the observed Pn and Sn arrivals. We found that the same crustal model used for the study works well for both clusters (Table A-1).

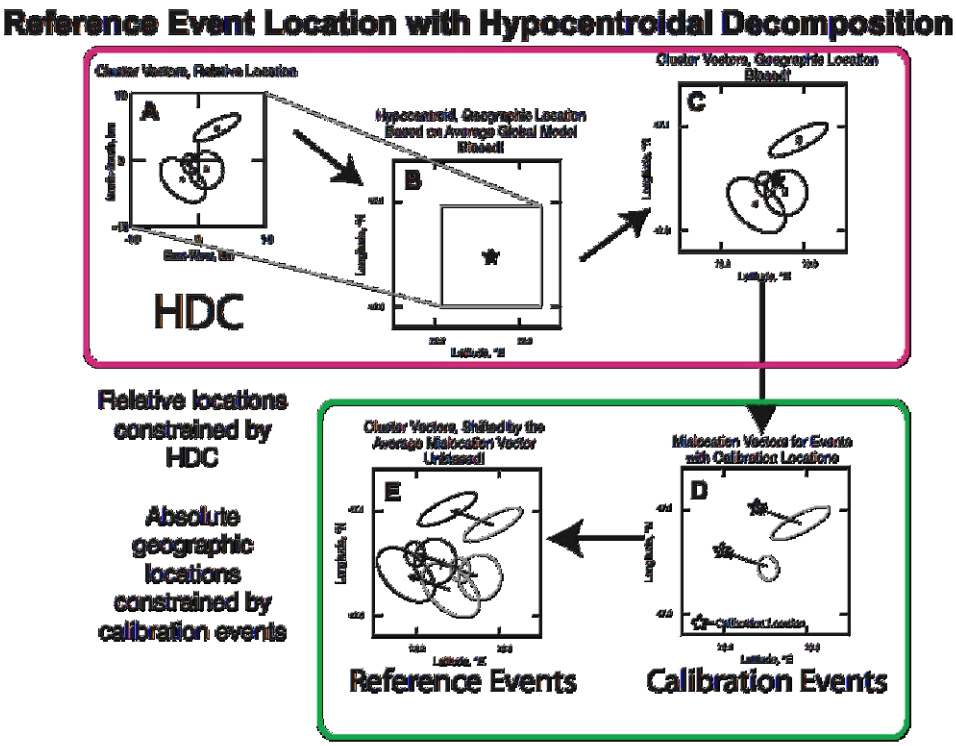

Figure A-1. Schematic of the indirect calibration technique used in this study. PNEs with known locations other than those of the target sequence were selected as the calibration events for the cluster and their reference locations were set according to parameters determined by Mackey and Fujita (2014) and this report.

Table A-1. Crustal velocity model used for the Butane and Urtabulak clusters.

Thickness (km)	P Velocity (km/s)	S Velocity (km/s)
12	5.60	3.15
4	5.80	3.26
19	6.20	3.60
halfspace	8.15	4.60

The crustal thickness of this model is 35 km. Because of the lack of direct crustal arrivals, the details of the layering in the crust are not significant in this case; only the average velocity is constrained by data. These crustal velocity model parameters are influenced by the assumed focal depths of the events contributing the arrival time data, but in these cases we are able to specify shallow depths for the PNEs with high confidence and the associated readings were used to constrain the velocity model. There is some uncertainty remaining about the tradeoff between assumed velocity model and origin times, but the relative times reported by Sultanov et al. (1999)

for the PNEs agree very closely with the relative times as constrained by seismic data, lending confidence to the reported origin times. This will be discussed further in the later sections.

6.1.3. Butane Cluster

The Butane cluster was formed especially to attempt to determine reliable locations of four PNEs with code names "Butane" detonated in pairs 15 years apart:

- Butane 1-1 on March 30, 1965
- Butane 1-2 on June 10, 1965
- Butane 2-1 on June 16, 1980
- Butane 2-2 on June 25, 1980

Russian reports are contradictory concerning the exact locations of these shots and seismic data are very sparse for them, with few stations reporting and poor azimuthal coverage. Standard single-event location procedures applied to such data would have very large uncertainties, in this case even larger than those that Sultanov et al. (1999) proposes for his seismically-determined epicenters. To make best use of the available data we searched the Bulletin of the International Seismological Centre (2015) for other seismic events in the region and added 18 other events that had sufficient observations to support a calibrated multiple event relocation. These events include 13 other PNEs, most of which have fairly well-determined locations, either from Sultanov et al. (1999) or from revisions based on research by Mackey and Fujita (2014) and this report. The initial fit of data to travel-time curves is shown in Figure A-2.

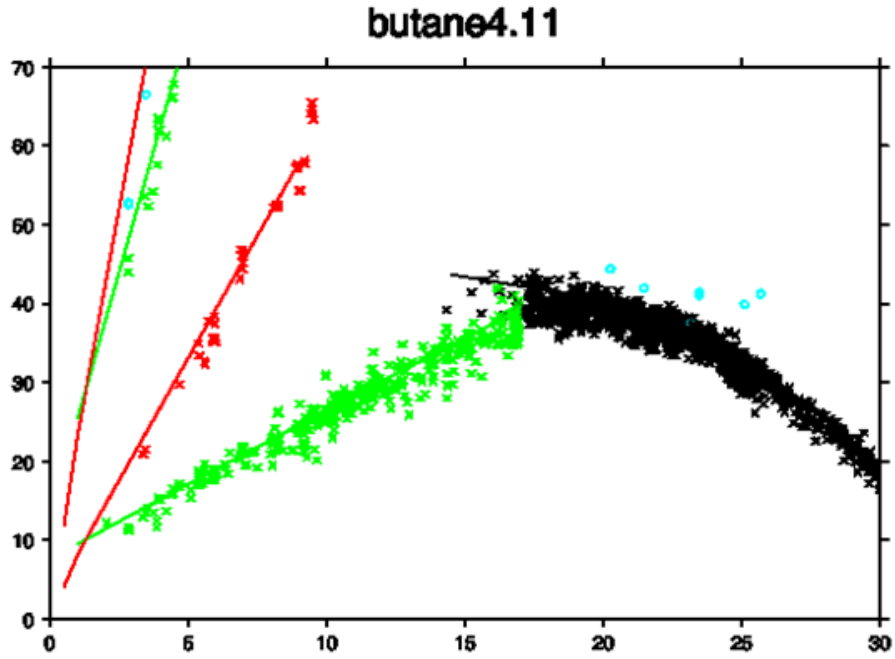

Figure A-2. Reduced travel time vs. distance for the Butane cluster out to 30° epicentral distance. Reduction time is 11.67 s/degree (~9.5 km/s). Pg and Sg readings and theoretical curves are in red. Pn and Sn are in green. Teleseismic P is in black.

Preliminary relocation analysis revealed serious difficulties in obtaining useful locations of most of the Butane series (the four events noted above). The linearized inversion process used in *mloc* is not well-suited to extremely poor data sets, which tend to prevent convergence. In this case, we were able to salvage one of the series, Butane 2-1. It is still the weakest event in the cluster because of a relatively small number (12) of readings that have connectivity to the other events for constraining cluster vectors and because those readings have poor azimuthal coverage (open azimuth 211°). The cluster analyzed for this report, then, includes 19 events, 14 of which are PNEs, and only the third member, Butane 2-1, of the Butane sequence.

6.1.3.1 Relocation

The HD algorithm decomposes the location problem into two separate estimation problems, 1) the "cluster vectors", the relative locations in space and time of the cluster events, which are specified relative to a common reference point, and 2) the "hypocentroid", the reference point for the cluster vectors. The two estimation problems differ in the number of parameters, the particular data that are used and the sources of uncertainty that must be accounted for. The absolute coordinates (epicenter in geographic coordinates, focal depth and origin time) are estimated only for the hypocentroid. Absolute coordinates for individual events is found by adding the cluster vector for that event to the hypocentroid. In this analysis we held focal depths fixed because the dataset contained no data that can constrain focal depth) and solved for epicenter and origin time.

An important aspect of HD analysis is so-called "cleaning" in which the observed distribution of residuals for each station-phase combination is analyzed with a robust statistical method to estimate a scale parameter (spread) that is insensitive to the presence of outliers and which does not depend on a measure of central tendency. With this measure of spread, outlier readings are identified and removed from the inverse problem, and each datum is inversely weighted according to the spread for that station-phase. This procedure is iterated until the dataset satisfies, in broad terms, the assumption that all samples are drawn from a normal distribution.

For indirect calibration of the Butane cluster we estimated the hypocentroid using only teleseismic P arrivals between 30 and 90° epicentral distance and minimizing residuals against the *ak135* global model. This by itself does not provide a calibrated location, but it provides a stable and reasonably accurate location that is usually not more than about 10 km away from a calibrated location. The teleseismic P branch has been found to be the most accurate portion of the *ak135* model globally, and there is generally good azimuthal coverage for a cluster when all the associated teleseismic P readings are combined. For the Butane cluster there were 1407 such readings after cleaning that were used to estimate the three parameters of the hypocentroid.

The cluster vectors of the Butane cluster were estimated with all phase readings at all epicentral distances that passed the cleaning criteria, with the exception that a station-phase combination that has only one sample cannot contribute any information regarding relative location, and so it is not used. In the estimation of cluster vectors, only travel-time differences are processed, so baseline errors in the theoretical travel-time model do not influence the result and there is no hazard in using readings for which the theoretical model may be quite in error. For the Butane cluster the cluster vectors (19 x 3 = 57 free parameters) were estimated using 2771 readings.

After the initial phase of HD analysis, when the hypocentroid has been determined by fitting the teleseismic P arrivals to the ak135 model, all locations are considered uncalibrated. Then the hypocenter of the calibration events, the PNEs, are compared with their reference parameters and a shift vector is calibrated that brings the uncalibrated hypocenters of the reference events into agreement with the respective reference locations. In this case the uncalibrated HD epicenter must

be shifted 6.6 km northeast (azimuth 67°). When this shift is applied to the hypocentroid, updating the absolute locations of all cluster events, the epicenters of all events in the cluster are considered to be calibrated. Similar corrections are made for focal depth and origin time. The calibrated locations of the Butane cluster are shown in Figure A-3 and listed in Table A-2.

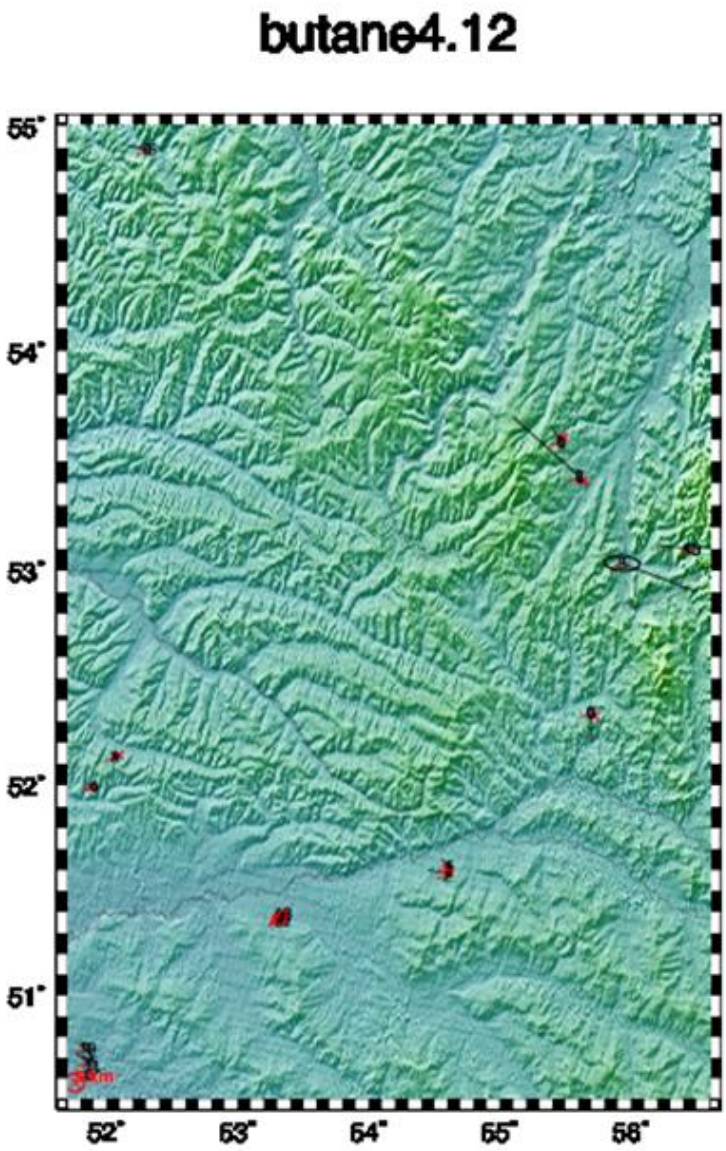

Figure A-3. Calibrated locations for the Butane cluster. Each event is represented by a 90% confidence ellipse for the relative location. Full location uncertainty would require addition of the uncertainty of the hypocentroid. The black vector for each event shows the change in location from the location given in the arrival time data file, for the earthquakes in the cluster the starting epicenter is from the ISC Bulletin; for the 14 PNEs it is from Sultanov et al. (1999). A circle of 5 km radius is shown for scale in the lower left of the figure.

Table A-2. Calibrated hypocenters for the Butane cluster.

Year	Mo	Da	Hr	Mi	Sec	Lat	Long	Depth	Mag	Az1	L1	Az2	L2	Cal	Comment
1970	6	25	4	59	56.18	52.34124	55.69465	0.50	5.8mb	84	2.12	174	2.89	CH03	Magistral
1971	10	22	5	0	1.93	51.57977	54.61057	1.00	5.2mb	52	1.62	142	1.81	CH02	Sapphire-1
1972	9	21	8	59	59.78	52.13437	52.06739	0.40	5.0mb	76	1.67	166	1.93	CH02	Region-1
1972	11	24	9	0	0.18	51.99336	51.90417	0.60	4.5mb	72	2.09	162	2.47	CH02	Region-2
1973	9	30	5	0	0.07	51.61740	54.61761	1.00	5.2mb	82	1.60	172	1.83	CH02	Sapphire-2
1973	10	26	6	0	0.22	53.58864	55.47176	1.80	4.8mb	82	1.67	172	2.29	CH02	Kama-2
1974	7	8	6	0	0.01	53.42838	55.61281	1.90	4.6mb	83	1.82	173	3.17	CH03	Kama-1
1980	6	16	6	0	0.65	53.03187	55.93275	1.40		4	3.99	94	10.69	CH11	Butane 2-1
1983	7	10	4	0	0.05	51.35827	53.31938	0.80	5.3mb	67	1.45	157	1.61	CH02	Lira 1-1
1983	7	10	4	4	60.00	51.36286	53.32936	0.80	5.3mb	64	1.42	154	1.58	CH02	Lira 1-2
1983	7	10	4	9	60.00	51.37275	53.33905	0.80	5.3mb	63	1.43	153	1.60	CH02	Lira 1-3
1984	7	21	2	59	59.86	51.36431	53.33268	0.80	5.4mb	71	1.45	161	1.58	CH02	Lira 2-1
1984	7	21	3	4	59.80	51.39339	53.34802	0.90	5.3mb	74	1.43	164	1.56	CH02	Lira 2-2
1984	7	21	3	9	59.91	51.38049	53.34174	0.80	5.4mb	75	1.43	165	1.57	CH02	Lira 2-3
2008	4	26	13	14	53.29	50.68219	51.87031	10.00	4.8mb	271	1.64	1	2.25	CT02	
2008	5	29	11	3	26.50	54.90478	52.31438	10.00	3.8mb	90	1.94	180	2.61	CT03	
2008	7	18	19	36	40.10	50.61996	51.87597	10.00	3.8mb	275	2.01	5	2.96	CT03	
2011	3	11	23	15	8.54	53.09732	56.46045	10.00	-	27	2.26	117	4.13	CT04	
2011	12	30	23	58	17.16	50.74579	51.84991	10.00	3.8mb	54	1.85	144	3.16	CT03	

Notes: Calibration was based on the reference locations for the listed PNEs (except Butane 2-1), with names given under 'Comment'. Hypocenters listed here for the reference events are the ones from calibrated relocation, not the reference locations. The 90% confidence ellipse for epicenter is given by parameters Az1, L1, Az2, and L2 (azimuth and length in km of the two semi-axes). "Cal" is a code providing information about the calibration status. The letter portion of the code reflects which hypocentral parameters are considered calibrated (CH = all parameters, CT = epicenter and "provisional" origin time, based on an assumed focal depth). The numeric portion of the code gives a length scale, to nearest km, for calibration of the epicenter.

The vector describing the location of each PNE's calibrated epicenter relative to that reported by Sultanov et al. (1999) is listed in Table A-3.

Table A-3. Difference between calibrated epicenters and Sultanov locations

Year	Mo	Da	Name	Dist	Azim
1970	6	25	Magistral	15.6	358
1971	10	22	Sapphire-1	11.1	102
1972	9	21	Region-1	1.9	350
1972	11	24	Region-2	2.3	082
1973	9	30	Sapphire-2	5.7	129
1973	10	26	Kama-2	8.2	146
1974	7	8	Kama-1	45.1	132
1980	6	16	Butane 2-1	41.0	291
1983	7	10	Lira 1-1	0.9	134
1983	7	10	Lira 1-2	0.5	190
1983	7	10	Lira 1-3	1.1	202
1984	7	21	Lira 2-1	1.0	046
1984	7	21	Lira 2-2	2.5	012
1984	7	21	Lira 2-3	1.5	217

Notes: 'Dist' in km, 'Azim' in degrees clockwise from north.

These vectors are shown in black in Figure A-3. Clearly, there are cases in which the calibrated locations are significantly different from those reported by Sultanov et al. (1999), e.g., Magistral, Sapphire-1, Kama-1 and Butane 2-1. Several others, e.g., Sapphire-2 and Kama-2 have discrepancies that are marginally significant. The remainder, including all the Lira PNEs have differences that are a few km at most. Even for these, however, estimates of the reference locations that are likely more accurate than those reported by *Sultanov* can be made. These are discussed in the sections below that deal with individual PNE sequences.

6.1.3.2. Tests of the Statistical Consistency of the Calibrated Locations

A check of internal consistency is made after the calibrated locations (and their uncertainties) have been calculated. If all is well, the residual differences between the calibrated locations and the reference locations should be well described by the uncertainties of the calibrated locations. There are several ways to consider this issue. One is a statistical test of the null hypothesis that all residual vectors (vector difference between calibrated and reference epicenters) are zero. This implies that the residual vectors as a group can be explained as random variations with the underlying distribution described by the uncertainties of the calibrated epicenters. For the Butane cluster, the null hypothesis cannot be rejected; on this basis we conclude that the calibrated locations are statistically consistent with the reference locations.

A second test is also made, one that is only applicable when there are a fairly large number of reference events, as here (13 reference events). This is a "coverage" test, which considers how many of the reference locations are covered by the confidence ellipse of the respective calibrated location. Crudely, since the confidence ellipses are calculated at 90% level of confidence, we should not be surprised if, in about one out of ten cases, the confidence ellipse does not cover the reference location. The coverage test is based on the cumulative binomial probability distribution, which gives the probability of the observed number of "uncovered" reference locations, given the number of reference events. If that probability is greater than 10% (since we are using 90% confidence ellipses) we conclude that the calibrated locations are consistent with the reference locations.

What happens if either or both of these tests are failed? This can be caused by one or more of the HD locations or the reference locations being significantly in error. In some cases it is possible to go back to the HD analysis and identify outlier readings that were previously missed, or to reconsider the uncertainty of the reference locations (i.e., increasing the uncertainty for one or more of them). If no such corrections are implemented, there is no alternative but to increase the uncertainty of all of the calibrated locations, which is done by adding a small circular uncertainty (increments of 200 m) to the covariance matrix that describes each confidence ellipse. Then the test (either of them) is repeated. This sequence is continued until the statistical test is 'satisfied' at which point the cumulative circular uncertainty is termed the "radius of doubt".

For the Butane cluster, the test of the null hypothesis of zero-length residual vectors did not require any radius of doubt, but the coverage test required a radius of doubt of 1.0 km. When both tests are applicable (as in this case), the larger of the two estimates of radius of doubt is taken. Therefore, the final estimate of uncertainty for all events in the Butane cluster includes a 1.0 km radius of doubt. This is done by adding the covariance matrix for a circle of 1 km radius to the covariance matrix of each event and calculating a new confidence ellipse from the covariance matrix; the amount that the resulting confidence ellipse is increased in size is less than 1 km in any direction. The confidence ellipses in Table A-2 include the contribution of the radius of doubt.

The radius of doubt represents an additional uncertainty in the calibration process with unknown source(s). However, in a cluster that is large in area, such as the Butane cluster, it is likely that the need for a radius of doubt arises from distortion in the cluster vectors (relative locations) of the HD analysis, due to using a single 1-D crustal model across the entire region. To imagine that that simplification in our analysis hides only ~1 km of location bias is not especially troubling.

6.1.3.3. Reference Locations

For convenience the reference locations used in this study are listed in Table A-4. Based on the calibrated HD relocation and the confidence with which the reference location can be specified, a judgement of GT level is made. GT0 implies accuracy of 500 m or better in the epicenter.

Table A-4. Reference Locations for the Butane Cluster.

Year	Mo	Da	Name	Hr	Mi	Sec	Lat	Long	Depth	GT	Source
1970	6	25	Magistral	4	59	55.5	52.3265	55.7238	0.5	GT0	Mackey and Fujita (2014)
1971	10	22	Sapphire-1	5	0	01.0	51.5874	54.6146	1.0	GT0	Mackey and Fujita (2014)
1972	9	21	Region-1	9	0	0.31	52.1402	52.0929	0.4	GT1	Mackey and Fujita (2014)
1972	11	24	Region-2	9	0	0.04	51.9934	51.8823	0.6	GT0	This study
1973	9	30	Sapphire-2	5	0	0.35	51.6052	54.5991	1.0	GT0	Mackey and Fujita (2014)
1973	10	26	Kama-2	5	59	59.5	53.607	55.483	1.8	GT1	Mackey and Fujita (2014)
1974	7	8	Kama-1	5	59	59.95	53.4097	55.6387	1.9	GT1	Mackey and Fujita (2014)
1983	7	10	Lira 1-1	3	59	59.99	51.3584	53.3198	0.8	GT0	Mackey and Fujita (2014; Lira 2-2)
1983	7	10	Lira 1-2	4	4	59.94	51.3660	53.3258	0.8	GT1	Mackey and Fujita (2014)
1983	7	10	Lira 1-3	4	9	59.85	51.3717	53.3357	0.8	GT0	Mackey and Fujita (2014; Lira 2-2)
1984	7	21	Lira 2-1	2	59	59.81	51.3646	53.3338	0.8	GT1	This study
1984	7	21	Lira 2-2	3	4	59.71	51.3916	53.3497	0.9	GT0	Mackey and Fujita (2014; Lira 2-3)
1984	7	21	Lira 2-3	3	9	59.85	51.3802	53.3388	0.8	GT0	Mackey and Fujita (2014; Lira 1-3)

Note: The source for the epicenter is listed. In all cases, origin times were held at the values reported by Sultanov et al. (1999). Focal depths, in km, are from Sultanov et al. (1999), corrected for surface elevation.

6.1.3.4. Individual PNE Sequences

In the section we review the calibrated relocations for the different named PNE sequences included in this cluster, in chronological order to the extent possible.

6.1.3.4.1. Magistral

Magistral is a singlet PNE, detonated on June 25, 1970. Mackey and Fujita (2014) have argued that a more likely location than the one reported by Sultanov et al. (1999) is at 52.3265°N, 55.7238°E, based on strong evidence in other Russian reports and satellite imagery. This location was taken as the reference location for Magistral in the calibrated HD analysis. The calibrated epicenter differs from the reference location by 2.6 km, the largest discrepancy observed for this cluster and the reference location is not quite covered by the 90% confidence ellipse of the calibrated location. The location reported by Sultanov et al. (1999) is over 15 km from the epicenter determined in the calibrated HD analysis.

6.1.3.4.2. Sapphire

The Sapphire sequence consists of two PNEs, detonated on October 22, 1971 (Sapphire-1) and September 30, 1973 (Sapphire-2). The calibrated locations and the reference locations are shown in Figure A-4. The reference locations are taken from Mackey and Fujita (2014). The calibrated locations of Sapphire-1 and Sapphire-2 differ from those of Sultanov et al. (1999) by 11 and 6 km, respectively (Table A-3), much more than the uncertainty (1.6-1.8 km) of the calibrated locations. The residual vectors (between calibrated and reference epicenters) are 0.8 and 1.8 km, respectively. The Sapphire-1 reference location is covered by the 90% confidence ellipse of the calibrated location, but that of Sapphire-2 is not.

Figure A-4. Satellite imagery of the source region of the Sapphire-1 (#2) and Sapphire-2 (#5) PNEs (*Google Earth, 2015*). Large red icons are the locations from calibrated relocation. Pushpins mark the reference locations (Table A-4).

6.1.3.4.3. Region

The Region sequence consists of five PNEs in three very different locations. Two of them (Region-3 and Region-4) were detonated in the Caucasus region. Region-5 was detonated in northern Kazakhstan. They were not relocated in this study. The remaining two members of the Region sequence occurred in the region covered by this cluster: Region-1, detonated on September 21, 1972, Region-2 on November 24, 1972.

Mackey and Fujita (2014) see no evidence of a shot site within 1 km (the quoted uncertainty) of the location reported by Sultanov et al. (1999) for Region-1. They propose several possible alternative sites in the area, including "Alternate B" which is about 3 km NNE of the Sultanov et al. (1999) location, with visual characteristics in satellite imagery that is typical of other known PNEs. After preliminary calibrated relocations that did not use this event as a reference event showed that the calibrated location of Region-1 would be close to this site, I have used it (Table A-4) as the reference location for Region-1 in subsequent runs for the calibration study. The calibrated location is about equidistant (~1.8 km) from both this reference location and the Sultanov et al. (1999) location, but the visual evidence cited by Mackey and Fujita (2014) lead us to prefer it as the reference location.

The Sultanov et al. (1999) location for Region-2 is close to the calibrated location of the event when it is not used as a calibration event, but inspection of satellite imagery (Figure A-5)

reveals a very likely-looking site about 1 km away, and this is the reference location used for subsequent relocations (Table A-4). The calibrated location, with an uncertainty of 2.1-2.5 km, is ~1.4 km from the reference location and ~2.6 km from the Sultanov et al. (1999) location.

Figure A-5. Satellite imagery of the source region of the Region-2 PNE (Google Earth, *2015*). Large red icon is the location from calibrated relocation. Pushpins mark the location from Sultanov et al. (1999) and the reference location used in this study (Table A-4).

6.1.3.4.4. Kama

The Kama sequence consists of two PNEs, detonated on October 26, 1973 (Kama-2) and July 8, 1974 (Kama-1) — sequence numbers are not in date order.

For Kama-2 Sultanov et al. (1999) gives a location with very low precision, to the nearest ~1 km in latitude but only to the nearest ~10 km in longitude. Mackey and Fujita (2014) were unable to identify an unambiguous location, but suggest three possibilities based on the observation of "disturbed areas". Preliminary calibrated relocation that do not use Kama-2 as a reference event place the location close to Mackey and Fujita's (2014) Kama-2B site (Figure A-6) and we have used that reference location in subsequent relocations of the Butane cluster (Table A-4). The calibrated location, with an uncertainty of 1.7-2.3 km, is ~2.1 km from the reference location and ~8.2 km from the Sultanov et al. (1999) location. Both the Kama-2A and Kama-2C sites proposed by Mackey and Fujita (2014) are much further away and are very unlikely to be associated with this event.

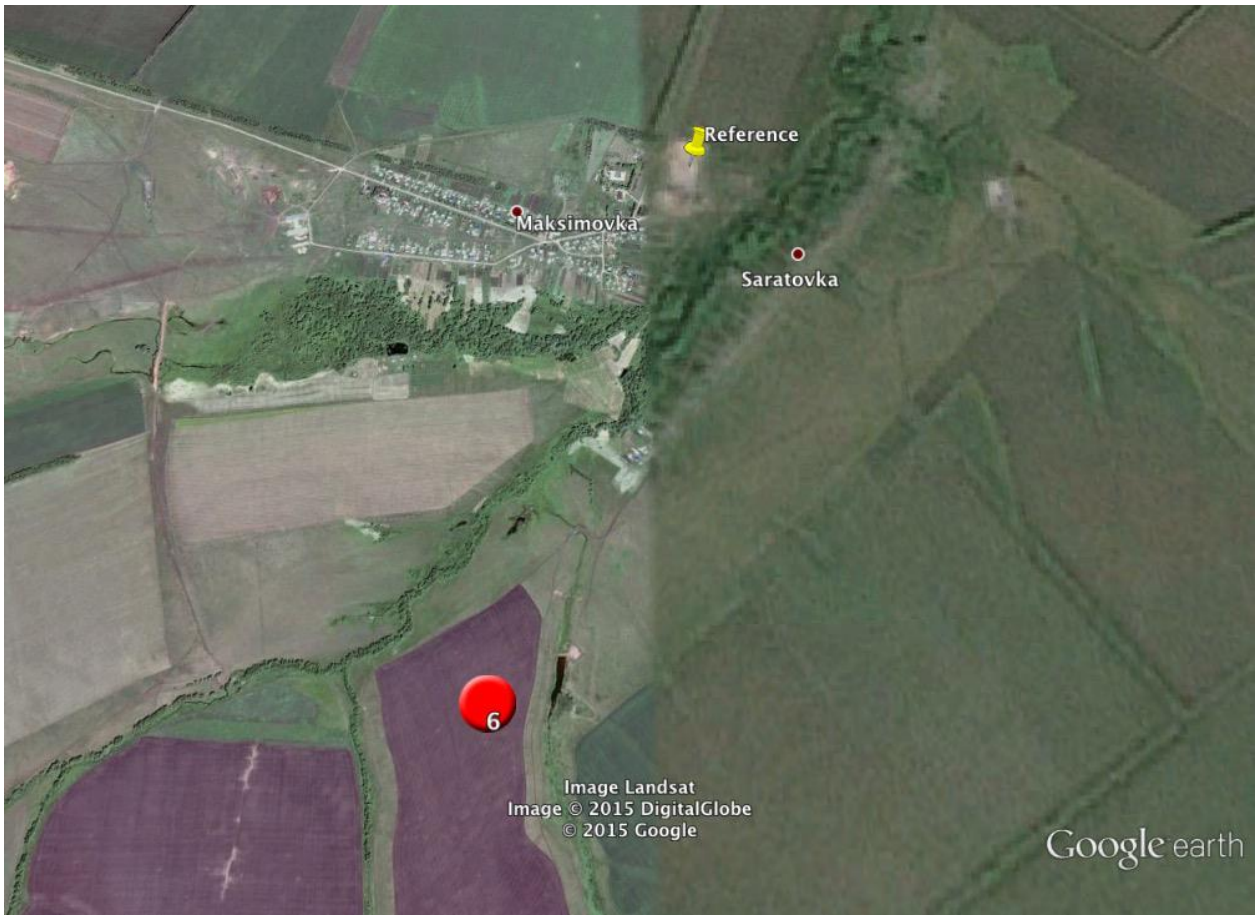

Figure A-6. Satellite imagery of the source region of the Kama-2 PNE (*Google Earth, 2015*). Red icon (#6) is the location from calibrated relocation. Pushpin marks the reference location (Table A-4).

For Kama-1, the location determined by Mackey and Fujita (2014), based on inspection of satellite imagery and Russian reports, is very consistent with the calibrated location in relocations that do not use this event as a reference event (Figure A-7), and I used their location as the reference location in subsequent relocations (Table A-4). The calibrated location, with an uncertainty of 1.8-3.2 km, is located 2.7 km from this reference location. The location reported by Sultanov et al. (1999) is 45 km away.

Note: *The Kama-2 PNE was located with certainty in this study subsequent to this cluster analysis. Please see Section 2.24.*

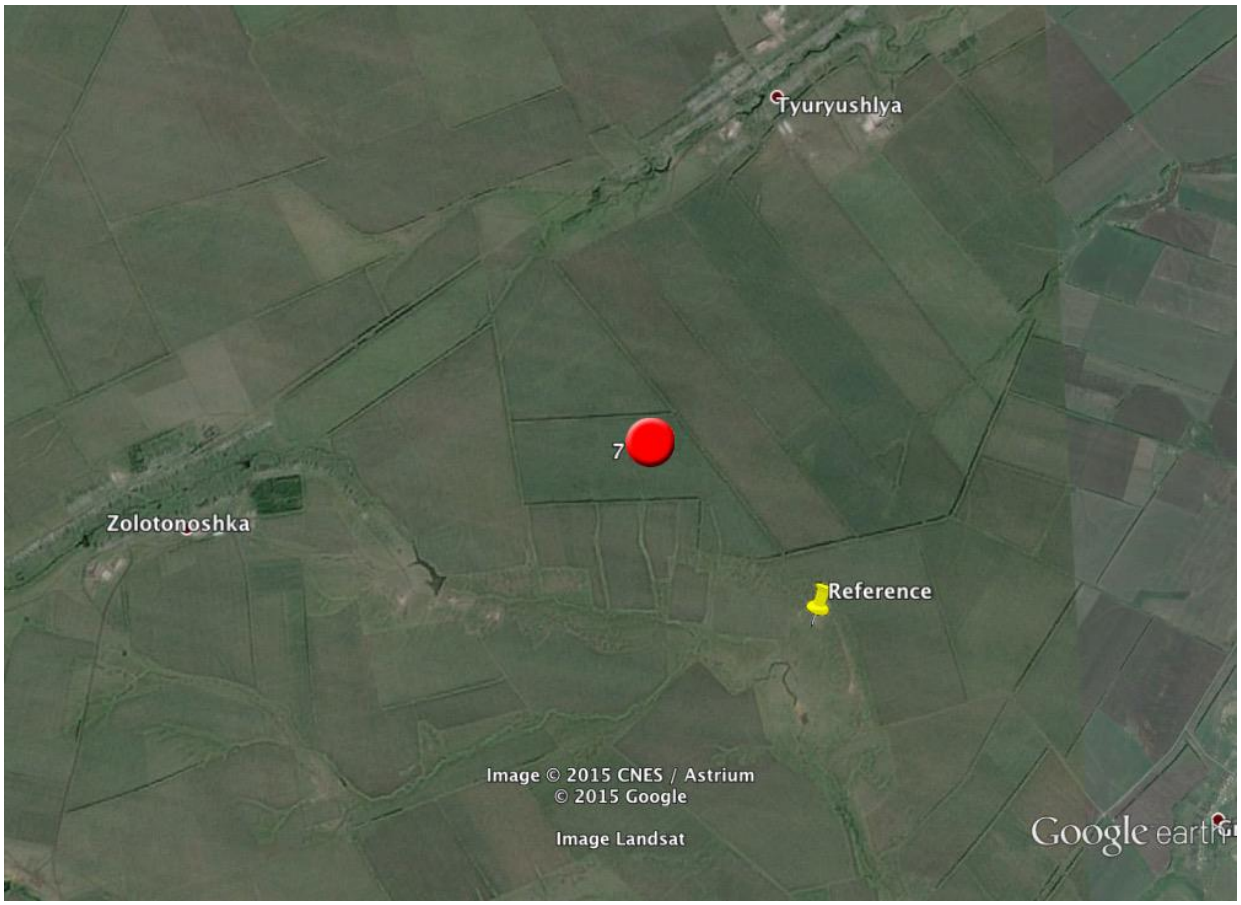

Figure A-7. Satellite imagery of the source region of the Kama-1 PNE (*Google Earth, 2015*). Large red icon is the location from calibrated relocation. Pushpin marks the reference location used in this study (Table A-4).

6.1.3.4.5. Butane

As discussed above, the sequence for which this cluster was named consists of four PNEs, but only one of them (Butane 2-1, on June 16, 1980) was well-enough recorded to be included in the cluster for calibrated relocation. There are a number of reports, beside Sultanov et al. (1999), that discuss the details of these explosions, but they tend to be contradictory regarding the locations. According to Mackey and Fujita (2014) it is likely that all four Butane PNEs were detonated in close proximity to one another.

Lacking convincing *a priori* knowledge concerning the epicenter of Butane 2-1, this PNE (alone among all the PNEs in the Butane cluster) was not used as a reference event for calibration. It was treated in the same way as the five earthquakes in the cluster, such that the calibrated HD location is the best estimate of the location for this event. The dataset of arrival time readings for this event is better than that of any of the other Butane PNEs, but it is still very weak, with only 12 readings that are connected to the other events in the cluster and a large open azimuth of 211°. As a result the calibrated location for this event has much greater uncertainty than for any other event in the cluster, with a confidence ellipse with semi-minor axis of 4 km oriented N-S and a semi-major axis of 10.7 km oriented E-W. These axes are shown schematically in Figure A-8.

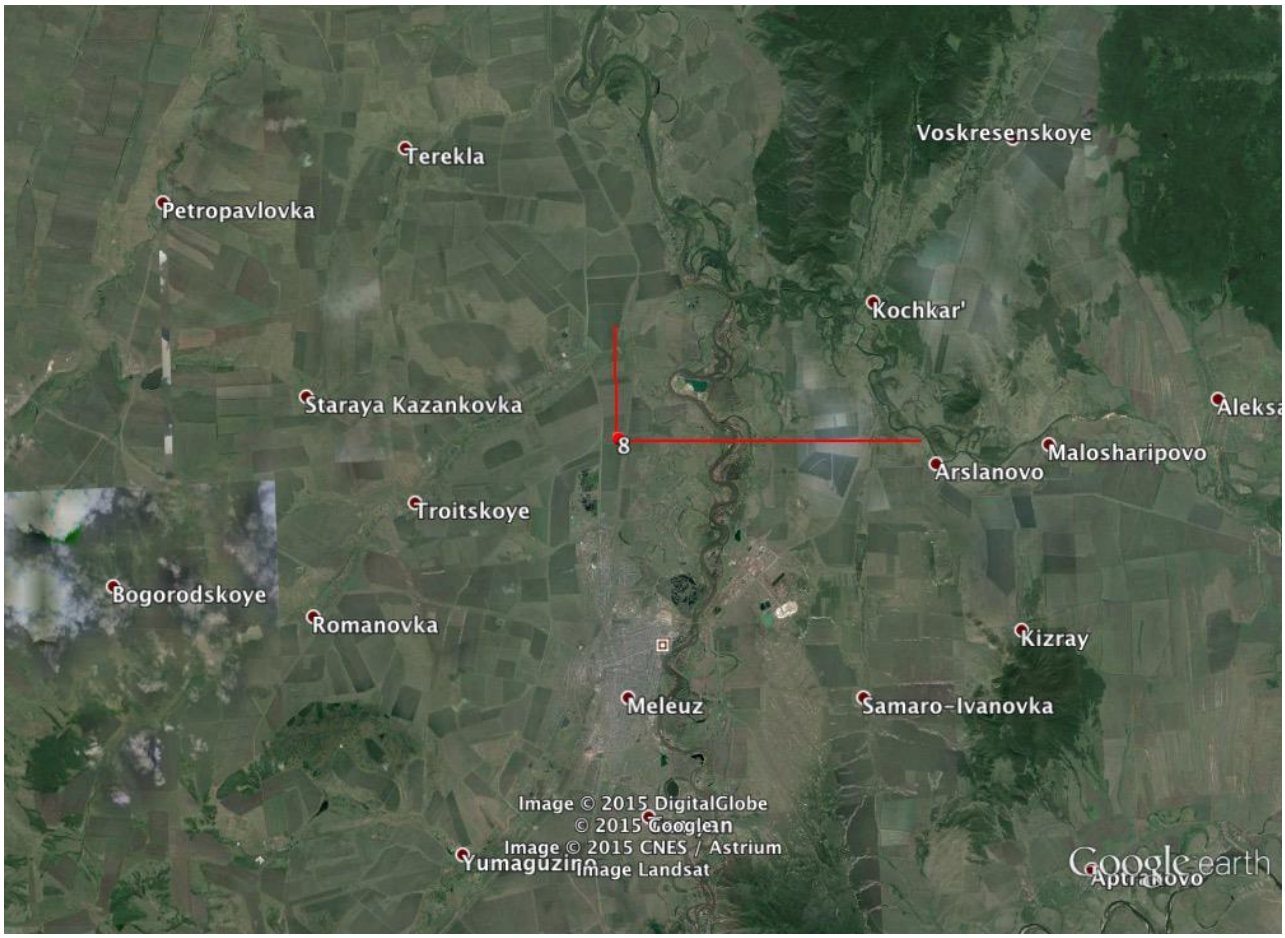

Figure A-8. Satellite imagery of the source region of the Butane 2-1 PNE (Google Earth, 2015). Red circular icon (#8) is the location from calibrated relocation. Red vectors indicate the orientation and length of the semi-minor (4 km) and semi-major (10.7 km) axes of the 90% confidence ellipse of the calibrated epicenter.

The location for Butane 2-1 found here is compatible with the tentative conclusion of Mackey and Fujita (2014) that it likely was detonated at a site NW of Meleuz, but not with the location reported by Sultanov et al. (1999) and other authors, which are ~40 km east of Meleuz.

6.1.3.4.6. Lira

The Lira sequence of six PNEs was detonated in two sets of three events each, the first set on July 10, 1983 and the second on July 10, 1984. Based on the reported locations of the Lira PNEs by Sultanov et al. (1999), Mackey and Fujita (2014) estimated refined GT locations by associating the events with shot sites identified from satellite imagery. Of necessity those associations were made mainly on the basis of proximity of Sultanov et al.'s (1999) locations to observed shot sites, which have a characteristic appearance. In Figure A-9, the calibrated locations are shown together with the Mackey and Fujita (2014) shot sites, all identified by the Lira sequence number. The calibrated HD analysis rearranges the relative locations of some of the Lira PNEs, making different associations more probable. Based on this approach we assigned new reference locations to five of the Lira PNEs, as follows:

- Lira 1-1: 51.3584°N, 53.3198°E. This is the site Mackey and Fujita (2014) assigned to Lira 2-1.
- Lira 1-2: 51.3660°N, 53.3258°E. The same as Mackey and Fujita (2014).
- Lira 1-3: 51.3717°N 53.3357°E. This is the site Mackey and Fujita (2014)assigned to Lira 2-2.
- Lira 2-1: 51.3646°N 53.3338°E. This site was not associated with any PNE by Mackey and Fujita (2014)
- Lira 2-2: 51.3916°N, 53.3497°E. This is the site Mackey and Fujita (2014) assigned to Lira 2-3.
- Lira 2-3: 51.3802°N, 53.3388°E. This is the site Mackey and Fujita (2014)assigned to Lira 1-3.

Calibrated relocation indicates that Lira 1-2 and 2-1 occurred very near one another, potentially at the same shot site. However there appear to be two other possible shot sites close to the one associated by Mackey and Fujita (2014) with Lira 1-2, and we have associated Lira 2-1 with one of these. In fact, either Lira 1-2 or Lira 2-1 could be associated any one of the three potential sites without violating the seismological constraints on their locations, in either a relative or absolute sense.

Because the Lira sequence events are very close to one another, the particular association of PNE to shot site makes little difference with regard to the location calibration of the cluster as a whole. However, different assumptions concerning the associations have consequences for the estimated uncertainty of the calibrated locations, as a poor association leads to larger residuals in location and greater uncertainty in the location calibration process.

On the other hand, the uncertainty of the cluster vectors for the Lira sequence events that describe the relative locations are small enough that they provide a quite strong basis for making the associations used here. This is illustrated in Figure A-10.

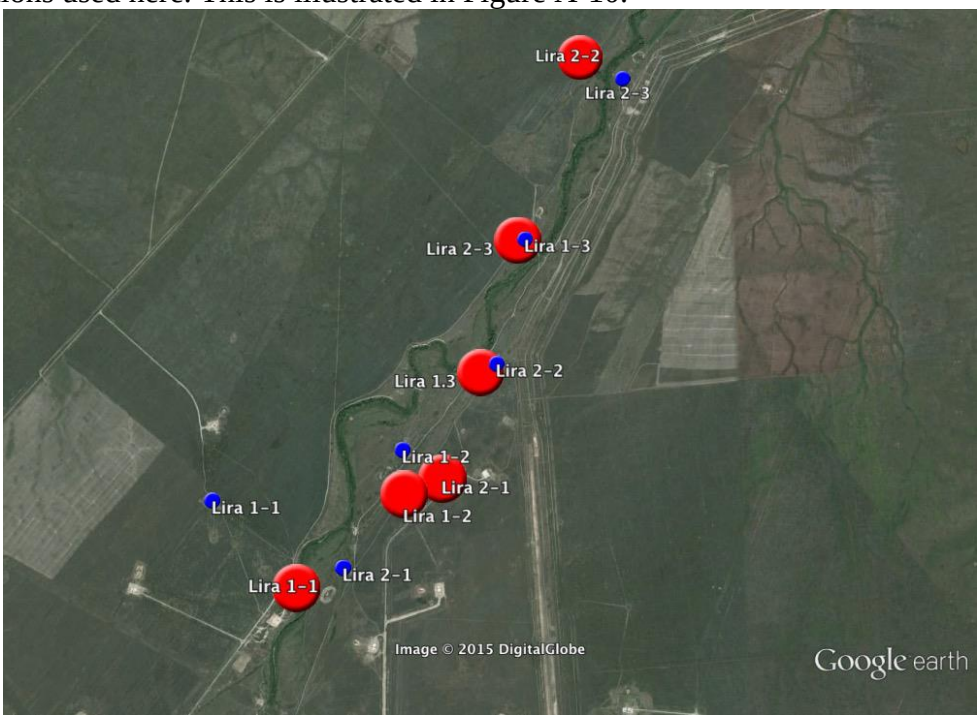

Figure A-9. Satellite imagery of the source region of the Lira PNE sequence (Google Earth, 2015). Large red icons are the locations from calibrated relocation, using reference locations for all PNEs in the cluster except Butane 2-1. Smaller blue icons are the GT locations reported by Mackey and Fujita (2014) based on comparison of locations reported by Sultanov et al. (1999) and likely shot sites identified in the satellite imagery.

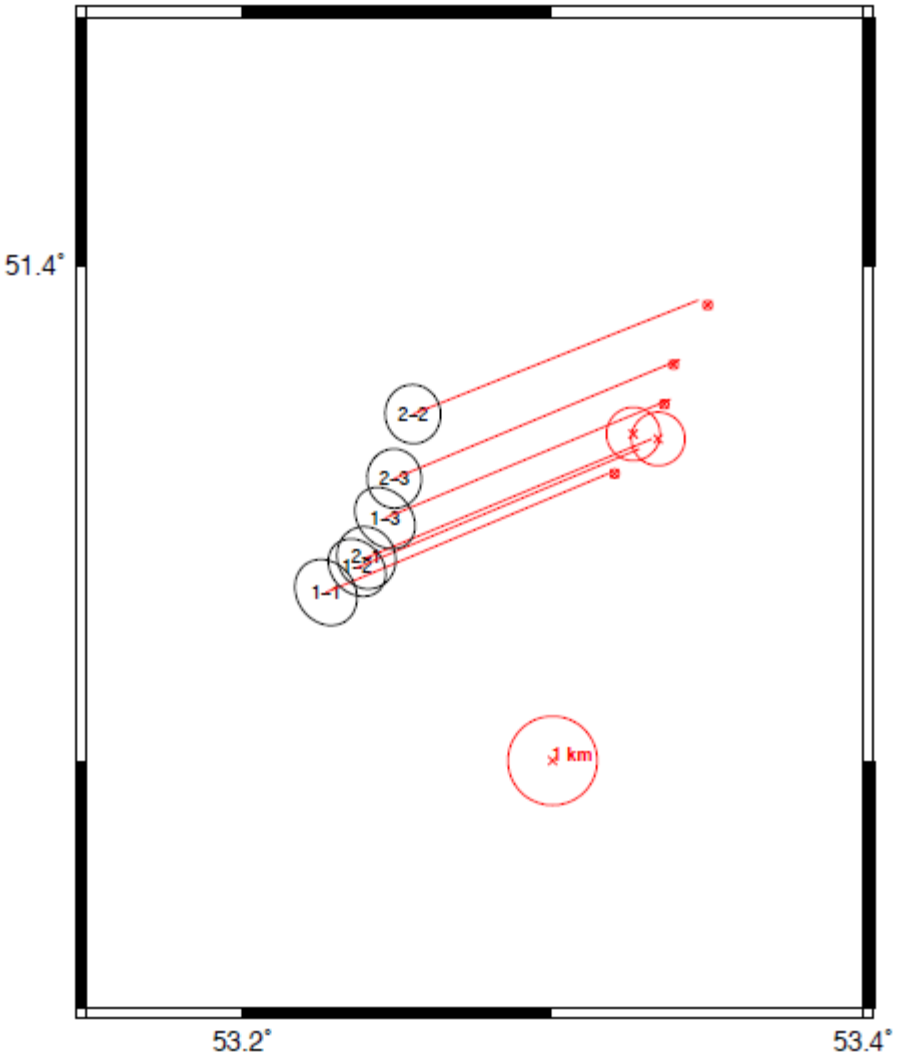

Figure A-10. Relative locations of the Lira PNEs (identified by sequence number) from uncalibrated HD analysis, and the shift required to bring them into concordance with the assumed shot sites, averaging over the 6 vector differences for the individual PNEs. The average shift vector, shown in red for each event, is 6.8 km @ 067°. Residuals from the average shift vector range from 111-374 m. The confidence ellipses (90% confidence level) for relative location (cluster vectors) are shown in black; their semi-axis lengths range from 570-780 m. The locations of the reference locations that were used to calculate the calibration shift of the cluster as a whole are shown as red x's, and a circle around each site represents a measure of the uncertainty in the location. For four of the PNEs the association is rather unambiguous and an uncertainty of 100 m is used. For Lira 1-2 and 2-1 there is uncertainty about which of three nearby sites (separated by 400-600 m) is the correct association, so the uncertainty for these two reference locations is represented by a circle of 600 m. A circle of 1 km radius is shown for scale.

6.1.3.5. Origin Times

In the calibrated relocation analysis we have taken the origin times reported by Sultanov et al. (1999) as the reference times. As with epicenters, we can examine the residuals in origin time after the calibration shift has been made in order to evaluate the consistency of those reference times. These residuals are listed for the 13 reference events in Table A-5.

Table A-5. Origin time residuals from calibrated locations of the Butane cluster.

Year	Mo	Da	Name	OT Res
1970	6	25	Magistral	**0.679**
1971	10	22	Sapphire-1	**0.933**
1972	9	21	Region-1	**-0.532**
1972	11	24	Region-2	0.140
1973	9	30	Sapphire-2	-0.278
1973	10	26	Kama-2	**0.716**
1974	7	8	Kama-1	0.058
1983	7	10	Lira 1-1	0.056
1983	7	10	Lira 1-2	0.057
1983	7	10	Lira 1-3	0.148
1984	7	21	Lira 2-1	0.051
1984	7	21	Lira 2-2	0.091
1984	7	21	Lira 2-3	0.056

Notes: Origin time residuals (calibrated OT - reference OT) in seconds. All reference origin times are from Sultanov et al. (1999). Outliers are in bold.

The residuals in origin time of four events (Magistral, Sapphire-1, Region-1 and Kama-2) appear as possible outliers. Sultanov et al. (1999) gives the origin times of Kama-2, Magistral and Sapphire-1 only to the nearest tenth of a second and his epicenters are ‘seismic’ locations (to the nearest hundredth of a degree) so the accuracy of the reference origin times of these three events can be questioned. The origin time and epicenter of Region-1 PNE is given to higher precision by Sultanov et al. (1999), suggesting greater confidence. The residual for Region-1 (-0.53 s) is the smallest of the four apparent outliers, however, and perhaps this residual represents a valid measure of the uncertainty of the calibrated origin times. The HD calibration process estimates the uncertainties of the origin times of all the calibration events in the range 0.18-0.20 s (with a zero mean) so Region-1 would not be a gross outlier on that basis.

On the basis of the consistency and small residuals of the origin times that were reported with higher precision (nearest hundredth of a second) by Sultanov et al. (1999), it seems justified to take those reported origin times as accurate to at least a tenth of a second. On the other hand, origin times reported only to the nearest tenth of a second by Sultanov et al. (1999) should be treated as less accurate, probably not reliable to better than the nearest second, and possibly biased (if they were based on seismological analysis rather than field reports).

6.1.3.6. Butane Cluster Summary and Conclusions

A calibrated relocation analysis was conducted for a cluster of 19 seismic events in southern Russia, near the border with western Kazakhstan. The cluster includes 14 known PNEs from the sequences Butane, Kama, Lira, Magistral, Region and Sapphire. The calibrated relocations help validate reported GT-quality locations for some PNEs, localize likely shot sites for

some other PNEs and bring other events (presumed to be natural earthquakes) in the cluster into a status as reference events in their own right. Lacking seismic data at near-source distances, calibrated hypocenters could only be obtained by taking some of the better-characterized PNEs as reference events and using consistency arguments to evaluate the likely accuracy of proposed or suspected coordinates for less well-characterized PNEs.

Locations reported by Sultanov et al. (1999) for these PNEs are accurate to within his stated uncertainties in some cases, but not all. The preferred reference locations for all PNEs in this cluster are revised from Sultanov et al. (1999). Revised reference locations by Mackey and Fujita (2014) were validated for many of the events, and further adjustments were made for some events in the relocation analysis. In particular, five of the six events in the Lira PNE sequence were assigned to new reference locations. In four of those cases, the associations were simply switched around among the sites identified by Mackey and Fujita (2014). The only member of the Butane sequence (Butane 2-1) that could be relocated with any confidence still has much greater uncertainty than any of the other PNEs, but the calibrated relocation requires the epicenter to be 5-15 km north of Meleuz and within about 10 km east or west of the longitude of Meleuz. With the exception of Butane 2-1, the epicenter of the PNEs in this cluster. For the 13 PNEs in this cluster that were used as reference events (i.e., except for Butane 2-1), the reference locations adopted here are considered to be validated at the GT0-1 level of accuracy.

The five non-PNE events in the cluster, which are assumed to be natural earthquakes, were all held at 10 km depth. Their epicenters are calibrated with accuracy ranging from 2-4 km. The calibrated origin times are contingent on the accuracy of the assumed focal depths. The epicenters should not be very sensitive to variations in focal depth unless the error in depth is quite large. It may be that some or all of these events are in fact man-made explosions at shallow depth. That possibility has not been seriously explored.

The origin times reported to high precision (two decimal places) by Sultanov et al. (1999) appear to be accurate to within 0.1 s. Origin times reported by Sultanov et al. (1999) to only one decimal place may be biased if they were derived from seismological analysis and are likely not accurate to better than the nearest second.

6.1.4. Urtabulak Cluster

Calibrated relocation analyses for the Urtabulak cluster was carried out for a clusters of seismic events, comprised of Peaceful Nuclear Explosions (PNEs), natural earthquakes and presumed chemical explosions in the territory of the former Soviet Union. Focal depths of earthquakes included in these clusters are set to a reasonable default value. The Urtabulak cluster was formed to attempt to validate the reported locations of two PNEs in western Uzbekistan, near the border with Turkmenistan, with code names “Urtabulak” on September 30, 1966 and “Pamuk” on May 21, 1968. These two events are only ~45 km apart making them good subjects for a calibrated relocation. A third PNE, “Crater” on April 11, 1972, was added to the cluster even though it is much further away, about 270 km to the southwest, in south-central Turkmenistan. This was done because there are no other well-recorded seismic events near the Crater PNE. Although we gain some insight into the source of Crater from this analysis, the great distance from other events means that our results are subject to greater uncertainty than usual. The quality of the statistics (i.e., parameter uncertainties) of a calibrated relocation analysis depend on repeated observations of the same phases at the same stations; therefore it is advantageous to add other seismic sources to the cluster. We searched the Bulletin of the International Seismological Centre (2015) for seismic events in the region and formed the cluster from 34 events that had sufficient observations to support a calibrated relocation.

The Urtabulak PNE was selected as the calibration event for this cluster and its calibration location was set according to an analysis of satellite imagery that reveals a clear, circular feature around the borehole location (at a depth of 1532 m below the surface), as shown in the Figure A-11.

Figure A-11. Satellite imagery of the source region of the September 30, 1966 Urtabulak PNE (Google Earth, 2014). Pushpins show the epicenter reported by Sultanov et al. (1999) and the reference location used in this study.

The coordinates assigned to the Urtabulak PNE for indirect calibration are 38.9672°N, 64.5193°E. In comparison, the coordinates published by Sultanov et al. (1999) are 38.968°N, 64.517°E. The coordinates differ by only about 200 m to the northwest of, but the Sultanov et al. (1999) coordinates are only given to the nearest ~100 m and they cite an uncertainty of 0.2-1.0 km. In other words, there is close agreement. If this location of the Urtabulak PNE is accurate, the calibrated relocation analysis should provide estimates of the epicenters of the other two PNEs, based on their locations relative to Urtabulak, that are similarly accurate, and with realistic uncertainties. The initial fit of data to travel-time curves are shown in Figure A-12.

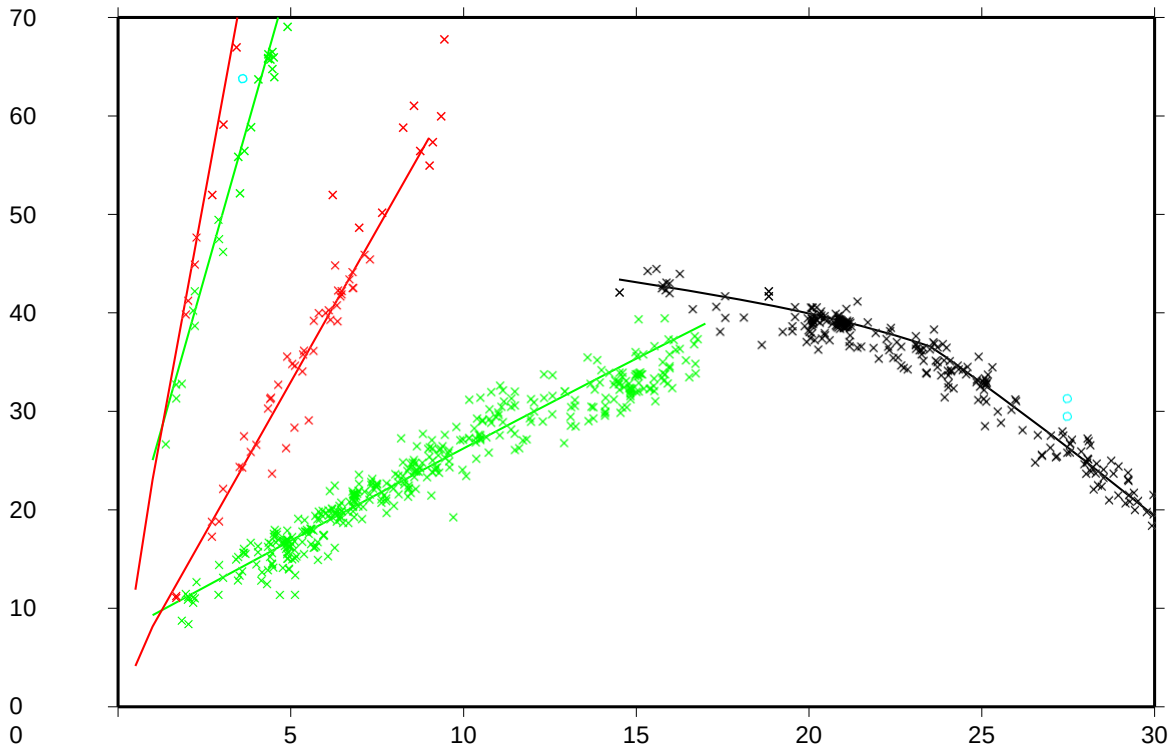

Figure A-12. Reduced travel time vs. distance for the Urtabulak cluster out to 30° epicentral distance. Reduction time is 11.67 s/degree (~9.5 km/s). Pg and Sg readings and theoretical curves are in red. Pn and Sn are in green. Teleseismic P is in black.

6.1.4.1. Preliminary Relocation

The HD algorithm decomposes the location problem into two separate estimation problems, 1) the "cluster vectors", the relative locations in space and time of the cluster events, which are specified relative to a common reference point, and 2) the "hypocentroid", the reference point for the cluster vectors. The two estimation problems differ in the number of parameters, the particular data that are used and the sources of uncertainty that must be accounted for. The absolute coordinates (epicenter in geographic coordinates, focal depth and origin time) are estimated only for the hypocentroid. Absolute coordinates for individual events is found by adding the cluster vector for that event to the hypocentroid. In this analysis we held focal depths fixed because the dataset contained no data that can constrain focal depth) and solved for epicenter and origin time.

An important aspect of HD analysis is so-called "cleaning" in which the observed distribution of residuals for each station-phase combination is analyzed with a robust statistical method to estimate a scale parameter (spread) that is insensitive to the presence of outliers and which does not depend on a measure of central tendency. With this measure of spread, outlier readings are identified and removed from the inverse problem, and each datum is inversely weighted according to the spread for that station-phase. This procedure is iterated until the dataset satisfies, in broad terms, the assumption that all samples are drawn from a normal distribution. For indirect calibration of the Urtabulak cluster I estimated the hypocentroid using only teleseismic P arrivals between 30 and 90° epicentral distance and minimizing residuals against the *ak135* global model. This by itself does not provide a calibrated location, but it provides a

stable and reasonably accurate location that is usually not more than about 10 km away from a calibrated location. The teleseismic P branch has been found to be the most accurate portion of the ak135 model globally, and there is generally good azimuthal coverage for a cluster when all the associated teleseismic P readings are combined. For the Urtabulak cluster, there were 884 such readings after cleaning that were used to estimate the three parameters of the hypocentroid.

The cluster vectors of the Urtabulak cluster were estimated with all phase readings at all epicentral distances that passed the cleaning criteria, with the exception that a station-phase combination that has only one sample cannot contribute any information regarding relative location, and so it is not used. In the estimation of cluster vectors, only travel-time differences are processed, so baseline errors in the theoretical travel-time model do not influence the result and there is no hazard in using readings for which the theoretical model may be quite in error. For the Urtabulak cluster the cluster vectors (34 x 3 = 102 free parameters) were estimated using 1363 readings.

After the initial phase of HD analysis, when the hypocentroid has been determined by fitting the teleseismic P arrivals to the ak135 model, all locations are considered uncalibrated. Then the hypocenter of the calibration event, the Urtabulak PNE, is compared with its calibration parameters (Figure A-11) and a shift vector is calibrated that brings the two estimates of the hypocenter into agreement. In this case the uncalibrated HD epicenter must be shifted 1.7 km almost due west (azimuth 265°). When this shift is applied to the hypocentroid, updating the absolute locations of all cluster events, the epicenters of all events in the cluster are considered to be calibrated. Similar corrections are made for focal depth and origin time.

The calibrated locations of the Urtabulak cluster are shown in Figure A-13. The vector describing the shift of each PNE from its starting location (Sultanov et al., 1999) to its calibrated location is

- Urtabulak: 0.2 km @ 114°
- Pamuk: 2.2 km @ 147°
- Crater: 7.5 km @ 073°

For other events in the Urtabulak cluster, for which the starting location was taken from the ISC Bulletin, epicentral shifts by as much as 40 km to the calibrated location are observed. Given that we have taken only the location of the Urtabulak PNE to be known (with an uncertainty of 200 m) in this case, it is of interest to consider the uncertainties of the calibrated locations for Pamuk and Crater to decide if there is a statistically-significant difference between the calibrated locations and Sultanov et al.'s (1999). Taking into account the uncertainty of their relative locations (cluster vectors) and the uncertainty of the calibration shift (0.8-1.4 km), the final uncertainty (90% confidence level) of the calibrated epicenter of Pamuk is 1.2-2.0 km and that of Crater is 1.5-2.5 km, where the range in uncertainties is taken from the semi-axes of the confidence ellipse.

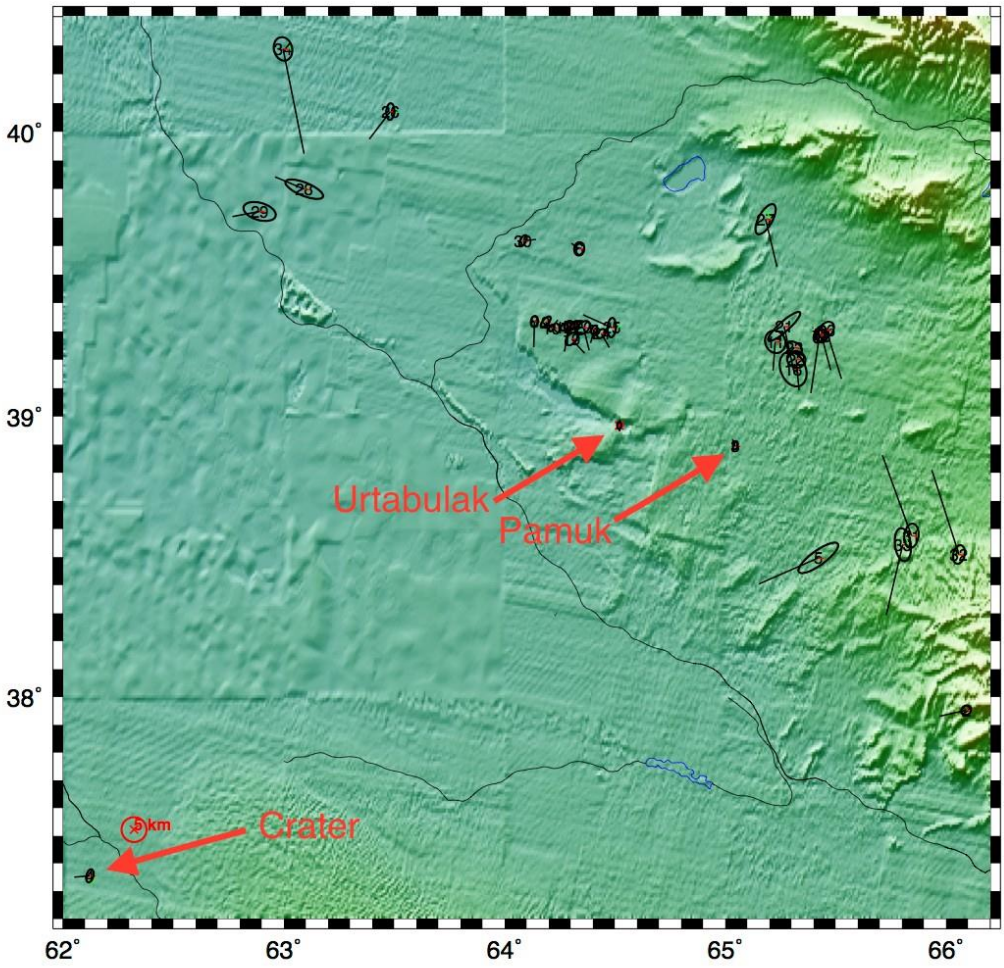

Figure A-13. Calibrated locations for the Urtabulak cluster. The three PNEs in the cluster are indicated. Each event is represented by a 90% confidence ellipse for relative location. Full location uncertainty would require addition of the uncertainty of the hypocentroid. The black vector for each event shows the change in location from the location given in the arrival time data file, in most cases the starting epicenter is from the ISC Bulletin; for the three PNEs it is from Sultanov et al. (1999). A circle of 5 km radius is shown for scale in the lower left of the figure.

To evaluate the consistency of the alternative locations the uncertainties of Sultanov et al.'s (1999) locations must also be considered. The locations for Urtabulak and Pamuk are "geodetically-determined" and considered to be accurate within 0.2-1.0 km, but that for Crater is a "seismically- determined" location that is considered accurate only to about 5-10 km. Given these uncertainties for the locations reported by Sultanov et al. (1999) and those determined in the calibrated relocation, it is clear that there is no statistically-significant difference between the epicenters from Sultanov et al. (1999) and the HD analysis, even for the Crater PNE, for which there is a relatively large difference in the two locations.

Even so, the accuracy of the epicenter of the Crater PNE may be somewhat better from the HD analysis. Formally this is obviously true, considering the uncertainties of each estimate (1.5-

2.5 vs. 5-10 km), but it is likely that the HD location is biased to some extent because this single event is so far away (~275 km) from the rest of the events in the cluster (Figure A-13) and the cluster vector for this event could easily be biased by unmodeled heterogeneity in the crustal structure over such a distance. Such bias would not be reflected in the formal uncertainty of the location. Since there is no means of evaluating this possibility at present, the location of the Crater PNE should most likely be considered unknown to any degree approaching "ground truth", unless clear evidence of the shot site can be found from inspection of satellite imagery or from ground-based inspection.

Note: The Location of PNE Crater was determined subsequent to this cluster analysis. Please see section 2.14.

6.1.4.2. Focal Depths and Origin Times

For many seismological purposes it is highly desirable to have unbiased estimates of focal depth and origin time in addition to epicenters. Focal depth and origin time are highly correlated in the earthquake location problem. If the depth of an event in a calibrated relocation cannot be constrained somehow, then the origin time cannot be considered to be calibrated in the fullest sense but it is may still be an improvement over existing catalog locations to specify that origin time is calibrated provisionally, depending on the true depth of the event. In the Urtabulak cluster the only events with useful constraint on focal depth are the three PNEs, for which reliable borehole depths ranging from 1.3-2.2 km below sea-level have been reported by *Sultanov,* and an earthquake on July 24, 2005 for which a large number of teleseismic depth phases were reported that are consistent with a depth of about 22 km. A subset of events in the Urtabulak cluster during 1983-84 were found to have calibrated epicenters and other characteristics which lead to the conclusion that they were probably chemical explosions used for civil engineering projects, namely, canal-building. This is discussed further, below. These events have been held at zero depth for relocation. The remaining events have been held at a depth of 15 km for relocation.

If the shot times reported for the three PNEs by Sultanov et al. (1999) are accurate, the calibrated origin times should be in close agreement with each other. Because we have used the Urtabulak PNE as the calibration event, the calibrated origin times of the other two PNEs should be very close to the origin times reported by Sultanov et al. (1999). The differences are listed in Table A-6.

Table A-6. Comparison of origin times reported by Sultanov et al. (1999) and those from the relocation calibrated with the Urtabulak PNE.

PNE	Sultanov	Calibrated	Difference, s
Pamuk	**0359:11.98**	**0359:12.09 ± 0.131**	**+0.11**
Crater	**0600:01.92**	**0600:02.37 ± 0.144**	**+0.45**

The origin time of the Urtabulak PNE is only given to the nearest tenth of a second by Sultanov et al. (1999) while those of the Pamuk and Crater PNEs are given to the nearest hundredth of a second. We specified the uncertainty for the Urtabulak calibration origin time as 0.1 s. The final uncertainty of the calibrated origin times shown in Table A-7 combines that baseline uncertainty with the uncertainty of the origin time component of each event's cluster vector. Thus, even assuming zero error in the calibration origin time for Urtabulak, the residual for Pamuk is less than 1σ and the residual for Crater is ~3σ, a marginal outlier. This is

observation is undoubtedly coupled with the likelihood of some remaining bias in the HD epicenter of the Crater PNE due to its great separation from the rest of the cluster. For this reason we think the data support the view that the origin times reported by Sultanov et al. (1999) for these three PNEs are consistent with each other and therefore they are likely to be accurate to a level of 0.1 s or better.

Table A-7. Calibrated hypocenters for the Urtabulak cluster.

Year	Mo	Da	Hr	Mi	Sec	Lat	Long	Depth	Mag	Az1	L1	Az2	L2	Cal	Comment
1966	9	30	5	59	50.94	38.97644	64.51380	1.30	5.1mb	275	1.19	5	1.97	CH02	PNE Urtabulak
1966	12	22	12	30	0.29	37.96071	66.09622	15.00	4.8mb	292	2.13	22	2.50	CT03	
1968	5	21	3	59	12.04	38.91036	65.04057	2.20	5.4mb	278	1.21	8	1.94	CH02	PNE Pamuk
1972	4	11	6	0	2.31	37.37853	62.12595	1.50	4.9mb	281	1.46	11	2.50	CH03	PNE Crater
1972	11	1	4	6	45.98	38.50409	65.41278	15.00	4.5mb	324	2.48	54	9.41	CT09	
1982	4	20	5	39	13.39	39.59391	64.33579	15.00	4.0mb	276	2.14	6	2.98	CT03	
1983	3	5	11	37	52.09	39.30744	64.40348	0.00	4.7mb	286	1.33	16	2.16	CH02	chemical explosion
1983	3	23	11	7	57.51	39.33892	64.13281	0.00	4.6mb	276	1.48	6	2.35	CH02	chemical explosion
1983	4	11	8	31	40.36	39.33632	64.18037	0.00	4.9mb	306	1.60	36	3.10	CH03	chemical explosion
1983	4	22	3	56	22.53	39.31637	64.21094	0.00	4.8mb	290	1.31	20	1.98	CH02	chemical explosion
1983	4	28	12	18	51.56	39.26811	65.22549	0.00	3.9mb	54	4.12	144	5.15	CH05	chemical explosion
1983	5	16	12	7	51.99	39.32106	64.26607	0.00	4.7mb	296	1.54	26	2.09	CH02	chemical explosion
1983	5	26	12	18	12.48	39.28444	65.43824	0.00	4.7mb	90	2.51	180	2.92	CH03	chemical explosion
1983	5	26	12	46	19.67	39.32596	64.29005	0.00	4.5mb	286	2.16	16	2.44	CH02	chemical explosion
1983	6	3	12	9	59.96	39.29919	65.42461	0.00	4.5mb	290	2.38	20	3.96	CH04	chemical explosion
1983	6	11	12	57	28.27	39.31052	65.45050	0.00	4.6mb	307	2.76	37	3.74	CH04	chemical explosion
1983	6	15	13	34	4.04	39.32658	64.31413	0.00	4.8mb	294	1.46	24	2.13	CH02	chemical explosion
1983	7	1	6	8	53.49	39.16898	65.30648	0.00	4.4mb	60	4.87	150	7.31	CH07	chemical explosion
1983	7	2	11	42	19.10	39.27916	64.30471	0.00	4.8mb	305	2.15	35	3.17	CH03	chemical explosion
1983	7	11	14	47	53.80	39.31899	64.35135	0.00	4.6mb	307	2.32	37	3.42	CH03	chemical explosion
1983	7	16	4	32	0.09	39.32214	65.26204	0.00	4.5mb	318	2.37	48	8.27	CH08	chemical explosion
1983	8	4	5	22	54.23	39.20362	65.31612	0.00	4.5mb	30	3.47	120	4.25	CH04	chemical explosion
1983	8	12	9	24	16.94	39.24728	65.31129	0.00	4.3mb	39	2.37	129	3.09	CH03	chemical explosion
1983	8	27	5	4	49.61	39.29771	64.43172	0.00	4.5mb	298	1.71	28	2.40	CH02	chemical explosion
1984	3	3	9	24	30.24	39.31656	64.48039	0.00	4.3mb	274	1.75	4	4.03	CH04	chemical explosion
1984	3	20	10	44	11.45	40.07525	63.48111	15.00	4.4mb	272	1.67	2	3.50	CT03	
1984	4	3	8	15	21.32	39.71372	65.17617	15.00	4.4mb	283	1.79	13	6.52	CT07	
1986	2	8	6	46	22.24	39.80995	63.07737	15.00	4.2mb	24	3.08	114	7.88	CT08	
1986	7	17	14	58	5.10	39.72461	62.89127	15.00	4.3mb	16	3.81	106	6.28	CT06	
2005	7	24	18	5	59.31	39.61416	64.08138	22.00	5.0mb	295	1.49	25	2.90	CH03	
2009	6	15	1	40	46.18	38.58730	65.81396	15.00		281	3.53	11	5.62	CT06	
2010	3	27	13	10	0.67	38.49590	66.05333	15.00	3.3mb	291	2.96	21	3.89	CT04	
2014	1	11	12	58	4.75	38.53212	65.79653	15.00	3.5mb	80	3.26	170	5.81	CT06	
2014	5	24	23	44	30.30	40.28991	62.98151	15.00	3.5mb	48	3.26	138	3.43	CT03	

Notes: Calibration was based on the reference locations for the Urtabulak and Pamuk PNEs shown in Figures A-11 and A-14. Hypocenters listed here for these two events are the ones from relocation, not the reference locations. The 90% confidence ellipse for epicenter is given by parameters Az1, L1, Az2, and L2 (azimuth and length in km of the two semi-axes). "Cal" is a code providing information about the calibration status. The letter portion of the code reflects which hypocentral parameters are considered calibrated (CH = all parameters, CT = epicenter and "provisional" origin time, based on an assumed focal depth). The numeric portion of the code gives a length scale, to nearest km, for calibration of the epicenter.

6.1.4.3. Calibrated Relocation of the Urtabulak Cluster, Revisited

From the review of results of calibrated relocation using only the Urtabulak PNE as a calibration event we conclude that the source parameters of the Pamuk PNE reported by Sultanov et al. (1999) are likely to be equivalently accurate, making Pamuk suitable for use as a calibration event as well. On the other hand the location of the Crater PNE is not sufficiently well-known from either Sultanov et al. (1999) or the calibrated HD relocation exercise to justify use as a reference event.

Therefore we performed a second relocation analysis of the cluster, using both Urtabulak and Pamuk as calibration (reference) events. As with the Urtabulak PNE (Figure A-11) we examined satellite imagery of the Pamuk site and identified a likely shot site (38.9197°N, 65.0350°E, Figure A-14) that differs slightly (300 m northeast) from the coordinates supplied by Sultanov et al. (1999), but within the claimed uncertainty. This location was used as the reference epicenter for the Pamuk PNE in the HD relocation. The calibrated hypocenters of all events in the Urtabulak cluster from this relocation are listed in Table A-7.

When using more than one calibration event for indirect calibration in *mloc*, it is not expected that all calibration locations can be fit exactly and there is a rather complex series of calculations that determines the shift (and its uncertainty) of the uncalibrated cluster that gives the best match to the available calibration locations. If there are two calibration events and the uncertainties of the calibration points and the HD cluster vectors are similar, as in the present case, the effect of these calculations is, essentially, to split the difference of the misfit vectors. Therefore the revised calibration of the Urtabulak cluster leaves all relative locations the same as before, but the entire cluster is shifted ~1 km to the northwest from the previous calibration. The calibrated location of the Urtabulak PNE is about 1 km northwest of the reference location (Figure 1-11), and that of the Pamuk PNE is about 1 km southeast of the reference point (Figure A-14). Given the uncertainties of the epicenters for these two events in the HD analysis, in the range 1.2-2.0 km, both reference locations are "covered" by the respective calibrated epicenters and the calibration is considered successful in this respect.

In judging the success of the HD calibration analysis it is necessary also to consider the consistency of calibrated origin times. In the HD analysis the shift in origin time (from the values calculated to fit the average global model *ak135*) needed to best fit the reference values for Urtabulak and Pamuk PNEs is +0.58 s, and the residuals after that shift (against the Sultanov et al., 1999 origin times) are -0.06 s and +0.06 s, respectively, for Urtabulak and Pamuk, well within the uncertainty of the origin times (0.16 s) for these events in the HD analysis. Therefore, origin times are also considered to be well-calibrated in this analysis.

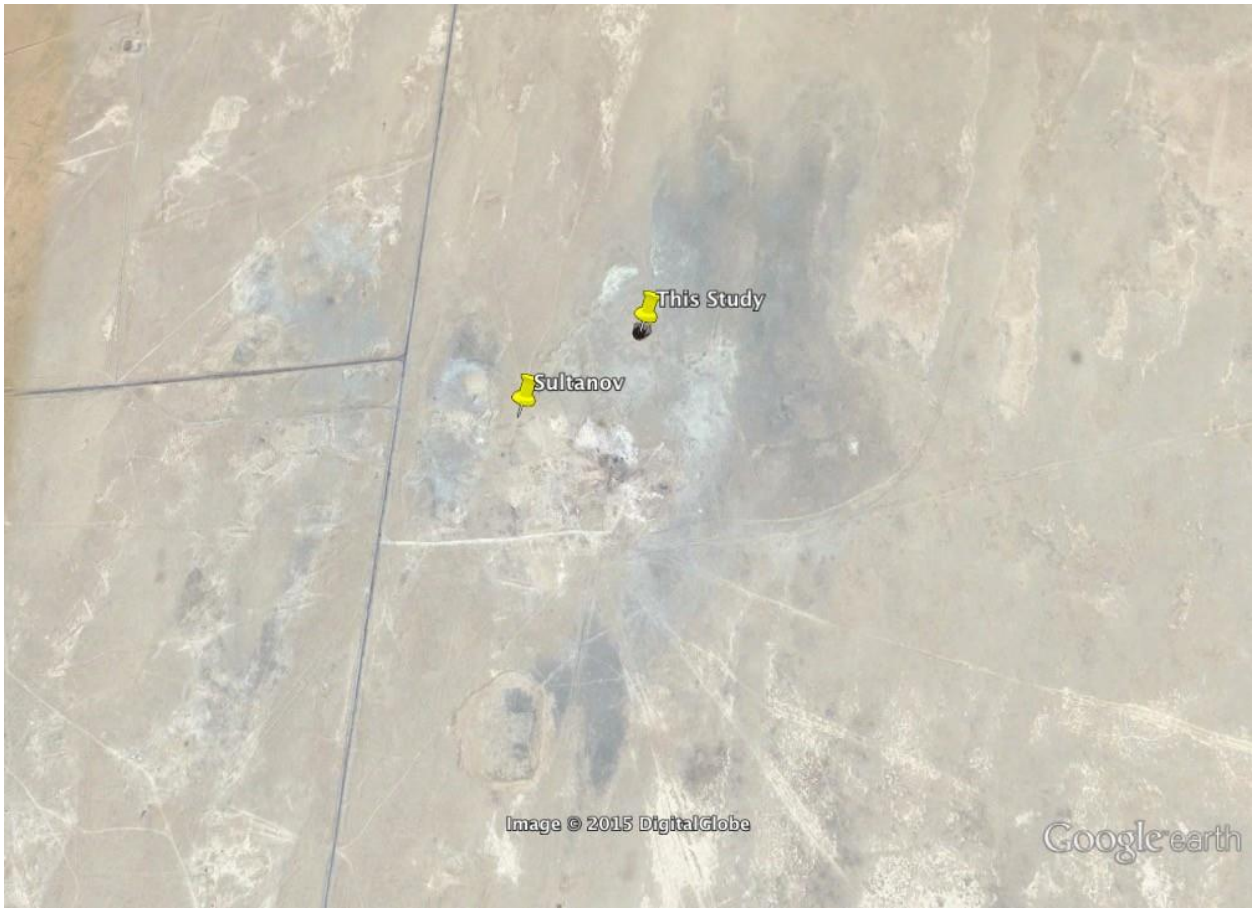

Figure A-14. Satellite imagery of the source region of the May 21, 1968 Pamuk PNE (*Google Earth, 2014*). Pushpins show the epicenter reported by Sultanov et al. (1999) and the reference location used in this study.

6.1.4.3.1. Chemical Explosions

In reviewing the HD calibrated relocations for the Urtabulak cluster I noticed two subsets of events in 1983-84 that were strongly clustered, with similar magnitudes (mb 3.9-4.9), and daytime (8am to 7pm local time) origin times. Taken together these observations are suggestive of man-made explosion sources, often conducted in the course of mining activities and large-scale civil engineering projects. An investigation of the source areas with satellite imagery reinforced that view, as both sets of events appear to be closely related to linear features that are clearly man-made. It seems likely that these are irrigation canals, but I have not researched the issue. The western set of events, north of Lake Dengizkul, is shown in Figure A-15.

The second set of events, near the town of Mubarek, that are suspected of being chemical explosions are shown in Figure A-16.

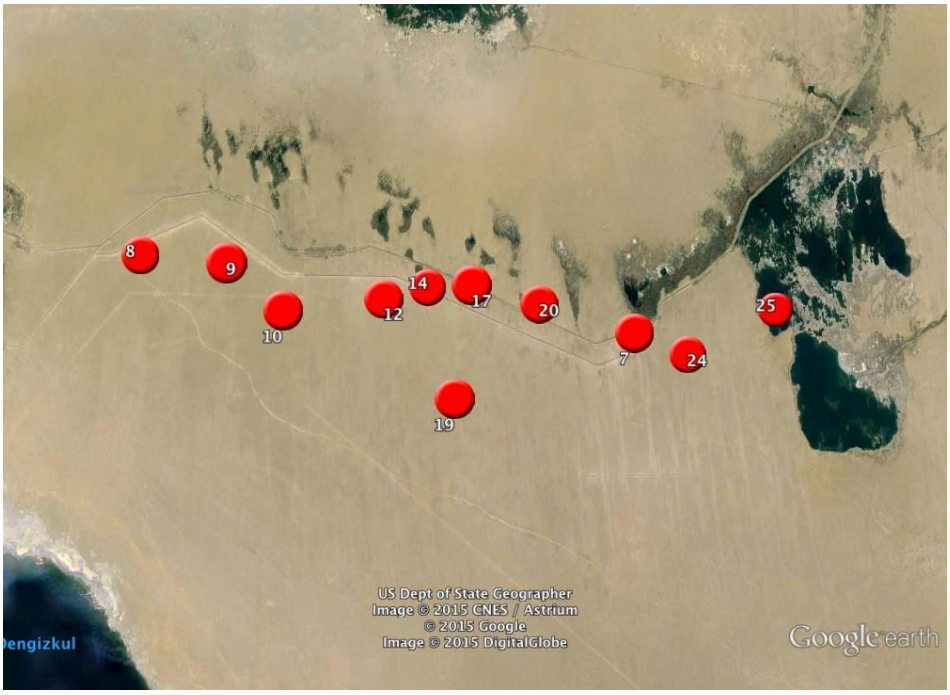

Figure A-15. Satellite imagery of a region of western Uzbekistan near Lake Dengizkul with eleven events thought to be chemical explosions related to the construction of irrigation canals (*Google Earth, 2014*). Numbers on the event icons refer to the event number in the Urtabulak cluster, in chronological order as in Table A-7.

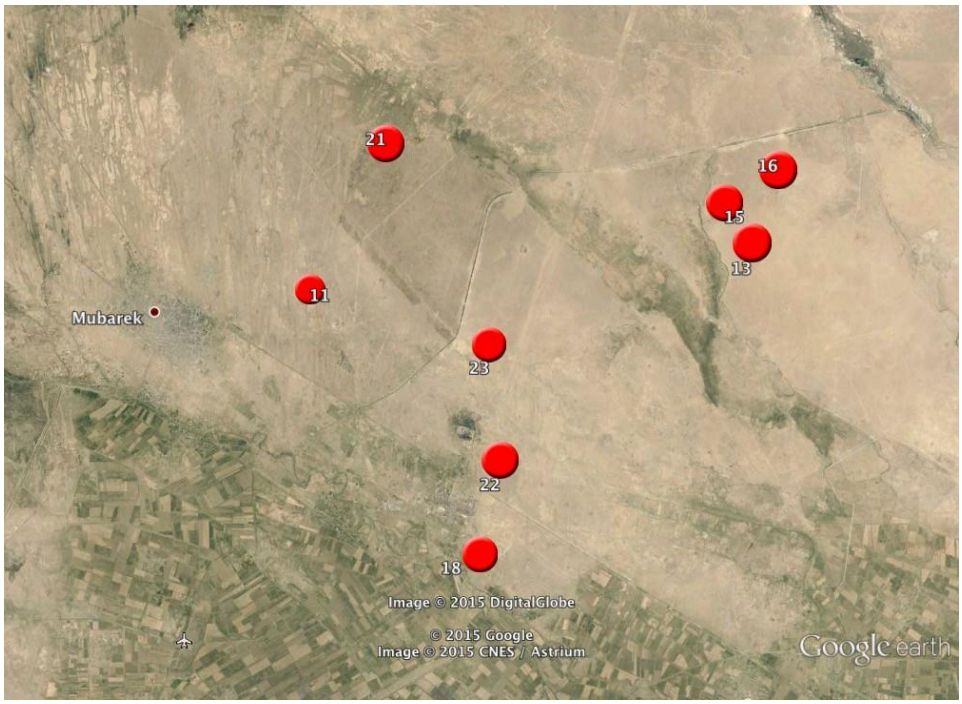

Figure A-16. Satellite imagery of a region of western Uzbekistan near Mubarek with eight events thought to be chemical explosions related to construction of irrigation canals (Google Earth, 2014). Numbers on the event icons refer to the event number in the Urtabulak cluster, in chronological order as in Table A-7.

The uncertainties of the epicenters for these events in the calibrated relocation analysis (Table A-7) range from about 2-8 km, such that most of the 90% confidence ellipses could overlap with a portion of the observed structures.

Because of the probable explosive nature of the sources of the events shown Figures A-15 and A-16, their focal depths have been held at zero depth in the HD relocation analysis. Because focal depth in the relocation analysis is referenced to mean sea level and the surface elevation in these two areas is 200-300 m, the assumed depths for these presumed explosions are in the range 200-300 m below the surface. They may in fact have been shallower, but differences in assumed depth of this magnitude have no significant effect on the relocation analysis.

It seems likely that some of the remaining events in the Urtabulak cluster are also chemical explosions, as they occur close to apparent irrigation canals. Even the apparently deep event on July 24, 2005 (event #30) could in fact be a pair of shallow explosions, with the second blast delayed appropriately to be reported as a depth phase of the first by many teleseismic stations. The epicenter is very close to what appears to be an irrigation canal. This theory could be tested through an inspection of waveform data. Obviously, the calibration status of such events is compromised if they have been located with focal depths far from the true depth, and this issue should be investigated if the Urtabulak cluster is to be used in additional studies as a set of reference events.

6.1.4.3.2. The Crater PNE

The epicenter of the Crater PNE on April 11, 1972, as reported by Sultanov et al. (1999) and as estimated here from calibrated HD relocation (Table A-7), is shown in Figure A-17.

Figure A-17. Satellite imagery of the source region of the April 11, 1972 Crater PNE (Google Earth, 2014), showing the epicenters reported by Sultanov and estimated in this study by calibrated relocation, using PNEs Urtabulak and Pamuk as reference events.

Although the disagreement is large (7.5 km) the Sultanov et al. (1999) epicenter is an uncalibrated seismic location with an estimated uncertainty of 5-10 km, so there is no significant discrepancy in that sense. The formal uncertainty of the calibrated HD relocation is 2.5 km or less, but we have discussed above why this location may well be biased because of its great separation from the remainder of the cluster.

It would therefore be highly desirable to observe some evidence in the satellite imagery to confirm (or not) the calibrated location. Inspection of the imagery available in Google Earth within several km of the calibrated location has failed to provide such evidence. It appears that there has been substantial development of this area in recent decades and that may have obscured the signs of an old shot site. Alternatively, the calibrated location may be more severely in error than we suppose, and we have been looking in the wrong place.

For most seismological purposes, therefore, we conclude that the epicenter of the Crater PNE is at present unknown.

Note: The Location of PNE Crater was determined subsequent to this cluster analysis. Please see section 2.14.

6.1.4.4. Urtabulak Cluster Summary and Conclusions

A calibrated relocation analysis was conducted for a cluster of 34 seismic events in Uzbekistan and Turkmenistan. Most events are on the Uzbekistan side of the border with Turkmenistan. The cluster includes 3 known PNEs, code-named Urtabulak, Pamuk and Crater. The calibrated relocations help validate reported source parameters for the PNEs and bring other events in the cluster into a status as potential reference events in their own right. Lacking seismic data at near- source distances, calibrated hypocenters could only be obtained by taking one event as a reference event and using consistency arguments among other events to evaluate the likely accuracy of hypocentral parameters, either those reported by Sultanov et al. (1999) for the PNEs or those estimated in the calibrated relocation analysis.

Comparisons with the results of the calibrated relocations suggests that the epicenters reported by Sultanov et al. (1999) for the Urtabulak and Pamuk PNEs are accurate to the claimed level of accuracy, although improved locations have been identified that differ by only a few hundred meters. The origin times reported by Sultanov et al. (1999) also appear to be accurate to within 0.1 s at the least, and perhaps to within a few hundredths of a second. This accuracy also pertains to the origin time of the third PNE, Crater, but the epicenter for that event cannot be confirmed to a high degree of accuracy. The calibrated location for Crater may be biased to an unknown extent because it is very far (280 km or more) from the remainder of the cluster and unmodeled lateral heterogeneity could introduce bias in the location. The formal uncertainty in epicenter is up to 2.5 km but the true error could easily be 5 km or greater. No evidence of a shot site could be found through inspection of satellite imagery but it may be obscured by recent development in the area.

Two sets of events in the cluster, 19 events total, were tentatively identified as chemical explosions, probably related to the construction of irrigation canals. Additional events in the cluster may well be explosions as well, but the evidence in those cases was less clear.

6.1.5. References

Aziz Zanjani, A., Ghods, A., Sobouti, F., Bergman, E. A., Mortezanejad, G., Priestley, K., et al. (2013). Seismicity in the western coast of the South Caspian Basin and the Talesh Mountains. *Geophysical Journal International*, *195*(2), 799–814. http://doi.org/10.1093/gji/ggt299

Croux, C., & Rousseeuw, P. J. (1992). Time-efficient algorithms for two highly robust estimators of scale. *Computational Statistics*, *1*, 411–428.

Google Earth, imagery accessed July 2015.

Hayes, G. P., Herman, M. W., Barnhart, W. D., Furlong, K. P., Riquelme, S., Benz, H. M., Bergman, E. A., Barrientos, S., Earle, P. S., and Samsonov, S. V. (2014). Continuing megathrust earthquake potential in Chile after the 2014 Iquique earthquake. *Nature*, *512*(7514), 295–298. http://doi.org/10.1038/nature13677

International Seismological Centre, *On-line Bulletin*, http://www.isc.ac.uk, Internatl. Seis. Cent., Thatcham, United Kingdom, 2015.

Jordan, T. H., & Sverdrup, K. A. (1981). Teleseismic location techniques and their application to earthquake clusters in the South-Central Pacific. *Bulletin of the Seismological Society of America*, *71*(4), 1105–1130.

Kennett, B. L. N., Engdahl, E. R., & Buland, R. P. (1995). Constraints on seismic velocities in the Earth from traveltimes. *Geophysical Journal International*, *122*(1), 108–124. http://doi.org/ 10.1111/j.1365-246X.1995.tb03540.x

Mackey, K. G., & Bergman, E. A. (2014). Ground truth locations for the Mangyshlak Peaceful Nuclear Explosion sequence, western Kazakhstan. *Bulletin of the Seismological Society of America*, *104*(4), 1–9.

Mackey, K.G., and Fujita, K., 2014. Improvement of GT Classification of Soviet PNEs, Final Report for contract SAQMMA11M2465, 282 pp.

McNamara, D. E., Benz, H. M., Herrmann, R. B., Bergman, E. A., Earle, P. S., Holland, A., et al. (2015). Earthquake hypocenters and focal mechanisms in central Oklahoma reveal a complex system of reactivated subsurface strike−slip faulting. *Geophysical Research Letters*, n/a–n/a. http://doi.org/10.1002/2014GL062730

Sultanov, D. D., Murphy, J. R., & Rubinstein, K. D. (1999). A seismic source summary for Soviet Peaceful Nuclear Explosions. *Bulletin of the Seismological Society of America*, *89*(3), 640–647.

6.2. APPNNDIX B – Borehole Photos of other PNEs

Figure B-1. Shpat-2 in 2011 (Abramov et al., 2012).

Figure B-2. Quartz-3 in 2010 (https://youtu.be/Drp7YQmfcH4).

Figure B-3. Rift-4 in 2010 (Abramov et al., 2012).